Neuroprotective Effects of Sulforaphane and the Involvement of Autophagy

Sandra Bednar MSc (pharm.)

A thesis submitted to the University of East Anglia in accordance with the requirements of the Degree of Doctor of Philosophy

Norwich Medical School, Faculty of Medicine and Health Sciences

University of East Anglia

April 2016

ABSTRACT

Sulforaphane (SFN) is an isothiocyanate found mostly after consumption of broccoli, but also other cruciferous vegetables such as cauliflower or cabbage. Isothiocyanates have been researched for over 20 years in the field of cancer. They show many different bioactivities, of which the majority are positively associated with cell health and are possibly collectively responsible for protective effects of SFN against toxin-induced cell death.

This study aims to investigate the bioactivities of SFN on neuronal cells. PC-12 and SH-SY5Y cells were used to resemble neuronal-like systems to research especially autophagy as well as nuclear factor E2-related factor 2 (Nrf2) and how these pathways might influence neuroprotective abilities of SFN.

Basal assessments confirmed that SFN can induce Nrf2-driven phase II enzymes, as determined by qPCR as well as immunoblotting. The elevation of the main autophagy marker light chain 3-II (LC3-II) by SFN could be observed dose-dependently at protein level. In addition, SFN pre-treatment provided statistically significant cytoprotection against H_2O_2- and 6-hydroxydopamine- (6-OHDA) induced cell death.

Further, DJ-1, a multifunctional protein, was selected for investigation with SFN, since it is highly implicated with neuronal cell health. SFN induced DJ-1 protein levels dose-dependently. In addition, tunicamycin-induced ER-stress was significantly reduced by SFN, as shown using the ER-stress marker CHOP on protein and RNA levels.

To intensify the research of SFN and autophagy, primary neuronal cells (PNCs) were developed from embryos from Atg16L1 wild type and knock out (KO) mice. Atg16L1 is a protein necessary for autophagosome formation. Immunostainings assessed that autophagy was indeed fully supressed in KO cells. Preliminary results suggest that autophagy is involved in the neuroprotective effects of SFN.

Conclusively, SFN was able to significantly protect all neuronal cells investigated from H_2O_2- or 6-OHDA-induced cell death. SFN's ability to activate autophagy as well as DJ-1 may contribute to its protective effects.

TABLE OF CONTENTS

LIST OF TABLES

LIST OF FIGURES

LIST OF ABBREVIATIONS

3-MA	3-methyladenine
6-HITC	6-methylsulfinylhexyl isothiocyanate
6-OHDA	6-hydroxydopamine
AD	Alzheimer's Disease
ALS	Amyotrophic lateral sclerosis
AMPK, AMP	Activated protein kinase
APP	Amyloid precursor protein
ARE	Antioxidant response element
Atg	Autophagy-related gene
ATP	Adenosine triphosphate
BBB	Blood brain barrier
Beclin1	Bcl-2 interacting myosin-like coiled-coil protein 1
BH_4	Tetrahydrobiopterin
CHOP	C/EBP homologous protein
CHX	Cycloheximide
CMA	Chaperone-mediated autophagy
CNS	Central nervous system
COX-2	Cyclooxygenase
CV	Cruciferous vegetables
CYP	Cytochrome P-450
DA	Dopamine
DMEM	Dulbecco's Modified Eagle Medium
DMSO	Dimethyl sulphoxide
DTC	Dithiocarbamates
DTT	Dithiothreitol
ERK	Extracellular signal regulated protein kinase
ERN	Erucin

ESP	Epithiospecifier protein
FBS	Foetal bovine serum
GST-a	Glutathione-S-Transferase
h	Hour(s)
HD	Huntington's Disease
HO-1	Heme oxygenase
IR	Infra-red
ITC	Isothiocyanate
JNK	c-Jun-N-terminal kinase
Keap1	Kelch-like ECH-associated protein 1
KO	Knockout
LC-3	Light chain 3
LRRK-2	Leucine rich repeat kinase 2
min(s)	Minute(s)
MND	Motor neuron disease
MPTP	N-methyl-4-phenyl-1,2,3,6-tetrahydropyridine
mRNA	Messenger ribonucleic acid
mTOR	Mammalian TOR
MTT	3-(4,5-Dimethyilthiazol-2-yl)-2,5-diphenyltetrayolium bromide
NADH	Nicotinamide adenine dinucleotide
NDs	Neurodegenerative diseases
NFκB	Nuclear factor kappa B
NGF	Nerve growth factor
NQO1	NAD(P)H:quinone oxidoreductase
Nrf2	Nuclear factor E2-related factor 2
p62	Sequestosome 1,
PAS	Phagophore assembly site
PBS	Phosphate buffered saline
PCR	Polymerase chain reaction
PD	Parkinson's Disease

PI3K	Phosphatidylinositol 3-kinase
PNCs	Primary neuronal cells
qPCR	Quantitative real time polymerase chain reaction
RES	Resveratrol
RNase	Ribonuclease
ROS	Reactive oxygen species
RT-PCR	Reverse transcription polymerase chain reaction
SD	Standard deviation
SDS-PAGE	Sodium dodecyl sulphate polyacrylamide gel electrophoresis
SFN	Sulforaphane
siRNA	Small interfering RNA or silencing RNA
SNCA	a-synuclein
SOD	Superoxide dismutase
SXR	Steroid and xenobiotics receptor
tBHQ	Tertiary butylhydroquinone
TNF-a	Tumour necrosis factor
TOR	Target of rapamycin
TR-1	Thioredoxin reductase 1
U	Unit(s)
UDP	Uridine 5'-diphosphate
UEA	University of East Anglia
UGT	UDP-glucuronosyl transferase
UK	United Kingdom
USA	United States of America
UV	Ultraviolet light
Vps34	Vacuolar protein sorting 34
WT	Wild-type

ACKNOWLEDGEMENTS

Firstly, I am extremely grateful to my primary and secondary supervisors, Dr Yongping Bao, Professor Aedín Cassidy and Professor Tom Wileman for their help and support throughout the duration of my research project and the completion of this thesis. In addition, I would like to thank all members of the Bao lab group, especially Wei Wang, for their assistance and reassurance over the past years, as well as all other members of the Department of Nutrition. A special thanks to my bench neighbours Wouter Hendrickx and Michael Edwards for their wonderful support. Equally, I am grateful to all members of both the Wileman and Robinson lab group for their lending hands and time for fruitful discussions.

I would like to thank Bertalan Bicsak for the collaboration and David Vauzour for teaching me how to work with primary neuronal cells. Also, big thanks go out to Darren Sexton and Andy Goldson for helping with anything concerning flow cytometry.

I know I am deeply indebted to Jasmine Buck, Fiona O'Neill and Christina Stratford for their support and comfort, celebrating the highs and fighting through the lows of our UEA experience together. Also a special thanks to Johanna Nader for sharing her home with me during my follow up visits in Norwich.

Being part of the UEA women's basketball team gave me the necessary balance to life in the lab. Thanks, fellow panthers - players and coaches - for the fun and the good exercise, and for the trophy collection we managed to achieve together.

I am much indebted to the support of my boss and colleagues at the Millennium Apotheke in Vienna throughout the write up of the thesis.

Finally, I would like to thank my favourite Mom, Dad and brother, as well as my family in Minnesota, California and Arizona, US, and in Brighton, UK, plus my friends back home in Vienna, Austria, for their visits and continuous support and belief in me, without which I would have not been able to complete this thesis.

1 INTRODUCTION

1.1 SULFORAPHANE

1.1.1 GENERAL INTRODUCTION

Since the 1990s, epidemiological and human intervention studies have suggested an inverse association between the intake of plant foods like turmeric, garlic or cabbage, and risk of cancer or a number of other chronic diseases (Surh 2003; Ferrari et al. 2010). A variety of phytochemicals, i.e. chemicals naturally occurring in plants, have been shown to enhance the metabolism and elimination of xenobiotics, like drugs, pesticides or carcinogens, thus antagonising their carcinogenicity (Zhang et al. 1992).

Cruciferous vegetables (CV) of the family *Brassicaceae* have become a research area of particular interest, since they have been associated with a reduced risk of development of a range of cancers (Verhoeven et al. 1996; Talalay & Fahey 2001). Such vegetables include broccoli, cabbage, kale, Brussels sprouts, cauliflower, mustard, wasabi, cress and radish (Verkerk et al. 2009; Fahey et al. 2001; Fimognari et al. 2008). They contain many beneficial dietary compounds, such as vitamin C, carotenoids, fibre, flavonoids and glucosinolates (McNaughton & Marks 2003). The sulphur containing glucosinolates are present in almost every CV and are responsible for their distinct aroma (Fahey et al. 2001; Vermeulen et al. 2006). Anticarcinogenic properties of CVs were first reported in the 1980s (Albert-Puleo 1983). A decade later, sulforaphane (SFN) was identified as the chemical primarily responsible for the bioactivity of broccoli, leading to further research in this area (Dinkova-Kostova & Kostov 2012; Zhang et al. 1994; Zhang et al. 1992). Studies on the molecular targets of SFN have led to a greater understanding of its mechanism of action. SFN shows a range of potential therapeutic effects and therefore is a potential candidate for therapeutic use in humans (Guerrero-Beltrán et al. 2010).

One CV can contain several glucosinolates, some with "anti-nutritional" properties, such that their inclusion in the diet can reduce the nutritional value of a meal (Griffiths et al. 1998). For example, the hydrolysis of β-hydroxyalkenyl glucosinolates creates β-hydroxyalkenyl isothiocyanates, which can further cyclise to oxazolidine-2-thiones - which may have goitrogenic effects (Fahey et al. 2001). Conversely,

"nutritional" or "functional" glucosinolates may have therapeutic and prophylactic properties (Fahey et al. 2001). Over 120 different glucosinolates have been identified in cruciferous plants, however few occur in dietary crucifers (Juge et al. 2007). Glucosinolates are β-thioglucoside N-hydroxysulfates with a side chain (R) and a sulphur-linked β-D-glucopyranose moiety (Fahey et al. 2001).

Glucosinolates, as opposed to their metabolites, are mostly biologically inactive (Vermeulen et al. 2006). In plants, they are accumulated in vacuoles in close proximity to myrosin cells, which are separate cells with vacuoles containing the enzyme myrosinase (Kissen et al. 2009). A natural defence mechanism is activated by cutting, grinding or chewing of plant tissue, when myrosinase is released and hydrolyses the glucosinolates into isothiocyanates (ITCs) and other metabolites (Fimognari et al. 2008; Kissen et al. 2009). ITCs are considered the major metabolite at pH 5-8, whilst at pH 2-5 in the presence of Fe^{2+} or guided by the heat-sensitive epithiospecifier protein (ESP) mostly nitriles and elemental sulphur are produced, and at pH >8 thiocyanates are generated **(Figure 1)** (Fimognari et al. 2008; Grubb & Abel 2006; Matusheski et al. 2004).

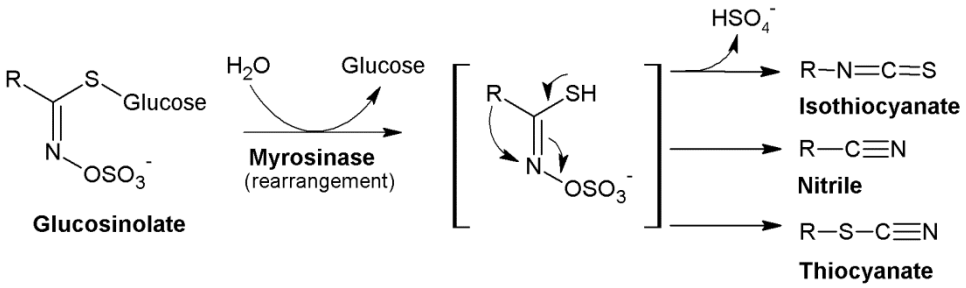

Figure 1: Metabolism of glucosinolates to their break down products.
Myrosinase catalyses the hydrolysis of glucosinolates to different end products, such as isothiocyanates, nitriles, or thiocyanates; depending on the reaction conditions. Adapted from (Dinkova-Kostova & Kostov 2012).

Cooking vegetables or applying pressure, which is often performed to inhibit activity of microorganisms and spoilage enzymes and therefore enhance storage life (preferably without affecting the quality of the product), inactivates myrosinase (Ghawi et al. 2012). Exposure to temperatures between 35°C and 70°C, for a duration as short as three minutes, has been shown to reduce myrosinase activity considerably in broccoli (Ludikhuyze et al. 1999; Oliviero et al. 2014) or green cabbage (Ghawi et al. 2012). High pressure-thermal inactivation has presented

synergistic as well as antagonistic effects at pressures below 200MPa, which may also differ between *Brassica* species (Ghawi et al. 2012).

In humans, glucosinolates are metabolised to ITCs by the bacterial flora of the gastrointestinal tract, although their activity is considerably less than that of myrosinase (Fahey et al. 2001; Shapiro et al. 2001; Lampe & Peterson 2002). After absorption, ITCs are conjugated to glutathione and are eliminated through the mercapturic acid pathway **(Figure 2; shown for the example of SFN)** (Vermeulen et al. 2008).

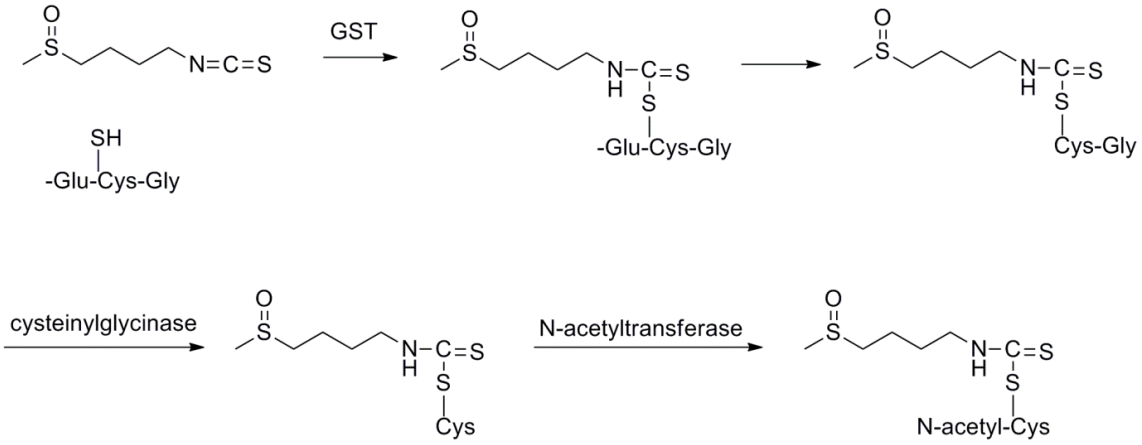

Figure 2: The mercapturic acid pathway shown for SFN

GST, glutathione-S-transferase

1.1.2 SULFORAPHANE AND ITS METABOLISM IN HUMANS

SFN [1-isothiocyanato-4-(methylsulfinyl)-butane] is the primary breakdown product of the glucosinolate glucoraphanin, which is found in cruciferous vegetables such as broccoli, cabbage, kohl rabi and cauliflower **(Figure 3)** (Juge et al. 2007).

SFN is subject to metabolism by glutathione γ-glutamyltranspeptidase, cysteinylglycinase and N-acetyltransferase to form mercapturic acid **(Figure 2)** (Shapiro et al. 2001). This compound can be easily measured in urine by HPLC (High performance liquid chromatography) and UV spectroscopy after cyclocondensation with 1,2-benzenedithiol to form 1,3-benzodithiole-2-thione, and therefore mercapturic acid serves as a reliable biomarker for the measurement of cruciferous vegetable intake (Fimognari et al. 2008).

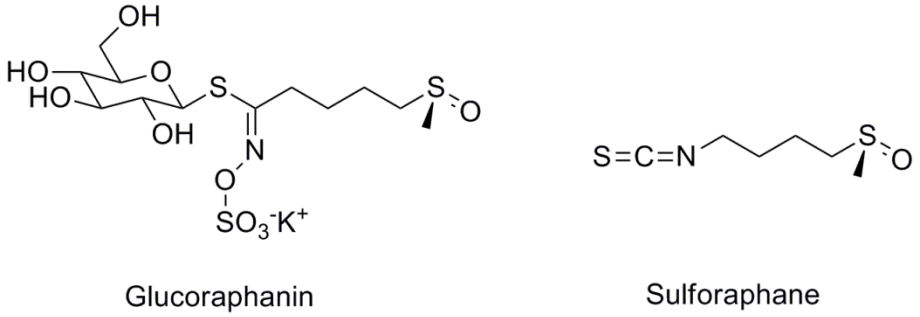

Figure 3: Chemical structures of glucoraphanin and sulforaphane.

1.1.3 BIOAVAILABILITY OF SULFORAPHANE

Ye *et al* (2002) performed the first human study of bioavailability of SFN, in which four volunteers consumed a single dose of 200μmol of ITCs obtained from broccoli sprouts. A peak concentration of 0.9-2.3μmol/l ITCs was detected in plasma, serum and erythrocytes 1 hour after consumption, with a half-life of 1.8h. At 8h, elimination of 58% of the dose was detected, whilst clearance in urine was 369±53ml/min, indicating active renal tubular secretion (Ye et al. 2002). During this study, a reliable and sensitive method to determine ITC levels in plasma and blood was created (Ye et al. 2002). All metabolites generated during the mercapturic acid pathway (Figure 2) belong to the class of dithiocarbamates (DTC), which can be quantified as their cyclocondensation product with 1,2-benzenedithiol by spectroscopy. As ITCs are rapidly and completely converted to DTCs in human tissues, this can be a very useful

analytical method, although it does not distinguish between ITCs and DTCs (Ye et al. 2002).

A more recent human randomised blinded cross-over study compared the bioavailability of broccoli sprouts and a broccoli supplement (Clarke et al. 2011). Consumption of six supplement pills (containing 121µmol glucoraphanin) by study subjects produced peak plasma concentrations of total SFN metabolites after 6 hours, whilst intake of 40g of broccoli sprouts (containing 150µmol glucoraphanin) resulted in a peak of total SFN metabolites after 3 hours and at a 7-fold higher concentration than the supplement pills, which did not contain any myrosinase. Urinary excretion of SFN metabolites following consumption of broccoli sprouts peaked between 3 and 6 hours, in contrast to a delayed excretion of later than 6 hours following consumption of the supplements (Clarke et al. 2011).

A number of studies in humans have shown significant differences in bioavailability, absorption and excretion kinetics depending on the cooking or storage method of the vegetables. Vermeulen *et al* (2008) observed a peak plasma concentration of SFN from consumption of 200g raw broccoli after 1.6 hours, compared to a peak after 6 hours following intake of cooked broccoli. The amount of ITCs derived from cooked vegetables was 2-10 times lower than from raw vegetables – as long as the raw vegetables were fully chewed. However, even after consumption of raw broccoli, only 37% of sulforaphane mercapturic acid was recovered in urine. This may be because glucoraphanin was not fully converted to SFN, or because SFN was not fully absorbed from the gut (Vermeulen et al. 2006; Vermeulen et al. 2008).

The effect of cooking time and type of cruciferous vegetables on SFN bioavailability has been investigated by several research groups, showing that blanching or short microwaving of ~2 minutes is to be favoured over cooking (Holst & Williamson 2004; Rungapamestry et al. 2007; Saha et al. 2012). Saha *et al* (2012) also presented a comparison between broccoli soup prepared from fresh or frozen broccoli, in which the bioavailability of SFN was tenfold higher for soups made from the former as compared to the latter.

Inter-individual variation in SFN bioavailability has been observed in a number of studies, and can be explained by a polymorphism in the GSTM1 gene, which results in lack of GSTM1-1 protein (Holst & Williamson 2004). A human cross-over study on a single meal of broccoli investigated the pharmacokinetics involved in this

polymorphism and found that GSTM1-null subjects excreted more SFN over 24 hours in urine and plasma, and at a greater rate, than GSTM1-positive individuals (Gasper et al. 2005). This lead to the assumption that GSTM1-positive persons benefit from the consumption of CVs more.

However, contrary to these findings, a nested case-control study in a female Shanghai-based cohort investigated the association between urinary isothiocyanate concentrations and colorectal cancer risk with the potential modifying effect of GST genotypes (Yang et al. 2010). Apart from finding an inverse association between urinary ITCs and colorectal cancer risk, this study also demonstrated that ITCs had protective effects in GSTM1-null patients. Urinary ITC concentration was lower in GSTM1-null women than in women who carried this gene, suggesting that the metabolic clearance rate varies by GST genotype. This supports the theory that individuals with GST deletion may be less efficient in metabolising and eliminating ITCs, and thus can be exposed to higher concentrations of ITCs, with an increased benefit from consumption of cruciferous vegetables in terms of their health-promoting effects (Lampe & Peterson 2002; Holst & Williamson 2004; Yang et al. 2010). The difference found in metabolic clearance rate and thus the different theories on GSTM1 being beneficial in reducing cancer risk can amount to the Chinese study being a population study, compared to a feeding study. A prolonged feeding study might reflect habitual dietary intake among populations that consume CVs routinely (Lampe 2009). These different results indicate that further understanding is necessary on how genotype influences the disposition of ITCs.

Of interest, more recent human bioavailability studies of SFN following r broccoli consumption have showed a bioconversion of SFN into erucin (ERN), another isothiocyanate (Vermeulen et al. 2006; Clarke et al. 2011; Tarozzi et al. 2013). A mouse study found this conversion to be tissue dependent, with a higher ratio of ERN in the liver, kidney and bladder, even when feeding SFN alone (Bricker et al. 2014). Although investigations into possible differences into the bioactivities of SFN and ERN exist, it is still not clear whether this conversion is important for the beneficial effects of glucosinolates (Jana Jakubikova et al. 2005; Tarozzi et al. 2013; Bricker et al. 2014).

1.1.4 BIOACTIVITY OF SULFORAPHANE

The bioactivity of SFN has been investigated in numerous studies, as outlined in the following sections. To date, induction of phase II enzymes by SFN is the most comprehensively researched effect of this compound.

A) Effects on detoxification enzymes.

Phase I enzymes – modification

Cytochrome P-450 (CYP) enzymes (phase I enzymes) are essential components in the metabolic pathways of numerous endogenous compounds, but may also cause the activation of carcinogens (Skupinska et al. 2009). SFN is known to inhibit several CYP enzymes such as CYP1A1, 1A2, 2B1/2, 2E1 and 3A4. CYP 3A4 is among the most important enzymes of the P-450 family, as it contributes to the metabolism of over 50% of clinically used drugs and xenobiotics (Gross-Steinmeyer et al. 2010). The nuclear hormone receptor, steroid and xenobiotic receptor (SXR), is one of the most important mediators of CYP 3A4 expression. SFN has been shown to inhibit SXR-co-activator interactions by binding directly to SXR (Fimognari et al. 2008).

Phase II enzymes – conjugation

As noted, the effect of SFN on phase II enzymes has been extensively studied. SFN is known to induce genes encoding phase II enzymes, which metabolise a variety of reactive carcinogens, mutagens and other toxins. These genes include those encoding NAD(P)H:quinone oxidoreductase (NQO1), GSTs, uridine 5-diphosphate-glucuronosyl transferase, ferritin, γ-glutamate-cysteine ligase, epoxide hydrolase and catalase. An increase in levels of the NR-E2-related factor 2 (Nrf2) transcription factor activity is thought to be responsible for induction of these genes (Fimognari et al. 2008). Under normal conditions, Nrf2 is bound tightly to the Kelch ECH associated protein 1 (Keap1), which results in ubiquitination and proteasomal degradation of Nrf2 (James et al. 2012). ITCs can react with the sulfhydryl groups of Keap1, liberating Nrf2, which then translocates into the nucleus and binds to the antioxidant response element (ARE), activating the transcription of phase II enzymes **(Figure 4;** a more detailed graph is presented in

Figure 13, p.44) (James et al. 2012; Dinkova-Kostova et al. 2002; Dinkova-Kostova & Talalay 2008).

Dinkova-Kostova *et al* (2007) have investigated the relationship between SFN and phase II enzymes in mouse and human skin after topical application of broccoli sprout extract, and detected an induction of NQO1 in humans and of NQO1, GST A1 and heme oxygenase (HO-1) in mice. Statistical analysis demonstrated increases of 1.5 – and 2.7-fold in mouse and 1.5- and 4.5-fold in humans after application of single and multiple doses (Dinkova-Kostova & Talalay 2008). An induction of phase II enzymes like transferases and catalases could also be found in liver, prostate, kidney and colon (Fimognari et al. 2008; Cheung & Kong 2009).

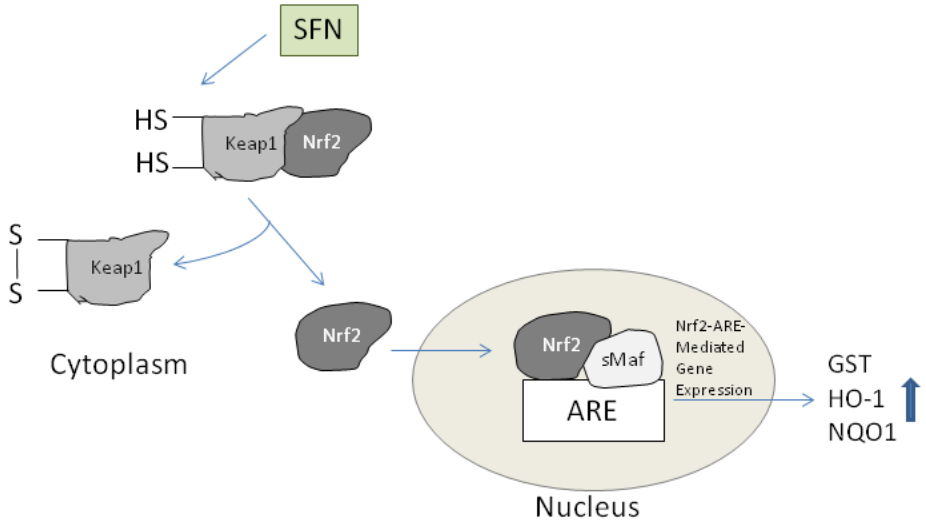

Figure 4: Overview of modulation of Keap1/Nrf2 by SFN
By modulating Keap1 via their sulfhydryl groups, Nrf2 is released from Keap 1 and translocates into the nucleus, where it binds to the ARE to activate the transcription of phase II enzymes. Nrf2, NR-E2-related factor 2; Keap1, Kelch ECH associated protein 1; ARE, antioxidant response element; sMaf, small musculoaponerotic fibrosarcoma; GST, glutathione-S-transferase; HO-1, hemeoxygenase-1; NQO1, NAD(P)H:quinone oxidoreductase.

A study by Zhao *et al.* (2007) has investigated the protective effects of SFN upon the permeability of the blood brain barrier (BBB). Using a rodent model of brain injury, it was demonstrated that through activation of Nrf2 regulated genes such as like GST and HO-1, the vulnerability of the BBB to injury is reduced by SFN. The loss of endothelial cell markers as well as tight junction proteins, which are the

two most critical components of the BBB, could be reduced by administration of SFN after brain injury.

SFN has been found to protect primary cultures of mouse cortical neurons from 5-S-cysteinyl-dopamine-induced neurotoxicity. Concentrations between 0.01-1μM SFN modulated the Keap1/Nrf2 pathway, leading to an increased expression of GST, TR-1 and NAD(P)H oxidoreductase (Vauzour et al. 2010).

Phase III transporters – transport and excretion

Phase III transporters belong to a family of ATP-binding cassette membrane transport proteins which are also called multidrug resistance proteins. As they transport not only unmetabolised drugs and endogenous substrates, but also products of phase I and II drug metabolism, they have been termed phase III of the detoxification system (Harris & Jeffery 2008). SFN is known to regulate the phase III transporters P-gp (P-glycoprotein) and MRP (multidrug resistance protein 1), which contribute, in part, to the detoxification of many xenobiotics (Fimognari et al. 2008; Harris & Jeffery 2008).

B) Cell cycle

Cell division is classified into two stages: mitosis (M) and interphase, which itself can be further divided into G1, S and G2 phases. The cell cycle is controlled by several mechanisms to ensure correct cell division (Vermeulen et al. 2003). Impairment of these mechanisms can lead to disease, thus the cell cycle has been investigated in relation to cancer, as alterations in genetic control may lead to unrestrained cell proliferation (Vermeulen et al. 2003). This mechanism represents an important target in the treatment of cancer as well as other diseases.

Research on SFN in the cell cycle has shown mostly induction of G1 or G2/M cell cycle arrest (Parnaud et al. 2004; Pledgie-Tracy et al. 2007; Shan et al. 2006; J Jakubikova et al. 2005), but in some cell lines S-phase induction has also been reported. A study investigating the effects of broccoli sprout extract on human bladder cancer UM-UC-3 cells has shown that 7.5-30μM extract leads to arrest in both S and G2/M phases (Tang et al. 2006).

C) Apoptosis

Lower concentrations of SFN have been shown to induce early apoptosis in human bladder cancer T24 cells (Shan et al. 2006). Pledgie-Tracy *et al* (2007) have reported that SFN induces apoptotic cell death in breast cancer cells; and studies in blood, brain, colon, ovary, pancreas, prostate and skin cancer cell lines have documented the ability of SFN to induce apoptosis (Zhang & Tang 2007).

The pre-treatment of SH-SY5Y cells, a neuronal-like cell line derived from a human neuroblastoma, with SFN before the addition of 6-hydroxydopamine (6-OHDA) resulted in a reduction in several apoptotic events such as mitochondrial depolarisation, caspase 3 and 9 activation and DNA fragmentation, as well as necrosis (Tarozzi et al. 2009). In healthy SH-SY5Y cells, SFN was able also prevent apoptosis.

D) Autophagy

Autophagy is a pathway mainly activated through starvation to degrade unnecessary cell organelles and consequently replenish the cells with amino acids and other small molecules. It is an important mechanism for cell homeostasis, and impaired autophagy is linked to many illnesses including neurodegenerative diseases (Rubinsztein et al. 2005; Pan et al. 2008). A study in 2006 first reported that SFN could induce autophagy as a human defence mechanism against SFN-induced apoptosis (Herman-Antosiewicz et al. 2006). This research was conducted using the human prostate cancer cell lines PC-3 and LNCaP. Subsequently, Nishikawa *et al* (2010) observed induction of autophagy after treatment with SFN, in the human colon cancer cell line WiDr.

Autophagy is discussed in more detail in Chapter 1.4.

E) NF-κB pathway

The nuclear factor kappa B (NF-κB) pathway has been linked to inflammation, cancer cell survival and progression, as this transcription factor binds to the promoter of many pro-inflammatory genes such as those encoding cyclooxygenase (COX-2), tumour necrosis factor a (TNF-a) and inducible nitric oxide synthase (iNOS) (Cheung et al. 2009). COX-2 is the key enzyme in the production of prostaglandins from arachidonic acid, and prostaglandins are

central mediators of inflammation (Tsatsanis et al. 2006). Over-expression of COX-2 too has been associated with human bladder cancer (Shan et al. 2009). Shan *et al* (2009) reported that SFN inhibits the binding of NF-κB to the COX-2 promoter, leading to down-regulation of COX-2 expression in human bladder cancer T24 cells. The exact mechanism by which SFN inhibits the pathway is not yet established, but it may block the "inhibitor of κB"-kinase (IκK), which is an upstream enzyme of NFκB (Cheung & Kong 2009).

F) Cell proliferation and mitosis

The potential beneficial effects of SFN upon reproduction of viable cells has also been the focus of several studies. Zanichelli *et al* (2011) observed increased proliferation in human mesenchymal stem cells after intake of low doses (0.25μM and 1μM) of *R*-SFN. However, higher doses (5μM and 20μM SFN) had a cytotoxic effect. In the breast cancer cell lines MCF7 and SUM159, SFN elicited antiproliferative effects with IC_{50} (half maximal inhibitory concentration) values of 16μM and 10μM SFN respectively (Li et al. 2010). Azarenko *et al* (2008) have discovered that the mechanism by which SFN elicits inhibition of mitosis is effective suppression of microtubules dynamics and stabilisation of microtubules.

G) Dopaminergic cells

Han *et al* (2007) demonstrated that SFN can protect dopaminergic (DAergic) cells from the cytotoxicity of tetrahydrobiopterin (BH4) and 6-OHDA, both compounds known to generate oxidative stress and cause selective death of DAergic cells. SFN does not protect DAergic cells from MPP^+-induced toxicity. MPP+, unlike the compounds mentioned above, does not produce DA quinone as its principle mechanism of toxicity. This suggests that SFN may elicit a protective effect in DA cells from toxicity resulting from quinone generation (Han et al. 2007).

H) Serotonin Receptor

Mastrangelo *et al* (2008) reported that SFN at 5, 10 and 20μM dose-dependently down-regulated the serotonin receptors $5HT_{1A}$, $5HT_{2C}$ and $5HT_{3A}$ in Caco-2 cells after exposure to SFN for 48 hours. In contrast, nAChR (Nicotinic acetylcholine receptor) was up-regulated after exposure to SFN. Previous studies have shown that induction of neurotransmitter receptors plays a role in the progression of

colon cancer cells like HT-29 (Mastrangelo et al. 2008). To our knowledge, only one study has explored the interaction between SFN and serotonin.

I) Antibiotic activity against *Helicobacter pylori*

Several researchers have documented activity of SFN as an antibacterial agent against *Helicobacter pylori* (Fahey et al. 2002; Haristoy et al. 2003; Yanaka et al. 2009). Studies in mouse models as well as human interventions have shown SFN to have both a direct antibacterial effect on *H. pylori* and an indirect, systemic effect by accessing the cytoprotective phase II response via Nrf2, as explained above (Yanaka et al. 2009). Direct effects in humans were explained by the activity of both glucoraphanin and its bioactive metabolite SFN on the gastric membrane mucosa, thus reducing gastritis. Since *H. pylori has been linked to the progression of stomach cancer, t*he findings support the suggestion that SFN can act as a dietary prophylactic agent against the development human gastric cancer (Yanaka et al. 2009).

Thus, SFN is a powerful phytochemical that can activate multiple molecular targets resulting in detoxification of a variety of carcinogens. SFN may also act to protect cells from neurotoxins, demonstrate antibiotic activity, and induce early apoptosis as well as autophagy **(Figure 5)**. However, these effects are not yet fully understood, and to date have been subject to limited investigation in neuronal cells. Hence, the research focus of this study was neuronal cells.

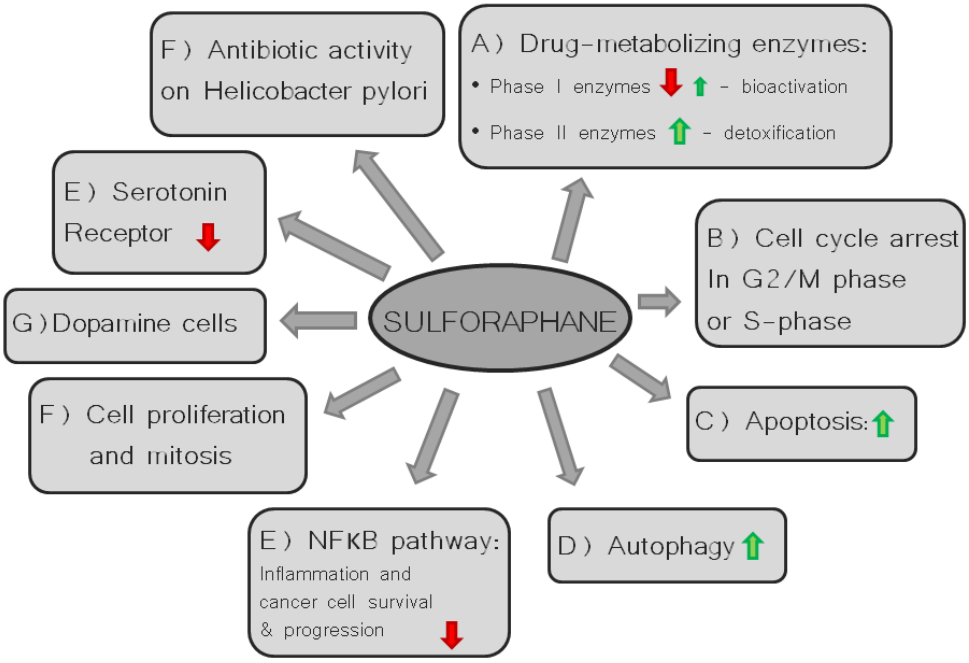

Figure 5: Overview of bioactivity of SFN
This graph highlights pathways which are influenced by SFN. Green arrows indicate an upregulation, while a red arrow shows a decrease.

1.2 NEURODEGENERATIVE DISEASES

Neuronal cells are electrically excitable cells that transmits information through electrical and chemical signals. They are the most important element of the central nervous system (Loeffler G. 2003).

1.2.1 CENTRAL NERVOUS SYSTEM

The central nervous system (CNS) is responsible for converting external stimuli as registered by the sensory organs into sensation, the control of motor skills, as well as the coordination of many vital functions (Loeffler G. 2003). It consists of the brain and the spinal cord.

The BBB isolates the CNS from the blood stream and thus from the rest of the body, and protects the nervous system from fluctuations in metabolism as well as from exposure to toxins. The major components of the BBB are a layer of brain capillary endothelial cells and the contiguous tight junctions between them (Zhao et al. 2007). Gases like O_2 and CO_2 and a wide range of lipid-soluble molecules (subject to factors such as molecular weight or number of rotatable bonds) can passively diffuse across the BBB (Abbott et al. 2010). Other essential substances such as amino acids must pass through this barrier by active transport (Loeffler G. 2003).

The integrity of the BBB is essential for maintaining brain function and homeostasis (Zhao et al. 2007). Several diseases such as stroke, epilepsy, brain tumours, and neurodegenerative diseases like Alzheimer's disease (AD) and Parkinson's disease (PD) have been associated with a dysfunctional BBB (Abbott et al. 2010). As noted above, SFN has been reported to protect endothelial cells of the BBB by increasing expression of Nrf2-regulated genes including HO-1 and GST (Zhao et al. 2007).

In order to elicit possible protective effects in neurodegenerative conditions or improve brain function, SFN should penetrate the BBB and accumulate in the CNS. According to Benedict *et al.* (2012) SFN is able to pass through the BBB in rats. This was also observed in various other animal models (Tarozzi et al. 2013).

1.2.2 NEURODEGENERATIVE DISEASES

Neurodegenerative diseases (NDs) can be characterised by a progressive loss of neuronal cell function or even cell death. As NDs are age-related and the elderly proportion of the population in developed countries is growing, the reported incidence of NDs is also increasing (Melo et al. 2011). Although many theories have been proposed, the underlying mechanisms of neurodegeneration remain unknown. Most neurodegenerative disorders are late-onset, progressing slowly, and clinical research suggests they have long asymptomatic phases before the first signs of illness appear (Golde 2009).

Parkinson's Disease (PD) is mainly characterised by a loss of dopaminergic cells in the substantia nigra, which is located in the midbrain and involved in the regulation of movement, but also by accumulation of the a-synuclein protein in specific brain regions (Lees et al. 2009). Through the reduction in dopamine production – typically a PD patient has lost 80% of dopamine-producing cells – the motor nervous system is unable to control coordination and movement (Zlokovic 2008). Symptoms of PD include muscle tremor, stiffness, and slow movement or inability to move, together with psychological symptoms such as insomnia, depression, and fatigue (Lees et al. 2009). PD is the second most common neurodegenerative disease, affecting approximately 6.3 million people worldwide and 120,000 in the UK (www.parkinsonsawareness.eu.com 2012; European Brain Council 2011). The age of onset of PD is usually over 60 years, but 10% of patients are diagnosed in their 40s or earlier (EuroPa 2014; Lees et al. 2009). Although most cases are sporadic, several genes have been linked to familial PD, such as the genes encoding Parkin, a-synuclein, PINK1, DJ-1 and LRRK-2 (Lees et al. 2009). To date, no cure is available, although levodopa and dopamine agonists can reduce symptoms of PD by replacing the lost dopamine. Dopamine itself cannot be used, since it cannot pass the BBB (Loeffler G. 2003).

In **Alzheimer's Disease** (AD), the synthesis of acetylcholine is reduced. AD is the most common form of dementia. Long-term memory loss, confusion and mood swings are the classic symptoms of AD. In 2011, over 600,000 cases were estimated in England (alzheimers.org.uk 2012). More than 25% of the population over 85 years old are believed to suffer from AD in Germany (Loeffler G. 2003). AD is typified by two classic changes within the brain; firstly an extraneuronal accumulation of

amyloid plaques consisting of β-amyloid peptide, and secondly intraneuronal deposits of neurofibrillary tangles composed of hyperphosphorylated tau protein (Lee et al. 2013). Although hardly distinguishable from sporadic AD in terms of phenotype and clinical manifestation, 5-10% of AD cases have been estimated to be genetic (Selkoe 2001). AD has been described as a multifactorial disease involving a variety of molecular triggers, including synaptic failure, mitochondrial dysfunction, inflammation, loss of calcium regulation and faulty cholesterol metabolism (Querfurt & LaFerla 2010). As with PD there is currently no curative therapy for AD, but acetylcholinesterase inhibitors such as donezepil or galantamine can retard the degenerative process.

Huntington's Disease (HD) is a neurodegenerative disease resulting from mutation of the "Huntington's gene", which encodes the protein huntingtin (Ross & Tabrizi 2010). According to the Huntington's Disease Association, over 6,000 patients in the UK have reported symptoms of HD (www.nhs.uk 2011). HD patients display random, uncontrollable movements (chorea), abnormal posture and difficulties in chewing and speaking. The symptoms usually develop in people between 30-50 years of age, progressing to death within 15-20 years (Walker 2007; Ross & Tabrizi 2010; Krobitsch & Kazantsev 2011). At present only symptomatic drug therapy is available. The chorea can be reduced by benzodiazepines, neuroleptics and tetrabenazine, while rigidity can be alleviated by levodopa or baclofen. However, use of all of these medications may also result in severe side effects (Ross & Tabrizi 2010). Research is therefore focusing on finding suitable biomarkers to investigate early-intervention strategies (Walker 2007).

One of the most common neuromuscular diseases is **Amyotrophic Lateral Sclerosis** (ALS), also known as Lou Gehrig's disease or Motor Neuron Disease (MND). ALS results from death of both upper and lower motor neurons. Muscle weakness and atrophy spread throughout the body, eventually affecting moving, swallowing and forming words. Worldwide, between 0.4 and 1.8 persons per 100 000 population develop ALS, although Guam is a notable exception with a 50 times higher prevalence (Europe 2014). The cause for this higher incidence of ALS may be environmental, as a seed of plant *Cycas cicinalis* L. is a traditional source of food and medicine in this country, but also contains a potent neurotoxin (Spencer et al. 1987). The age of onset of ALS is 40 to 70 years, with an average age of 55 at

diagnosis (Europe 2014). The drug riluzole reduces damage to motor neurons by activating the glutamate transporter and to date is the only treatment known to improve survival; however, it cannot repair damage already sustained by motor neurons (Europe 2014).

1.2.3 NEUROTOXICITY AND NEUROPROTECTION

As there are no known curative treatments for neurodegenerative diseases, current scientific research is focussed on investigating mechanisms of neuroprotection as well as neurotoxicity. However, without knowing the underlying mechanisms of cell death in NDs, it is challenging to establish targets for treatment (Melo et al. 2011). Dietary phytochemicals may represent a potential source of neuroprotective agents. Melo *et al.* (2011) have reviewed the role of oxidative stress in NDs, and discussed recent developments including clinical trials undertaken with several potential neuroprotective agents such as antioxidants, metal chelators and antiglutamatergic agents. Selegiline and rasagiline, which are selective monoamino oxidase B (MAO B) inhibitors, are the most promising drugs in PD tested in clinical trials, (Melo et al. 2011).

SFN has been shown to have neuroprotective effects in a number of animal models and in *in vitro* studies, using 6-OHDA and H_2O_2 as toxins to induce neuronal cell death (Guerrero-Beltrán et al. 2010). Most of the studies in that review observed a relationship between the induction of Nrf2 and cell protection (Innamorato et al. 2008; Soane et al. 2010; Vauzour et al. 2010).

1.3 NEURONAL CELL LINES

As neurodegenerative diseases are increasing in prevalence in the developed world, with no effective curative treatments available, animal and *in vitro* studies are important to gain insights into the mechanism underlying these diseases (Biedler et al. 1973). The following cell lines are of special value to the study of neuronal cells.

PC-12

Shape: round, elliptical, clumpy

Size: 5-31 µm

Cell cycle: 3-5 days

1.3.1 PC-12

Amongst all neuronal cell lines, the PC-12 cell line is one of the most studied to date (Green 1995). This line was cloned by Greene and Tischler (Greene & Tischler 1976) from a rat pheochromocytoma. In culture medium containing serum PC-12 cells undergo mitosis and show some properties of adrenal chromaffin cells. The cells are also able to synthesise acetylcholine and the catecholamines dopamine and norepinephrine, but not epinephrine (Greene 1978; Greene & Tischler 1976). When nerve growth factor (NGF) is added to culture medium, neurite outgrowth can be seen after about 7 days (**Figure 6**; Das et al. 2004).

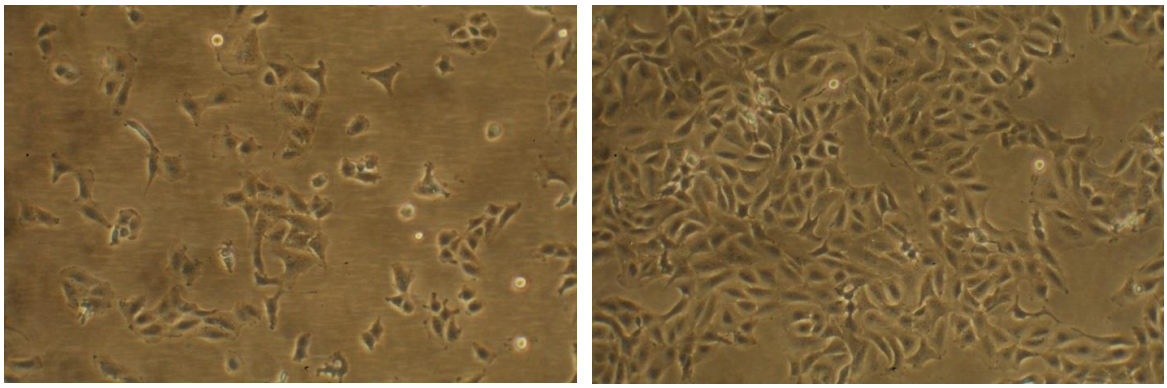

Figure 6: PC-12 cells day 1 and day 2 after seeding.

NGF is known to have a variety of effects on neurons, including increase in cell size, induction of certain enzymes involved in neurotransmitter synthesis and the stimulation of neurite outgrowth as well as increasing the survival of these neurones (Greene 1978).

As PC-12 cells have been utilised in scientific research for many years, a number of different cell culture protocols have been developed. Most employ a culture medium of DMEM (Dulbecco's Modified Eagle Medium) or RPMI 1640 (Roswell Park

Memorial Institute 1640) with glutamine, supplemented with heat-inactivated horse serum, foetal bovine serum and penicillin/streptomycin, at varying percentages. Cultures are maintained at 37°C with 5% (v/v) CO_2, and for experimental purposes the cells are used at 70-80% confluency (Aykin-Burns et al. 2005; Das et al. 2004; Fujii et al. 1982; Green 1995; Robinson & McGee Jr. 1985; Sadasivan et al. 2006).

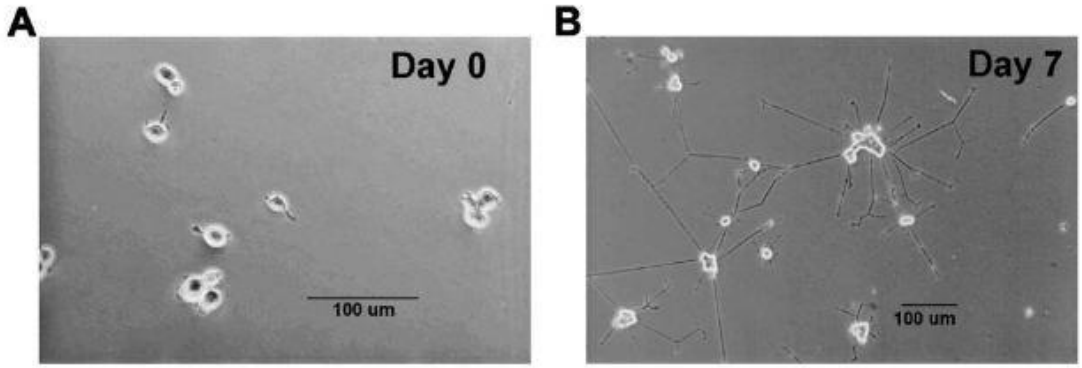

Figure 7: PC-12 cell differentiation observed following treatment with NGF after 0 (A) and 7 days (B) (Das et al. 2004).

1.3.2 SH-SY5Y

SH-SY5Y

Shape: round, elliptical

Cell cycle: 7-8 days

Number of generations after isolation: 20

In the early 1970s, SK-N-SH cells were established from a bone marrow biopsy of a neuroblastoma patient (Biedler et al. 1973). The SH-SY5Y cell line is a thrice cloned subline of the neuronal phenotype (N type) of SK-N-SH (Ciccarone et al. 1989). Culture medium for SH-SY5Y is composed of DMEM or MEM:F12 Ham 1:1 (Eagle's Minimum Essential Medium : Ham's F12 Medium) plus 10% (v/v) fetal bovine serum and penicillin/streptomycin.

The SH-SY5Y cell line shows many characteristics of dopaminergic neurons and therefore is potentially a useful cell model for PD. Not only do SH-SY5Y cells possess the ability to synthesize dopamine and noradrenaline, but they also can be differentiated into a more distinct dopaminergic neuronal phenotype in the presence of agents such as retinoic acid (Cheung et al., 2009).

Although SH-SY5Y is considered a good cell model for PD and is widely used, this cell line may not be a suitable model when the cells are in an undifferentiated state. Undifferentiated cells do not express high levels of dopaminergic synthetic

enzymes, and display fewer dopamine receptors; also, they are less sensitive to neurotoxins and neuroprotective agents (Xie et al. 2010).

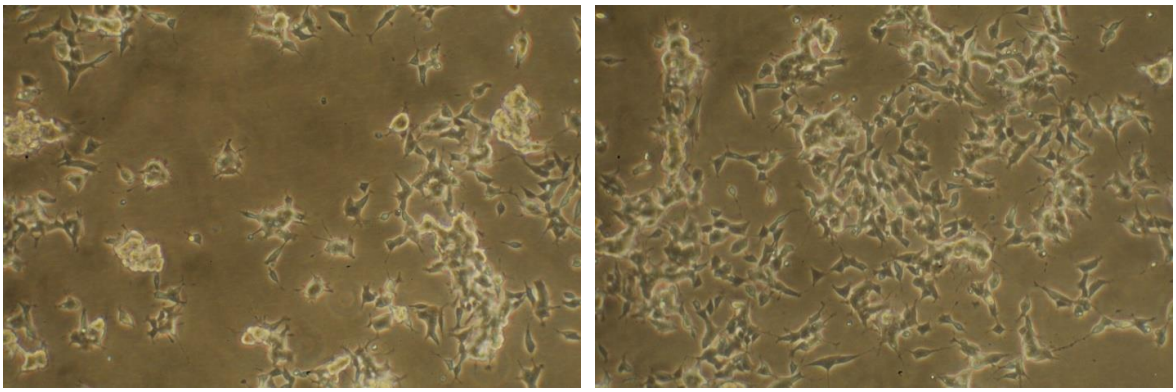

Figure 8: SH-SY5Y cells cultured at low and high density.

Upon differentiation of SH-SY5Y cells, cell proliferation ceases and neurite outgrowth can be observed, with morphological parallels to living neurons in the human brain. Several protocols for differentiation exist, and different agents induce alternative phenotypes which can therefore be used as different neuronal cell models (adrenergic/dopaminergic/cholinergic) (Xie et al. 2010).

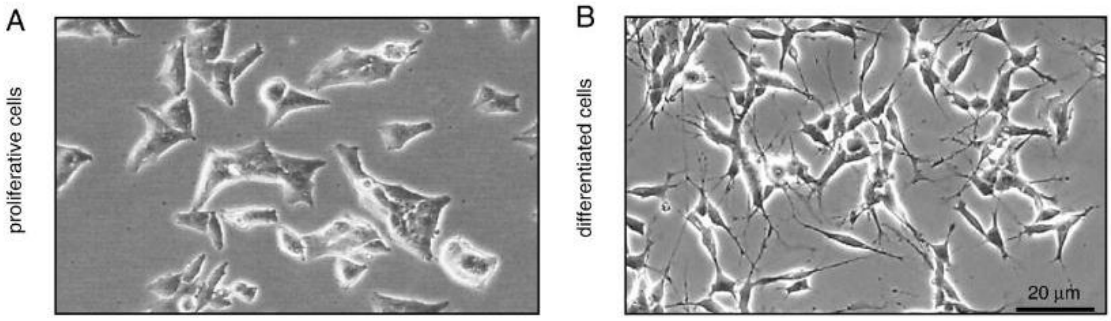

Figure 9: A: SH-SY5Y cells in regular culture medium B: SH-SY5Y cells differentiated with retinoic acid at day7 (Lopes et al. 2010).

1.3.3 PRIMARY NEURONAL CELLS

In contrast to the immortal cell lines mentioned above, primary neuronal cells (PNCs) do not divide in culture. They are plated directly after isolation from animal brain tissue (Gennaro Giordano and Lucio G Costa 2011). These cells are also used to study basic characteristics of neurons and the potential neurotoxicity of chemicals. After plating, PCNs form synapses and become electrically active, demonstrating a neuronal phenotype, before they eventually die (Gennaro Giordano and Lucio G Costa 2011).

The first primary neurons were cultured *in vitro* in the early 1900s, using 'hanging drop' method, which was simple to assemble and suitable for microscopic imaging, but problematic for cell and morphological identification (Millet & Gillette 2012). Many alternative methods have since been developed.

1.4 AUTOPHAGY

As one of the more recent target fields identified for SFN, autophagy has also been associated with neurodegeneration and is therefore a pathway of great interest for this study. Autophagy is one of the main degradation mechanisms within the cell, which is most often triggered by starvation (Rubinsztein et al. 2007). Various forms of autophagy have been identified, which all share the common element of transporting cytoplasmic organelles into the lysosome (Mizushima 2007). The three major types of autophagy in eukaryotic cells are macroautophagy, microautophagy and chaperone-mediated autophagy (CMA), which differ in the mechanism by which cellular components are imported into the lysosome. Some proteins contain certain pentapeptide motifs recognised by a lysosomal receptor protein, which enables these proteins to pass the lysosomal membrane, however a chaperone (CMA) is needed to unfold the substrates (Rubinsztein et al. 2007; Jaeger & Wyss-Coray 2009). In macroautophagy, a double-membrane vesicle (phagophore) sequesters cytoplasm and/or organelles into a double-membrane limited organelle (autophagosome). The autophagosome then fuses with a vacuole/lysosome, in which the contents undergo degradation owing to the acidic environment within the lysosome **(Figure 10)** (Yang & Klionsky 2009). In microautophagy, the lysosome secludes cytoplasmic content without a pre-lysosomal sequestration stage (Rubinsztein et al. 2007). As SFN has been linked to the activation of macroautophagy, it is the most relevant mechanism for this project and will now be referred to as autophagy.

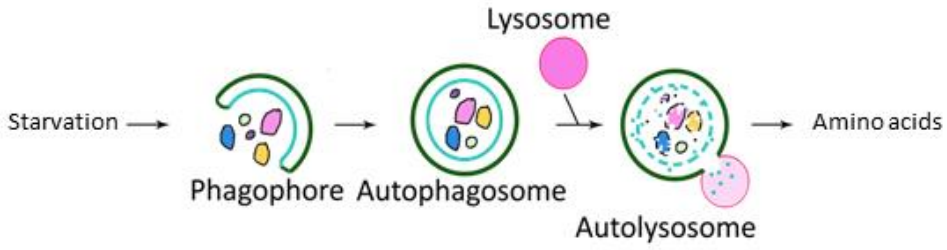

Figure 10: Outline diagram of autophagy.
This diagram shows the formation of the autophagosome in response to starvation, subsequent sequestration of damaged proteins and organelles, and fusion with the lysosome, which results in free amino acids.

The **induction** of autophagy starts with the activation of the Atg1-ULK complex **(Figure 11)**. The association of mTORC1 (TOR complex 1; TOR = target of rapamycin)

with this complex and the activity of mTORC1 is controlled by cellular nutrient status. During starvation, the amount of free amino acids within the cytoplasm is insufficient, which triggers the dissociation of mTORC1 from the ULK1/2 complex, which in turn leads to partial dephosphorylation of Atg13 and ULK1/2 (Yang & Klionsky 2010). **Nucleation** begins with the recruitment of Atg proteins for formation of the phagophore. Atg14, a Beclin1-binding protein and a specific subunit of the PI3K III complex (class III phosphatidylinositol 3-kinase), mediates nucleation of the phagophore membrane. The protein Bcl-2 (B-cell lymphoma 2) prevents this step by binding to and inhibiting Beclin1, another component of the PI3K-complex together with the catalytic subunit Vps34 (vacuolar protein sorting 34) (Yang & Klionsky 2010). Vps34 generates phosphatidylinositol triphosphate (PI3P) necessary for autophagy by targeting PI3P binding proteins, and initiates activation of the first of two ubiquitin-like reactions (Gottlieb & Carreira 2010; Nixon 2013). First, the Atg12-Atg5-Atg16 complex is formed and directed to the phagophore assembly site (PAS) for phagophore elongation (Nixon 2013). Atg7 (a ubiquitin-activating enzyme) and Atg10 (a ubiquitin-conjugating enzyme) mediate the covalent binding of Atg12 to Atg5, which then conjugates with Atg16 to form a tetrameric structure which assembles on the phagophore (Yang & Klionsky 2009; Gottlieb & Carreira 2010). The Atg12-Atg5-Atg16 complex induces a second ubiquitin-like reaction, which involves the removal of the terminal cysteine residue of LC3 (microtubule-associated protein 1 light chain 3; homolog of yeast Atg8) by Atg4, a cysteine protease, to form LC3-I (Klionsky et al. 2011; Nixon 2013). Cytosolic LC3-I is then lipidated by Atg7 (a ubiquitin-activating enzyme) and conjugated to phosphatidylethanolamine (PE) by Atg3 (a ubiquitin-conjugating enzyme) to form LC3-II (Gottlieb & Carreira 2010).

LC3-II is a useful marker of autophagosome formation. Although larger than the LC3-I form, it migrates faster during electrophoresis and is identified at an apparently lower molecular weight (LC3-I at 18kDa and LC3-II at 16kDa) owing to its lipidated state (Cherra 3rd et al. 2010). Alternative methods to assess autophagy are described subsequently (see p.42).

LC3-II is attached to both the interior and exterior of the phagophore, but once **autophagosome** formation is completed it is recycled from the outer membrane by the activity of Atg4, which separates LC3-II from PE (Yang & Klionsky 2009; He & Klionsky 2009). This is followed by fusion of the autophagosome with a lysosome to

form an **autolysosome**. The acidic environment of the lysosome facilitates the degradation of the inner autophagophore membrane, which is mediated by a number of lysosomal acid hydrolases (He & Klionsky 2009). Amino acids and other small molecules which result from the degradative process are transported into the cytosol through permeases, to be utilised in protein synthesis and maintenance of cellular function (Chen & Klionsky 2011).

Vacuole membrane protein 1 (VMP1) also interacts with Beclin1 and is necessary for autophagy, as it localises to the plasma membrane or the endoplasmic reticulum (ER) (Klionsky et al. 2011).

Induction of autophagy. Although the major physiological inducer of autophagy is nutrient depletion, it is also activated as a cellular response to various stress conditions including ER-stress, hypoxia, DNA damage and increased levels of ROS (Kroemer et al. 2010). Figure 12 displays most of the proautophagic pathways and their mechanisms of initiation. Sirtuin1, for example, is a deacetylase that senses environmental stress (Kroemer et al. 2010), while AMPK (5' adenosine monophosphate-activated protein kinase) is modulated by the energy status of the cell according to the AMP:ATP ratio (Efeyan et al. 2015).

Selection of defective cargo. Autophagy has many physiological roles. It is responsible for the disposal of damaged organelles, the turnover of long-lived proteins and the clearance of proteins susceptible to aggregation. Although autophagy is generally considered a nonselective pathway for the degradation of cytoplasmic bulk organelles, some types of selective autophagy also exist (Yang & Klionsky 2009). The protein p62 directly binds poly- or mono-ubiquitin via its ubiquitin-associated domain to LC3 and thus links ubiquitinated organelles to the autophagic pathway for degradation (He & Klionsky 2009; Klionsky et al. 2011). p62 is described in more detail on page 42.

When autophagy is impaired or inactivated, this can result in cytoplasmic protein inclusions composed of misfolded proteins and conglomeration of deformed organelles, which may underlie the development of conditions such as diabetes, myopathy and neurodegeneration (Komatsu & Ichimura 2010).

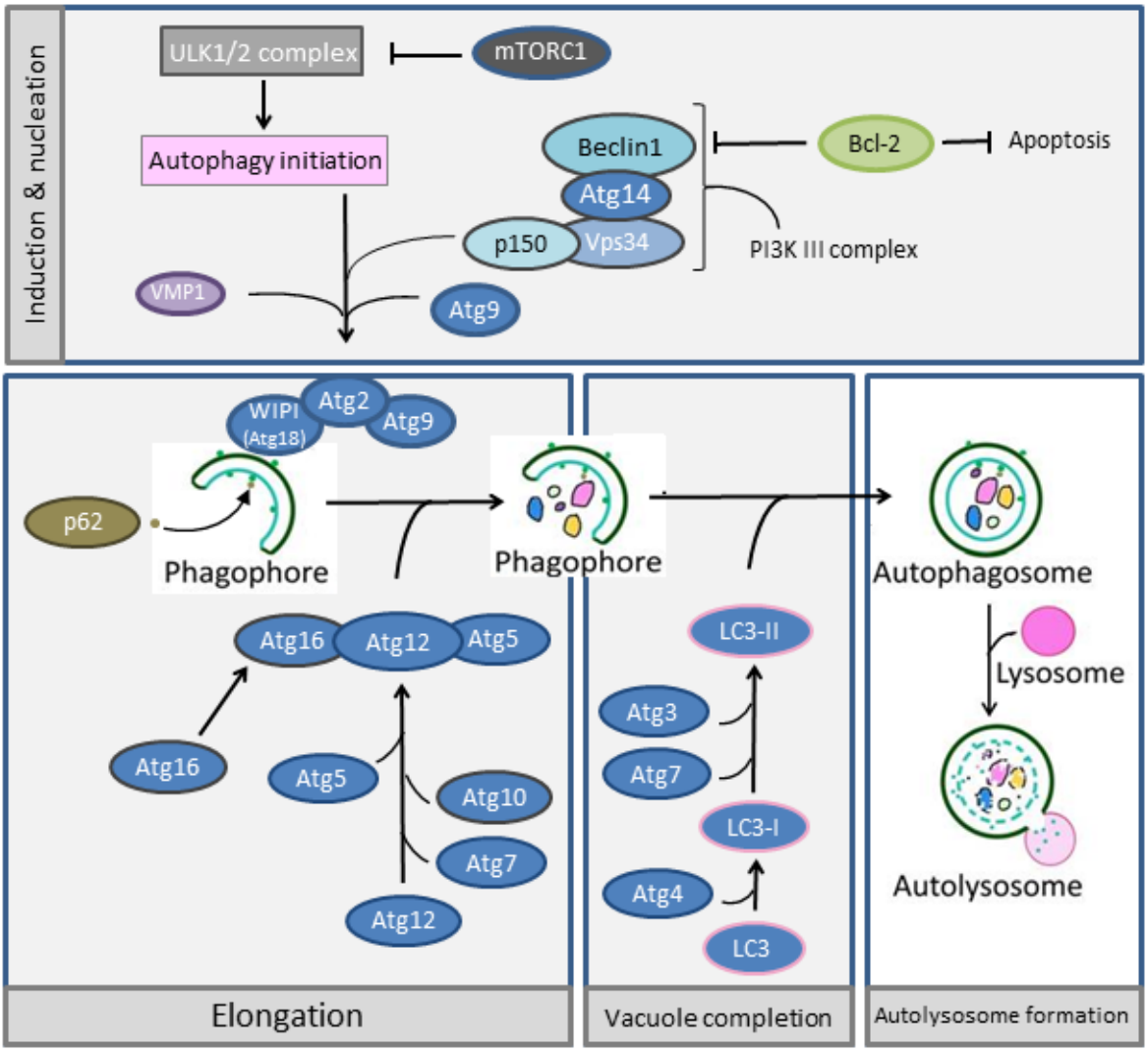

Figure 11: Schematic representation of the major components in the mammalian autophagy pathway.
Autophagy can be divided into induction, elongation and vacuole formation. The Atg proteins (shown in dark blue) can be grouped according to their different functions throughout the pathway. Atg1 (not shown) is important for the formation of the ULK1/2 complex. The Atg12-Atg5-Atg16 complex is necessary for vesicle expansion, while LC3-II (Atg8 in yeast) is involved in the completion of the autophagosome. (Arrows indicate activation, while blunted arrows show inhibition. Adapted from (Yang & Klionsky 2009; He & Klionsky 2009; Yang & Klionsky 2010; Gottlieb & Carreira 2010; Chen & Klionsky 2011; Klionsky et al. 2011; Nixon 2013).

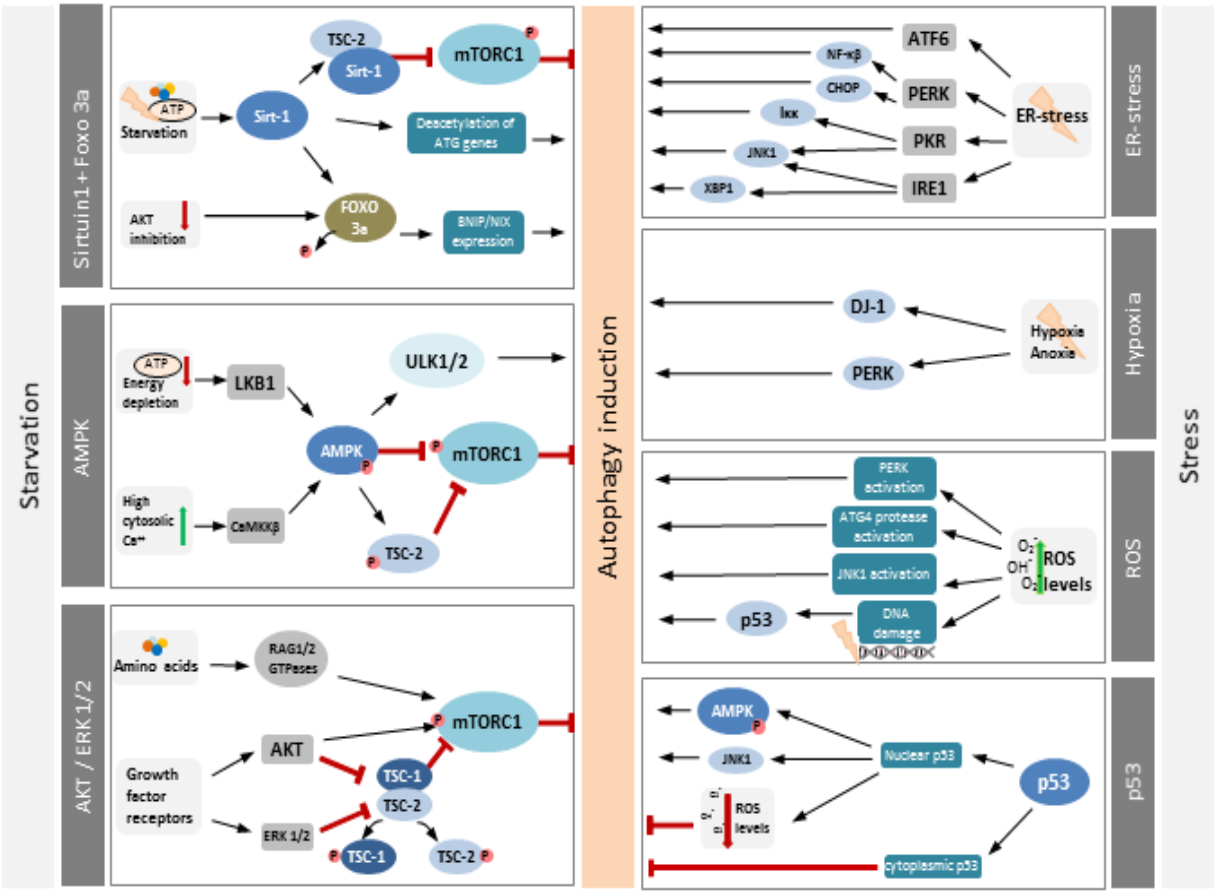

Figure 12: Selection of Autophagy Regulators

These diagrams show both starvation induced and stress induced signalling cascades. Displayed are the sirtuin-1, AMPK and AKT/ERK pathways on the left and pathways triggered by ER-stress, hypoxia, ROS and p53 on the right.

Sirtuin1, a deacetylase that senses environmental stress, (1) connects with tuberous sclerosis complex 2 (TSC-2) to further inhibit mTORC, (2) leads to deacetylation of Atg genes like Atg5, Atg7 and LC3, and (3) can deacetylate FOXO3 to enhance the expression of proautophagic Bnip3.

AMPK can be activated either by energy depletion (-> liver kinase B1(LKB1)) or through cytosolic Ca2+ (->calcium/calmodulin kinase kinase-β (CaMKKβ). When activated, it induces ULK1/2, inhibits mTORC, and can activate TSC-2 to in turn inhibit mTORC.

The inhibition of TSC-2 can also be initiated by AKT and ERK1/2 in response to growth factors.

ER-stress can lead to several unfolded protein response s(UPR) such as PERK (PKR-like eIF2a kinase), ATF6 (activating transcription factor-6) and IRE1 (inositol requiring enzyme 1), of which IRE is the only negative regulator of autophagy. Hypoxia can induce PERK and DJ-1, which regulates autophagy by an unknown mechanism.

Oxidative stress induces autophagy via ROS and p53. ROS can activate PERK, Atg4 and JNK1 (c-Jun N-terminal kinase-1). P53 is activated by different types of stress, including ROS. p53 plays a dual role, as nuclear p53can activate autophagy via AMPK and JNK1, but also inhibit autophagy via its cytoplasmic functions. Arrows indicate activation while blunted arrows in red indicate inhibition. Adapted from (Kroemer et al. 2010).

Methods to measure autophagy. The basic approach to investigating autophagy is assessing the number of autophagosomes present within the cell. This can be achieved either by counting the punctae produced in a GFP-LC3 puncta formation assay by fluorescence microscopy, or by detection of the LC3-conversion through immunoblotting (Mizushima et al. 2010). LC3 in general is an important marker, as it is involved in autophagosome formation, and the change from LC3-I to LC3-II should correlate with the number of autophagosomes produced (Mizushima & Yoshimori 2007). However, autophagy is a dynamic process that can be influenced at many steps, and the amount of LC3-II alone cannot indicate if a compound has induced autophagy, or alternatively if the degradation pathway/fusion of the autophagosome with the lysosome is inhibited (Klionsky et al. 2008). Therefore, several authors have recommended determining the so called "autophagic flux" and thus including autolysosome formation to cover both autophagosome synthesis as well as its degradation (Klionsky et al. 2008; Mizushima et al. 2010; Rubinsztein et al. 2009). By adding lysosomal inhibitors such as bafilomycin, which neutralises the lysosomal pH and therefore inhibits the degradation process; and comparing samples in the presence or absence of a particular compound, the more dominant pathway (synthesis or degradation) can be assessed (Rubinsztein et al. 2009).

Another option is to differentiate between autophagosome and autolysosome formation by using a tandem fluorescent-tagged LC3 plasmid (mRFP-GFP-LC3) which can be visualised by fluorescent microscopy. As GFP is degraded in the acidic environment of the lysosome, only a red signal is visible, whereas in the intact autophagosome yellow fluorescence results from the combination of mRFP and GFP (Kimura et al. 2007).

Another marker used to measure autophagy is p62, which is also called sequestosome 1(SQSTM1) in humans or ZIP in rats (Bjorkoy et al. 2009). It is a multifunctional protein containing several protein-protein interaction domains, suggesting that p62 is involved in the regulation of multiple signalling pathways (Salminen et al. 2012). p62 appears to selectively bind to toxic cellular waste and control its degradation or aggregation, by autophagy or proteasomes (Lamark et al. 2009; Salminen et al. 2012). Within the autophagic process, p62 is degraded **(Figure 11)**, but also interacts with Nrf2 (Rusten & Stenmark 2010). As a marker for

autophagy, p62 levels would be expected to decrease over time when autophagy is induced.

However, SFN can increase the levels of "free" Nrf2 by reacting with the thiol groups present in Keap1 and so disrupting the Nrf2-Keap1 complex, thus, especially after longer treatment times with SFN, p62 levels should be rising (Cheung & Kong 2009; Tufekci et al. 2011). Jain *et al.* (2010) reported a positive feedback loop between p62 and the Keap1-Nrf2 pathway, which in theory can be broken either by autophagy (degradation of p62) or the accumulation of small MAF proteins (repression of p62) **(Figure 13)**.

Autophagy and Neurodegenerative Diseases. A common factor in NDs is the presence of intracellular protein accumulations. As autophagy is an important pathway for degradation of such proteins, reduced activity of this process could contribute to the development of neurodegenerative diseases (Rubinsztein 2006; Rubinsztein et al. 2007; Sarkar 2011). A recent review has summarised the function of autophagy in development of PD, AD and HD, indicating different impairments within the autophagic pathway in each condition (Details **see Table 1;** Cheung & Ip 2011). Autophagy may therefore represent an interesting therapeutic target for these NDs, to reduce the levels of toxic protein aggregates and enhance the cellular response to stress (Nixon 2013). However, knowledge of alterations in molecular mechanisms of autophagy in NDs is incomplete; and to date studies have reported conflicting outcomes as to whether manipulation of autophagy can result in adequate neuronal survival (Cheung & Ip 2011; Jaeger & Wyss-Coray 2009).

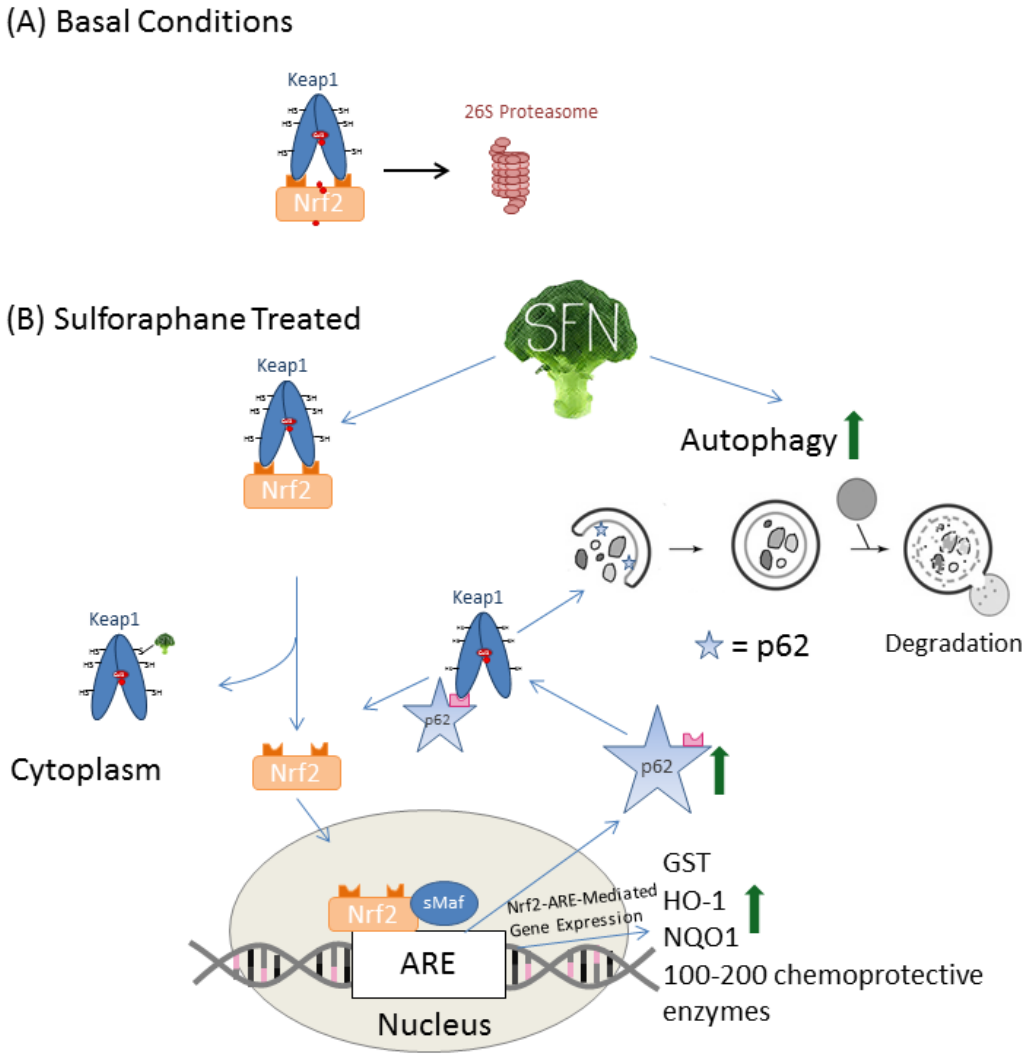

Figure 13: Modulation of the Nrf2 pathway and p62 by SFN.
In basal conditions, two Keap1 molecules bind to Nrf2, resulting in polyubiquitinated of Nrf2 and degradation by the proteasome. SFN can bind to Keap1 by interacting with cysteine thiol groups to impair the ubiquitination of Nrf2. Nrf2 then translocates into the nucleus, where it binds to the antioxidative response elements (ARE) upstream of cytoprotective genes such as GST and HO-1, but also p62. SFN increases autophagy, which results in degradation of p62. Binding of p62 to Keap1 results in further activation of Nrf2 and therefore leads to a positive feedback loop.

Neurodegenerative disease	Autophagy deregulation
PD	–Defective targeting of damaged mitochondria or mitophagy
	–Impaired lysosomal degradation
AD	–Generation of β-amyloid from autophagic vacuole
	–Impaired clearance of autophagic vacuole
HD	–Defective cargo recognition
	–Elevated autophagosome formation following mutant huntingtin expression
ALS	–Defective cargo recognition
	–Impaired autophagosome-lysosome-endosome fusion

Table 1 Autophagic impairment in Parkinson's disease (PD), Alzheimer's disease (AD), Huntington's disease (HD) and amyotrophic lateral sclerosis (ALS).

Mutation of Parkin and PINK1 are associated with targeting of damaged mitochondria to the mitophagy pathway in **PD**, but there is also increased autophagosome formation and possibly impaired lysosomal degradation. Pharmacological activation of autophagy can improve the clearance of a-synuclein and is neuroprotective. **AD** is characterized by increased autophagosome formation together with elevated β-amyloid production from the autophagic vacuole, as well as impaired clearance of autophagic vacuoles. **HD** has been associated with defective cargo recognition and - when challenged with mutant huntingtin - elevated autophagosome formation, although the application of an autophagy inhibitor can also alleviate accumulation of mutant huntingtin and toxicity. mTOR is sequestered into huntingtin inclusions, which causes activation of autophagy. **ALS** has been associated with p62 mutations, resulting in impaired substrate recognition. Mutant ALS2-mediated Rab5 [which has been associated with the Beclin1/Vps34 complex (Ravikumar et al. 2008)] suppression can result in dysfunctional fusion of the autophagosome with the lysosome or endosome, thus decreasing the rate of lysosome protein degradation, increasing autophagosome accumulation and subsequent neurodegeneration (adapted from Jaeger & Wyss-Coray 2009; Cheung & Ip 2011; Nixon 2013)

1.5 PROJECT AIMS

- To verify previously reported bioactivity of SFN in neuronal cell lines

  Based on the reviewed literature, the actions of SFN on neuronal cells have not been well researched. Some previously described bioactivities of SFN in other cell lines have been linked to potentially beneficial effects in NDs. The effects of SFN will be determined by measuring effects on the cell cycle, apoptosis, autophagy and the expression of phase II enzymes, as well as the capacity of SFN to protect neuronal cells from toxin-induced cell death. PC-12 and SH-SY5Y cell lines will be used to simulate neuronal cells.

- To investigate ER-stress regulators as potential downstream targets of SFN

  Targets tested will include DJ-1, a protein associated with PD, as well as CHOP, a marker for ER-stress, while ER-stress will be induced by tunicamycin. The role of DJ-1 in reducing ER-stress will be further researched by silencing DJ-1 using siRNA.

- To examine the importance of autophagy in SFN-mediated cell survival

  This study will examine whether primary neuronal cells generated from Atg16L1 deficient mice show a reduced capacity to recover from H_2O_2-induced cell death in the presence of SFN. The occurrence of autophagy will be compared in SFN-treated Atg16L1 knock out (KO) and wild type (WT) cells. Furthermore, the effect of impairment of autophagy on the protective effects of SFN will be determined.

2 MATERIALS AND METHODS

2.1 CELL CULTURE

2.1.1 PC-12 CELLS

2.1.1.1 MEDIA USED FOR ROUTINE CULTURE OF CELLS

The PC-12 cell line was maintained in Kaighn's Modification of Ham's F-12 Medium (F-12K; LGC Standards; contains 1.26 g/l D-glucose), supplemented with 2.5% (v/v) Fetal Bovine Serum (FBS; Invitrogen), 15% (v/v) Horse Serum (HS; LGC Standards) and 1% (v/v) Penicillin-Streptomycin (PEN/STREP 5000U/ml; Gibco). This media composition will be referred to as complete PC-12 media from this point forward. The cells were usually grown in 75cm^2 flasks with 12ml medium at seeding density of 1 – 1.5x10^6 cells.

2.1.1.2 SUBCULTURE OF CELLS

All flasks were labelled with name, date of seeding, cell line and passage number. Prior to subculture, the cells were checked for the ideal cell confluency (~70-80% growth density) and any signs of contamination. The cells were detached with TE (0.25% (w/v) trypsin/1mM EDTA; Gibco) and cell numbers were calculated using a haemocytometer.

At a seeding density of 1 – 1.5 x 10^6 cells were split every 3-4 days.

2.1.1.3 CRYOPRESERVATION AND CONTROLLED FREEZING OF CELLS

An estimated number of cryotubes were labelled with the user name, cell line, passage number, date and amount of cells (usually 1,5 x 10^6). The cells were then harvested as described above (2.1.2). The cells were spun down (5mins at 200G) and freezing medium (complete media + 5% (v/v) DMSO) was added. The resuspended cells were transferred into cryotubes in 1ml aliquots which were then put into a freezing container (Nalgene®Mr. Frosty, Sigma-Aldrich) at -80°C for one day and then kept in liquid nitrogen for long term storage.

2.1.1.4 DIFFERENTIATION OF PC-12 CELLS

Plates were coated with collagen at a concentration of 0,4mg/ml and placed in the incubator at 39°C for 30mins. PC-12 cells were then seeded into 12-well plates at a density of 10.000 or 20.000 cells/well using DMEM-Hi media (Gibco) supplemented with 15% (v/v) Foetal Bovine Serum (FBS; Invitrogen) + 1% (v/v) Penicillin-Streptomycin (PEN/STREP 5000U/ml; Gibco). After 2-3 days only ~75% of the media was changed to not stress the cells. 2 days later, at ~50% confluency, the media was replaced with NGF-containing media [DMEM-Hi + 15% (v/v) FBS + 1% (v/v) P/S + 50ng/ml NGF]. Going forward, fresh media was added every 2-3 days until differentiation was visibly confirmed (usually within 5-7 days after start of NGF treatment).

2.1.2 SH-SY5Y CELLS

2.1.2.1 MEDIA USED FOR ROUTINE CULTURE OF CELLS

The SH-SY5Y cell line (ATCC-CRL-2266) was kept in a 1:1 mixture of Eagle's Minimum Essential Medium (MEM; LGC Standards; contains 1 g/l D-glucose) and Ham's F12 Medium (F12-HAM; Sigma Aldrich; contains 1.802 g/l D-glucose) supplemented with 10% (v/v) FBS and 1% (v/v) PEN/STREP. The volume of medium used in routine cell culture was 12ml in a T75 flask. The cells were usually grown in 75cm^2 flasks with 12ml medium at seeding density of 2x10^6/flask.

1.1.1.1 SUBCULTURE OF CELLS

The cells were detached with TE (0.25% trypsin/1mM EDTA; Gibco) and counted with a haemocytometer. SH-SY5Y cells also include floating cells, which were spun down at 200G for 5mins, resuspended in fresh media and then added to the new flask.

When 2 x 10^6 cells were seeded, they could be harvested after 8-10 days.

1.1.1.2 CRYOPRESERVATION AND CONTROLLED FREEZING OF CELLS

See 2.1.1.3

2.2 MTT ASSAY

3-(4,5-Dimethyilthiazol-2-yl)-2,5-diphenyltetrazolium bromide (MTT; Sigma Aldrich) is a yellow coloured tetrazol, which is reduced into a purple formazan in living cells. 5mg/ml MTT was dissolved in sterile PBS. The MTT reagent was kept at 4°C, protected from light, and used within 3 months.

Cells were seeded in 96 well plates 100µl/well at 1 x 10^6/10ml (SH-SY5Y: 1.5 x 10^6/10ml). The first column was used as blank control samples. The following day, the cells were checked for complete attachment. The media was changed twice over the next two days, the second time replaced by different treatment solutions for each column. The plate was kept in the incubator for 24h. Prior to the MTT treatment, 800µl of MTT solution was added to 8ml pre-warmed media. The media was removed from the plate and replaced by the MTT/media mix. After a 1h incubation at 37°C, MTT/media was removed from the wells. 100µl DMSO, serving as a solvent of the purple formazan precipitate, was added to each well and mixed thoroughly by pipetting. The plate was then slightly tapped to ensure even and bubble-free distribution before reading it at 550nm test wavelength and 630nm reference wavelength.

$$\% \text{ Viability} = \frac{\text{Mean Absorbance of Sample}}{\text{Mean Absorbance of Control}} \times 100$$

2.3 WESTERN BLOT

2.3.1 PROTEIN EXTRACTION

To minimize protein degradation, samples and lysis buffer were kept on ice as much as possible. Cells were lysed in NP40 lysis buffer {Tris-EDTA pH8 (2mM), NaCl (150mM), Glycerol (10% (v/v)) and Nonidet P40 (1% (v/v))} plus Complete Protease Inhibitor mini tablet [EDTA-free], incubated on ice for 30min, dislocated from the plates using cell scrapers, and finally centrifuged at 13000rcf at 4°C for 15min. The supernatant was collected into cold 0.5ml Eppendorf tubes and stored at -20°C.

Nuclear protein extraction. Cells were washed with ice-cold PBS (incl. phosphatase inhibitors) before they were evenly covered with 1x Hypotonic buffer and incubated on ice for 30min while kept in motion. After dislocating the cells from the plates using cell scrapers and collecting them in individual Eppendorf tubes, detergent was added to each vial. These tubes were vortexed for 10sec at highest setting and centrifuged for 80sec at 14.000g at 4°C. The supernatant (cytoplasmic fraction) was transferred into a pre-chilled Eppendorf tube and stored at -80°C until used. The nuclear pellet was resuspended in complete lysis buffer and again vortexed for 10 sec at highest setting. After incubation for 30min at 4°C in motion, another 30sec vortex and centrifugation for 10min at 14.000g at 4°C, the supernatant (nuclear fraction) was transferred into a pre-chilled Eppendorf tube and stored at -80°C until used **(see appendix Table 8, p.135, for details on solution compositions)**.

Total protein was collected unless otherwise noted.

2.3.2 PROTEIN QUANTIFICATION (BRADFORD ASSAY)

The Bradford assay is a colorimetric protein assay based on the binding of the dye Coomassie Blue G-250 to protein. Bovine serum albumin (BSA; Thermo Scientific) was used to create a standard dilution series, for which samples were prepared within the range of 0.25 – 2mg/ml. All standards and samples were prepared in duplicates.

The samples were transferred into cuvettes and read in a spectrophotometer at 595nm. The absorbance was read from the standard curve to convert the results

into protein concentrations in mg/ml. Usually, 20ng of protein was used for separation and further investigation.

2.3.3 WESTERN BLOT

2.3.3.1 GEL ELECTROPHORESIS – SDS PAGE

Samples were mixed with 4x loading buffer (NuPage LDS sample buffer (4x); Invitrogen) and DTT (Sigma Aldrich) to obtain final concentrations of 70% (v/v) sample, 25% (v/v) loading buffer and 5% (v/v) DTT (1M). 10µl/20µl/30µl samples were prepared, from which a calculated volume containing 20ng protein was loaded on a gel. After mixing all contents with vortex, the samples were put in a heating block set to 98°C for 5min to denature the protein.

The gels contained either 10% (v/v) or 12.5% (v/v) resolving gel and were prepared not longer than 3 days before use, wrapped in cellophane and kept in the fridge. Depending on the amount of samples, either 10- or 15-well combs were used. The gels were placed in a MINI Protean Tetra Tank (Bio Rad) for four gels or a MINI Protean Tank (Bio Rad) for one or two gels, according to manufacturer's instruction. The electrophoresis was run at 200V for 30-35 minutes (Tetra Tank) or at 25mA for 40-60 minutes (Regular Tank). The run was stopped when the blue dye from the sample loading buffer has come close to the bottom of the gel.

2.3.3.2 SEMI-DRY GEL TO MEMBRANE TRANSFER

To transfer the proteins from the gel onto the membrane, the Trans-Blot SD Semi-Dry Transfer Cell (Bio Rad) was used. A transfer buffer was made up of 10% (v/v) transfer buffer (10x; Bio Rad), 20% (v/v) methanol (Sigma Aldrich) and 70% (v/v) water (MQ). Pre-cut filter paper was soaked in this transfer buffer. PVDF-membranes were incubated in methanol for 10sec before they also were left in transfer buffer for about 10mins. The filter paper, the membrane, the gel and again some filter paper were laid onto the plate. The filter paper is pressed a little with the fingers to remove most of the liquid before building this sandwich. After each layer is applied, a small glass pipette is rolled gently over it to remove unwanted bubbles. One gel was run at 15V, two at 25V for 50mins.

2.3.3.3 MEMBRANE BLOCKING AND STAINING

After the transfer, the membrane was washed in PBST 0.1% (PBS pH 7.4 containing 0.1% (v/v) Tween 20). Then the membrane was put into a box with 25ml of blocking buffer (Fisher Scientific) to block for 1-2 hours. The antibodies were prepared in a 1:1 solution of blocking buffer and PBST 0.5% (PBS pH 7.4 containing 0.5% (v/v) Tween 20) accorded to recommended dilutions **(see Table 2)**.

Type of AB	Antigen	Host	Dilution	Size / IR Dye	Supplier	Cat.no.
Primary	β-actin	goat	1:10000	42kDa	Santa Cruz Biotechnology	sc-1615
Primary	LC3	rabbit	1:2000-1:5000	18kDa + 16kDa	Sigma	L7543
Primary	p62	guinea pig	1:2500-1:5000	62kDa	Progen	GP62-C
Primary	Nrf2 (C-20) (cytosol)	rabbit	1:500	57/100kDa	Santa Cruz Biotechnology	sc-722
Primary	Nrf2 (H-300) (nuclear)	rabbit	1:500	57kDa	Santa Cruz Biotechnology	sc-13032
Primary	a-synuclein	rabbit	1:2000	14-19kDa	Millipore	AB5038
Primary	SAM 68 (C-20)	rabbit	1:10000	68kDa	Santa Cruz Biotechnology	sc-333
Primary	TR-1	rabbit	1:2000	55kDa	Abcam	AB16840
Primary	HO-1	mouse	1:2000	30/60kDa	Abcam	Ab13248
Primary	DJ-1	rabbit	1:1000	23kDa	Santa Cruz Biotechnology	sc-32874
Primary	CHOP (L63F7)	mouse	1:1000	27kDa	Cell Signalling	2895
Secondary	goat	donkey	1:10000	-/680	Li-Cor	926-68024
Secondary	rabbit	donkey	1:10000	-/800	Li-Cor	926-32213
Secondary	guinea pig	donkey	1:10000	-/800	Li-Cor	926-32411
Secondary	mouse	donkey	1:10000	-/800	Li-Cor	926-32212

Table 2: Antibodies used in western blotting

To the secondary antibody, SDS was added to reach a final concentration of 0.01% (v/v) to reduce the background of the red IR signal (680nm), as recommended by the supplier. The membrane then was incubated with the primary antibody with gentle movement over night at 4°C. After 15-18 hours, the membrane was washed 4 times with PBST, before the secondary antibody was applied and left for 1 hour. Again, the membrane was washed 4 times with PBST and once with PBS prior to finally keeping it in PBS at 4°C until imaging by the Odyssey® Imaging System. For long term storage, the membrane was dried out on tissue for 1-2 hours, then on a fresh tissue for another 1-

2 hours before put on labelled whatman paper and wrapped in cellophane. The membrane must be protected from light.

2.3.3.4 IMAGING WITH ODYSSEY

The membranes were imaged using the Odyssey® Infrared Imaging System and analysed using the Odyssey software. The intensity of each channel – 700 for the red and 800 for the green signal – was adjusted to receive the best image results. The intensity measured for each band was aimed to be at least 10, but not higher than 200. The box drawing feature in the software enables to quantify the value selected in this specific area. Quantifying the bands makes calculations possible, such as normalisation, simply by dividing the value of the protein of interest by the value of the loading control.

2.4 RNA/DNA EXPERIMENTS

2.4.1 RNA EXTRACTION

RNA extraction was carried out using the SIGMA RNA-extraction kit GenElute (Sigma-Aldrich) following the provided instructions. After lysing the cells, they were run through a filtration column for 2mins. The column binds the RNA, which is washed and 3 times prior to elution of pure total RNA.

2.4.2 RT-PCR

The RNA was transcribed into cDNA by using the SuperScript II kit (Invitrogen) following the provided instructions. In addition to the kit, Random primers, RNasin Plus (both Promega) and dNTP Mix (10mM; Invitrogen) were acquired. 1µg RNA was used in a 12µl reaction volume. After the SuperScript II RT is added, the mix is incubated at 25°C for 10min and at 42°C for 50min, before inactivating the reaction at 70°C for 15min.

2.4.3 PCR

The following reaction mix was assembled (Primers used can be seen in **Table 3**):

Component	**Volume (µl)**
cDNA from RT-PCR (~83ng/µl)	**4**
5x GoTaq Flexi Buffer	**10**
$MgCl_2$ (25mM)	**8**
dNTPs (10mM)	**1**
Fwd primer (10µM)	**2**
Rev primer (10µM)	**2**
dd H_2O	**22,5**
Go Taq (5u/µl)	**0,5**
Final volume	**50**

	Fwd primer	Temp. (C°)	Rev primer	Temp. (C°)
CHOP	CCTTGGAGACGGTGTCCAGC	69.4	CGCAGGGTCAAGAGTAGTGAAGG	68
Actin	GAGGCCCCCCTGAACCCTAAG	70.7	GAACCGCTCGTTGCCAATAG	66.7

Table 3: CHOP and actin composition forward and reverse primer and annealing temperature.

2.4.4 TAQMAN REAL-TIME PCR

mRNA levels were quantified by real-time RT-PCR (TaqMan®) using the AB 7500 PCR system. Probes and Primers were obtained by Applied Biosystems, as can be seen in **Table 4**. The experiments were carried out in a 96-well plate in a total volume of 25µl per well. The samples were set up in 3 technical replicates. A standard curve containing 2 technical replicates was also present on each plate. "No template controls" (no cDNA, just water) were added to each plate. Data were normalised against the housekeeping gene 18S ribosomal RNA.

	Gene name Reporter / Quencher	Primers and Probes	Supplier
GOI	GST - rat Glutathion-S-transferase FAM/TaqMan MGB	perfect probe	Applied Biosystems TaqMan Gene Expression Assay
	TR-1 - rat Thioredoxin reductase 1 FAM/TaqMan MGB	perfect probe	Applied Biosystems TaqMan Gene Expression Assay
	GST-a - human Glutathione-S-transferase FAM/TAMRA	Forward: 5' –CAGCAAGTGCCAATGGTTGA- 3' Reverse: 5' –TATTTGCTGGCAATGTAGTTGAGAA- 3' Probe: 5' –TGGTCTGCACCAGCTTCATCCCATC- 3'	Applied Biosystems TaqMan One-Step RT-PCR master mix reagents kit
	TR1 - human Thioredoxin reductase 1 FAM/TAMRA	Forward: 5'-CCACTGGTGAAAGACCACGTT -3' Reverse: 5' –AGGAGAAAAGATCATCACTGCTGAT- 3' Probe: 5' –CAGTATTCTTTGTCACCAGGGATGCCCA -3'	Applied Biosystems TaqMan One-Step RT-PCR master mix reagents kit
	APP – rat FAM/TaqMan MGB	perfect probe	Applied Biosystems TaqMan Gene Expression Assay
	SYN – rat FAM/TaqMan MGB	perfect probe	Applied Biosystems TaqMan Gene Expression Assay
HG	18S ribosomal RNA FAM/TAMRA	Forward: 5'–GGCTCATTAAATCAGTTATGGTTCCT-3' Reverse: 5'- GTATTAGCTCTAGAATTACCACAGTTATCCA-3' Probe: 5'TGGTCGCTCGCTCCTCTCCCAC-3'	Applied Biosystems

Table 4: Probes and primers used for qPCR

2.4.5 TRANSFECTION WITH PLASMIDS

Cells were seeded on cover slips in 24-well plates (30.000 cells in 500µl/well). The transfection reagent Xtreme Gene HP (Roche) was used for transient transfection on PC-12 cells according to the manufacturer's instructions. For this project, the following plasmids were used, which were a kind gift from Dr. R. Roberts, Babraham Institute, Cambridge:

- mRFP-LC3
- Atg16L1-GFP
- p62-tomatored
- mRFP/GFP-LC3

PC-12 cells were seeded at a density of 30.000/well. A 1:3 mixture of 1µg plasmid DNA and X-tremeGENE HP DNA Transfection Reagent was prepared in serum-free media and added drop-wise to the wells after a 15-30min incubation period at room temperature to allow complex formation. After 48h, cells were treated with DMSO (0.025%), SFN (2.5, 5 and 10µM) or HBSS for 4h, then the treatment medium was removed. To fix the cells, they were covered with 200µl ice cold pure MeOH/well and left for 5mins. Then cells were washed with PBS, before 200µl of DAPI (1:2000; Sigma) were added for 2mins. After this step, cells need to be protected from light. After removal of the DAPI solution, the cells were left in PBS. Cover slips were carefully removed from each well and washed first in PBS, then in water, before placed topside down onto a drop of Hydramount (national diagnostics) on labelled glass slides. The slides were left for 15mins to harden, after which they were put into a sample box and kept in the fridge until imaging. They were visualised under the ZEISS Axioplan 2 imaging microscope and analysed using the Axio Vision Release 4.8 software. All results were magnified to 100x objective.

2.4.6 TRANSFECTION OF PC-12 CELLS WITH SIRNA

siRNA experiments were carried out according to recommendations from QIAGEN using their HiPerfection Transfection Reagent Kit.

PC-12 cells were seeded at a density of $1x10^6$/96well plate. The next day they were treated with the siRNA-HiPerfect mix as recommended (see **Table 5**). Another 24h later treatment with SFN was initiated. One day later the plates were either measured using MTT or exposed to H_2O_2 for another 24h, to be then analysed according to the experiment layout.

The same procedure was followed for 6 well plate experiments at a seeding density of $1x10^6$/plate (~80 000/well).

	96 well plates (amounts/well)		**6 well plates** (amounts/well)	
Volume of HiPerFect Reagent (µl)	0.75		12	
Total volume of medium on cells (µl)	120		2300	
Final siRNA conc.	5nM	10nM	10nM	20nM
siRNA of a 2µM stock solution (µl)	0.375	0.75	12	24

Table 5: siRNA-HiPerfect mix components

2.5 FLOW CYTOMETRY

2.5.1 CELL CYCLE ASSAY

Cells were seeded in a 6 well plate (PC-12: 200 000; SH-SY5Y: 300 000 – 350 000/well). At 70-80% confluency, the wells were treated with different concentrations of SFN (2.5-20µM) for 24h. Then the media was collected in allocated tubes. The adhered cells were washed with PBS before detaching them from the plate with trypsin and adding them to the corresponding vial. The tubes were spun down at 270G for 5 minutes. The pellets were resuspended in PBS and spun down again. This time, ice-cold 70% (v/v) ethanol was added while vortexing the tube. Then the tubes were kept at -20°C.

Next, the tubes were spun down at 500G for 5mins. The ethanol was removed and the cells were washed with PBS. A mixture of PBS, RNase-A (0.5mg/ml) and Triton-X100 (0.3% v/v) was prepared, of which 25µl were added to each tube, after which the cells were resuspended in 50µl PBS. The samples were incubated at 37°C for 30mins.

After the incubation, 3µl propidium iodide (1mg/ml; Sigma-Aldrich) was added to each sample, which were then run on the BD Biosciences Accuri C6 flow cytometer. After gating the cells on a forward and side scatter plot excluding most likely debris (gate P1), forward scatter height and area data were used to gate for singlet cells. These were plotted on a histogram with FL2-A as filter setting for the x-axis. A minimum of 5000 events in gate P1 was collected. A method optimisation table can be found in the Appendix 1 (**Table 3**). Data was further analysed using the FlowJo Software.

2.5.2 ANNEXINV/PI APOPTOSIS ASSAY

The cells were seeded in and collected from 6-well plates as mentioned above (2.5.1), but instead of fixing the cells with ethanol, they were resuspended in 500µl binding buffer (1x!) provided with the AnnexinV-FITC Apoptosis Detection Kit (eBioscience). 100µl of this cell suspension was transferred into a new labelled tube. Next, 2µl AnnexinV-FITC (included in the kit, concentration information not provided) and 10µl PI (20µg/ml; included in the kit) were added. After incubation

at room temperature under light protection, the samples were run on the BD Biosciences Accuri C6 flow cytometer.

The gated cells (P1) where then filtered by FL1-A on the X-axis and FL3-A on the Y-axis on a new scatter plot. This could then be divided into 4 squares which show the different stages between healthy (AnnexinV$^-$/PI$^-$), apoptotic (AV$^+$/PI$^-$) and necrotic (AV$^+$/PI$^+$) cells. A minimum of 10000 events in gate P1 was achieved unless otherwise noted. Data was further analysed using the Kaluza Software.

In cytoprotection assays cells were treated with SFN at an earlier stage (at ~60-70% confluency) to avoid overgrowth of cells at the end of the experiment, when cells were treated with H_2O_2 or 6-OHDA for 24h after SFN-pre-treatment **(see method optimisation in appendix, Figure 48, p.136).**

2.6 MOUSE WORK

2.6.1 ANIMAL MAINTENANCE

The mice used for the experiments mentioned were a kind donation of Prof. Uli Mayer's lab at UEA. All mice were handled in accordance with Home Office regulations. They were kept in specific pathogen free conditions in individually-ventilated cages and were routinely screened for common mouse pathogens. For generating primary neuronal cells, pregnant female mice were killed by schedule 1 method 14-16 days into the pregnancy.

2.6.2 RETRIEVING EMBRYONIC BRAINS

The sacrificed pregnant mouse was dissected to extract the vitelline bag, which was then put into a Ca^{+2}- and Mg^{+2}-free PBS solution containing 33mM glucose (PBS-glucose) and kept at 4°C. The dead embryos were removed and placed into individual wells of 6 well plates containing PBS-glucose. After decapitation of the embryos, the heads were placed into fresh individual wells filled with PBS-glucose. Under a microscope an incision at the back and either side of the head was made and with gentle pressure on top of the head the brain was released into the solution and immediately removed with a small sieve and placed into a labelled 1.5ml Eppendorf tube filled with PBS-glucose.

2.6.3 GROWING PRIMARY NEURONAL CELLS

Fire-polished Pasteur pipettes were rinsed with heat inactivated FBS before gently dissociating the cells of each Eppendorf tube. After 5-10 minutes, the non dissociated elements formed a pellet. The supernatant was pipetted into a fresh Eppendorf tube and centrifuged at ~200g for 5mins at room temperature. After the supernatant was removed, the cells were mixed with DMEM/F12 +10% (v/v) mixed hormones (see **Table 6**) in an amount based on number of wells to be plated, and seeded into poly- D-lysine pre-coated (incl. coverslips; for immunohistochemistry) or poly-ornithine pre-coated plates (for AV/PI experiments) [Coating Procedure see Appendix 8.4.3].

After 2 days, first morphological signs of differentiation could be observed. After 4 days, the media was changed. After a week, treatment with SFN was started. For

AV/PI experiments, this was followed by a 4h exposure to H_2O_2 in Hepes buffered media (HBM) and further 20h of media + 10% (v/v) mixed hormones.

	MEDIUM FINAL CONCENTRATION	SUPPLIER + CAT.NO.
TRANSFERIN	100µg/ml	Sigma T-2036
INSULIN	25µg/ml	Sigma I-1882
PUTRESCINE	60µM	Sigma P-7505
SODIUM SELENATE	30nM	Sigma S-9133
PROGESTERONE	20nM	Sigma P-6149

Table 6: List of components of mixed hormones solution.
This mixture is added to DMEM/F12 1:1 (Gibco, 11320-740, (1x), liquid – with L-glutamine, without HEPES) as medium

2.6.4 MOUSE GENOTYPING

The tail of each embryo used mentioned above was kept at 4°C until genotyped using PCR. About 150µl of proteinase K lysis buffer was added to each tail biopsy and left over night in a rotating incubator at 55°C. The lysate was then diluted 10 times using distilled water, of which 3µl was used in a PCR reaction.

The following reaction mix was assembled:

Component	**Volume (µl)**
DNA (1:10 dilution from lysis)	3
10x buffer (containing $MgCl_2$)	5
dNTPs (25µM)	0.5
Primer mix (20pmol/µl)	1
Taq	2
dd H_20	X
Final volume	**50**

For amplification of genomic DNA, a touchdown PCR method was applied:

95°C – 10 min	
95°C – 45 sec 65°C – 1min/ minus one degree each cycle 72°C – 1 min	10 cycles
95°C – 45 sec 55°C – 1min 72°C – 1 min	25-30 cycles
72°C – 10 min	
4°C – on hold	

The PCR products were then run on a 1% agarose gel.

2.7 IMAGING

2.7.1 IMMUNOFLUORESCENCE

Cells were fixed by adding ice cold pure methanol for 5 minutes. After several washes with PBS, the slides were blocked with 2% (w/v) BSA in PBS at room temperature for 1h. This solution was then replaced by the primary antibody (see **Table 7**) at room temperature for 1h. After 3 washes with 2% (w/v) BSA in PBS the second antibody was left on for 40 minutes at room temperature. Once the antibody and BSA was washed off, a solution of DAPI 1:5000 was added to the wells for 5-10 minutes. Following more washes, the slides were finally mounted using Hydromount (national diagnostics) and dried under protection of light. The slides were imaged under the microscope.

2.7.2 MICROSCOPY

Fixed cell images were captured at x63 magnification on a Zeiss Axioplan 2 microscope, unless specified otherwise. Images were analysed with the Axioplan software version 4.7.1. IMARIS was used to calculate autophagy punctae.

TYPE OF AB	ANTIGEN	HOST	DILUTION	SUPPLIER	CAT.NO.
PRIMARY	LC3	rabbit	1:1000	Sigma	L7543
PRIMARY	p62	guinea pig	1:1000	Progen	GP62-C
SECONDARY	rabbit	donkey 594	1:500	Invitrogen	*
SECONDARY	guinea pig	goat 488	1:500	Invitrogen	*

Table 7: List of antibodies used for immunofluorescence
* These secondary antibodies were a kind gift from Matt Jefferson, Wileman lab, University of East Anglia.

2.8 STATISTICS

For all results with 2 or more biological replicates, standard deviation and, if appropriate, Student's t-test were calculated and, if statistically significant, were labelled with the P-value. Whenever more than pairwise comparisons were investigated within a data set, ANOVA was used to test for significance and post-hoc t-tests were adjusted according to Bonferroni.

3 BIOACTIVITIES OF SULFORAPHANE ON PC-12 AND SH-SY5Y CELLS

3.1 BACKGROUND & AIMS

Before this study was initiated, no publications reported the actions of SFN on PC-12 cells. However, Shibata *et al.* (2008) investigated cruciferous vegetable extracts on PC-12 cells on the search for the most potent natural enhancer of NGF-dependent neuritogenesis. Japanese horseradish (*Wasabia jabonica*) with its major ITC 6-methylsulfinylhexyl isothiocyanate (6-HITC) was identified as the richest source of neurotrophic inducers within the *Brassicaceae*, and was further investigated on neurite outgrowth and the involvement of NGF. It was shown that 6-HITC could enhance the NGF-induced neurite outgrowth.

Shavali & Sens (2008) demonstrated that SFN could protect SH-SY5Y cells from cytotoxicity caused synergistically by arsenite and dopamine. Concentrations between 0.1 and 2.5µM showed significant recovery of cell survival in a dose dependent manner, while the cell viability was reduced in 5µM SFN samples. In a different study, SFN could protect SH-SY5Y cells against H_2O_2 or 6-OHDA-induced cell death (Tarozzi et al. 2009). They also demonstrated significant increases in total GSH level, NAD(P)H quinone oxidoreductase-1, GSH-transferase and –reductase. The SFN concentrations used were between 1.25 and 2.5µM for 12 or 24h, followed by a 24h exposure to 300µM H_2O_2 or 100µM 6-OHDA.

SFN has been introduced in depth in chapter 1 (page 15). The aim of this chapter is to validate previous findings, therefore cell cycle, apoptosis, Nrf2 and Nrf2/ARE-driven genes as well as autophagy will be measured. To investigate SFN in PC-12 cells, basic assessments will be made to optimise concentrations of SFN and time lines for further experiments including toxins.

Initiation of autophagy by autophagy. The first report of SFN inducing autophagy by measuring autophagy endpoints like autophagosome formation also looked into

the mechanism of action involved. 3-methyladenine (3-MA, a class III PI3K blocker) was effective to inhibit SFN-induced autophagy, so PI3K III could also be a target of SFN (Herman-Antosiewicz et al. 2006). SFN has previously been reported to reduce Bcl-2, an inhibitor of Beclin-1 and thus autophagy (Singh et al. 2005). The production of mitochondria-derived ROS by SFN has also been found to be a trigger for autophagy induction (Xiao et al. 2009). A more recent study in SH-SY5Y cells and cortical neurons however has suggested that the ROS further activates ERK, which in turn induces autophagy (Jo et al. 2014). Interestingly, the initial investigation of SFN and autophagy has argued against an involvement of ERK in sulforaphane-induced autophagy. They reported an ERK activation by SFN, but since an inhibitor of ERK applied simultaneously failed to reduce LC3 production, it was concluded that ERK may not be involved in the mechanism of SFN on autophagy (Herman-Antosiewicz et al. 2006). It is possible that SFN has several targets to initiate autophagy, or that it works differently in separate experiment models. The mechanism of autophagy initiation by SFN will not be investigated in this study.

3.2 RESULTS

3.2.1 CELL VIABILITY OF SFN IN PC-12 CELLS

To determine a dose range of SFN which keeps cells intact, cell viability was assessed using the MTT assay. To estimate the IC_{50} value, the results were analysed using the GraphPad Prism software. In 80% confluent PC-12 cells, 50% of cell survival can be expected at approximately 36.9µM SFN in 24h-treatments (=IC_{50}) **(Figure 14)**.

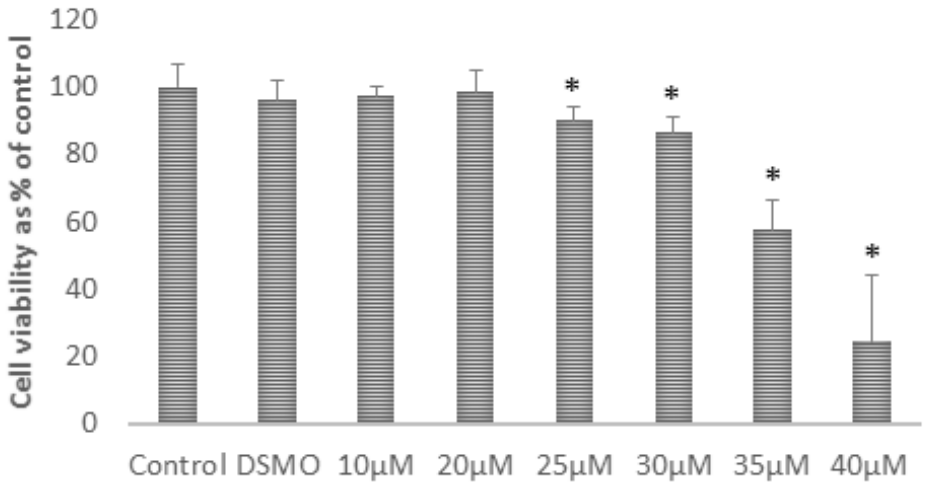

Figure 14: Cell viability of PC-12 cells following exposure to SFN for 24h. PC-12 cells were treated with DMSO (0.05%) or different concentrations of SFN (10-40µM) for 24h. Cell viability was assessed by MTT and measured on a plate reader using 550nm as test wavelength and 630nm as reference wavelength. Each bar represents the average of six biological replicates (± standard deviation; *P<0.05 compared to control).

3.2.2 EFFECT OF SULFORAPHANE ON CELL CYCLE ARREST IN PC-12 AND SH-SY5Y CELLS

SFN on cell cycle in PC-12 cells. The results shown in **Figure 15** indicate that SFN leads to S phase arrest in PC-12 cells. Untreated controls were primarily in the G1 phase (51.83%) with smaller percentages in the S phase (28.97%) and G2/M phase (17.1%). DMSO (0.01%) samples did not show a significant change compared to vehicle control samples. Following SFN treatment, the percentage of cells in the S phase increased in the 1.25 and 2.5µM samples to 42.39% and 42.35%, which was a significant change compared to control and DMSO samples. The 5µM samples of one batch were lost, therefore a statistical significance compared to control or DMSO samples could not be calculated. Although SH-SY5Y showed a similar tendency, we only present a single observation and thus this experiment would need to be repeated **(see appendix p.141, Figure 53)**.

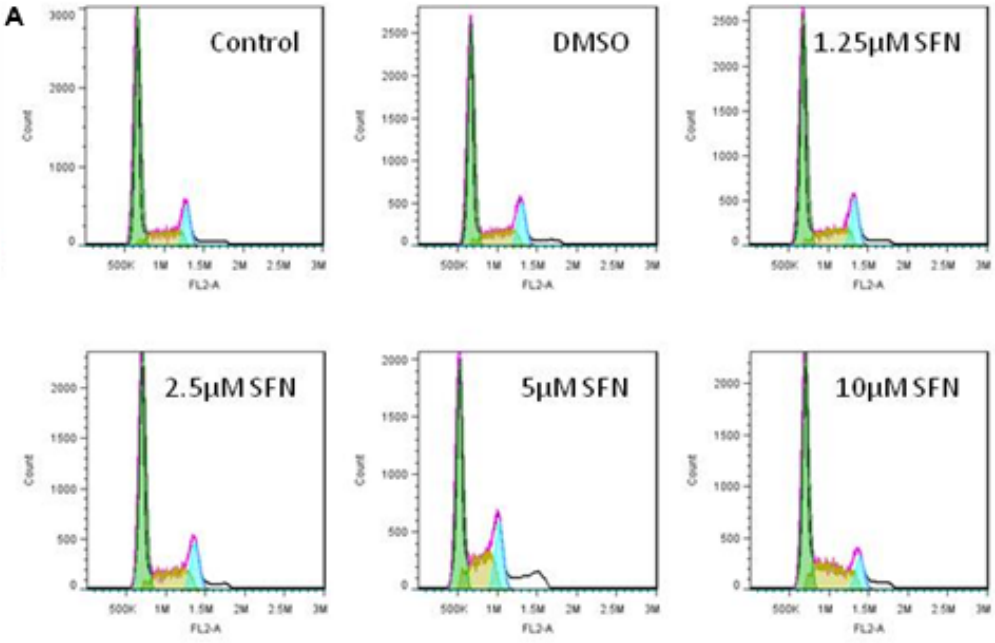

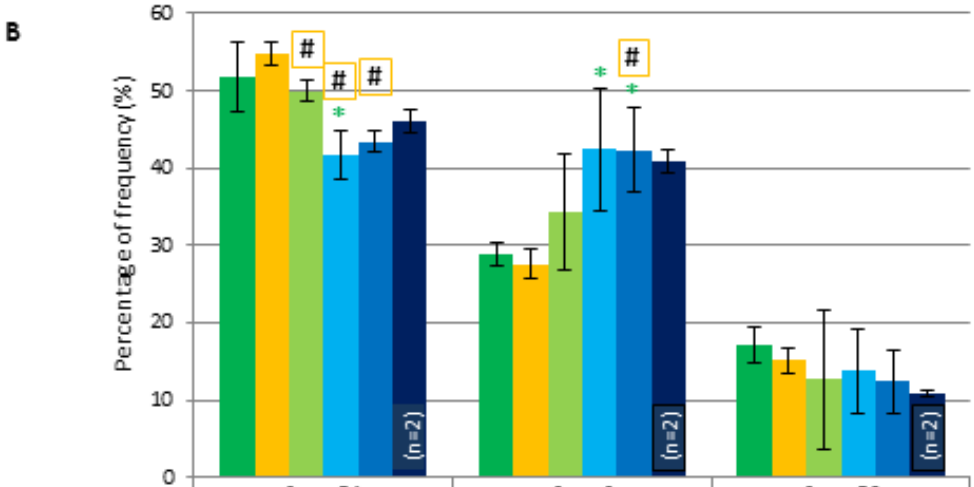

	StageG1	StageS	StageG2
Control	51.83	28.97	17.10
DMSO (0.01%)	54.75	27.60	15.15
0.625µM SFN	50.01	34.31	12.66
1.25µM SFN	41.69	42.39	13.77
2.5µM SFN	43.41	42.35	12.39
5µM SFN	46.18	40.80	10.81

Figure 15: Cell cycle assay of SFN in PC-12 cells.
Cells were exposed to media only, DMSO (0.01%) or different concentrations of SFN for 24h. The distribution of cells in different cell cycle stages was obtained by flow cytometry and FlowJo software. **A** shows sample figures with SFN concentrations from 1.25µM-10µM,, while **B** displays the average of 3 biological replicates of samples ranging 0.625-5µM SFN (n=3, unless otherwise marked; ±SD; * P<0.02 vs control, # P<0.02 vs DMSO).

3.2.3 EFFECT OF SULFORAPHANE ON PHASE II AND ANTIOXIDANT ENZYME EXPRESSION

First, 18S rRNA was assessed to be a suitable reference gene in PC-12 cells by using the GeNorm Kit provided by Primer Design (data not shown). After a 4h treatment with media only, DMSO (0.01%) or 5µM SFN, RNA was extracted, transcribed to cDNA and quantified via Taqman. This experiment was carried out in 4 biological and 2 technical replicates. 18S rRNA was amongst the most stable reference targets and was therefore used throughout all qPCR experiments.

Nrf2 nuclear protein levels in PC.12. Nrf2 levels of nuclear protein were investigated over a variety of time points. At 2h, Nrf2 protein levels showed a 3 fold induction for 5µM and 10µM SFN treatments **(Figure 16)**. Individual blots show a visible increase of protein expression from DMSO controls up to 10µM SFN. A dose dependent trend can be seen in an accumulated graph, showing 4 individual time points **(see appendix Figure 55, p.143)**.

SFN on TR-1 gene expression in PC-12. Results in **Figure 17** show a dose dependent increase in TR-1 expression on RNA level. After a 4h treatment with 2.5µM SFN, a 2.7 fold increase was determined, while a 3.3 fold increase was found for 5µM treatment. 10µM SFN presented a 3.1 fold increase. HBSS, a positive control of autophagy, halves TR-1 levels compared to control, indicating no involvement of the autophagic pathway in the induction of TR-1 levels by SFN. These results only reflect the average of two biological replicates. 2h and 6h samples were also investigated in single biological replicates, which also showed an increase in TR-1 expression in all SFN-treatment samples, the lowest in 2h samples **(see Appendix Figure 56, p.144)**. **Figure 18** presents a similar picture in protein expression, where the increase was strongest at 5µM SFN concentration after a 24h treatment with SFN.

SFN on HO-1 protein expression in PC-12. Results presented in duplicates show a several fold increase of HO-1 protein levels when cells were treated with 10µM (5 fold) and 20µM (25 fold) SFN for 24h. Lower concentrations (2.5µM and 5µM SFN) only produced minor change **(Figure 19).** This antibody presented itself as a dimer. Hardly any bands were visible at the expected size of 30-33kDa, however, at ~60kDa strong bands could be detected. This phenomenon has been described within the antibody data sheet, but also by Hwang *et al.* (2009) documenting that HO-1 is in fact more stable and functions better as a dimer/oligomer in the ER.

SFN on GST gene expression in PC-12. 4hour treatment with SFN shows a 6-8 fold increase in 2.5, 5 and 10µM treatments, however in a non-dose dependant manner **(Figure 20)**. HBSS, a positive control for autophagy, showed a decrease in GST levels, suggesting that autophagy does not play a role in the induction of GST by SFN, as would be expected. These results only reflect the average of two biological replicates. 2h and 6h samples were also investigated in single biological replicates, which showed a lower induction of GST by SFN **(see Appendix Figure 57, p.145).**

SFN on TR-1 and GST gene expression in SH-SY5Y. In SH-SY5Y cells, 2h exposure to SFN could not elevate TR-1 levels higher than 1.4-fold compared to control. However, after 6h of SFN treatment induction of up to 3.2 fold (2.5µM SFN) could be observed **(see Appendix Figure 58, p.145)**. Looking at GST levels, a dose-dependent response was observed. The lowest SFN concentrations presented a 2-fold increase compared to control samples both after 2 and 6 hours **(see Appendix Figure 59, p.146)**. The highest induction of GST gene expression levels was found in the 2hour sample of 5µM SFN treatment. These experiments were only carried out with one biological replicate, as they were preliminary investigations only, and therefore would need further repeats to be of significant value.

Short interfering RNA (siRNA) was introduced to mimic a knock down of both GST and TR-1, and an optimal dosage of 10nM siGST and siTR-1 could be determined by qPCR to be used in future experiments on cell protective effects of SFN in GST or TR-1 reduced PC-12 cells (data not shown).

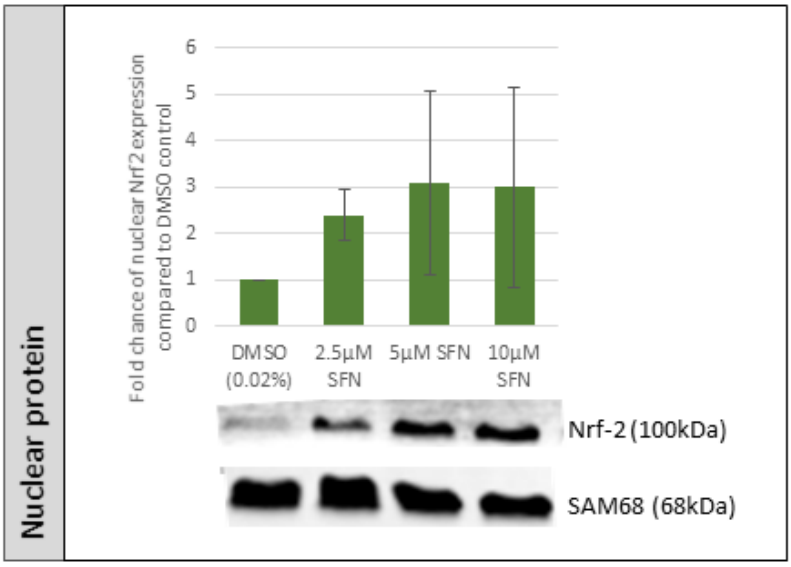

Figure 16: Nrf2 expression in PC-12 cells after 2h SFN treatment as determined by western blot.
PC-12 cells were treated with DMSO (0.02%) or various concentrations of SFN (2.5-10µM) for 2h. Nuclear protein was collected and blots were imaged using Odyssey. The graph shows the average of two biological replicates (n=2; ±SD).

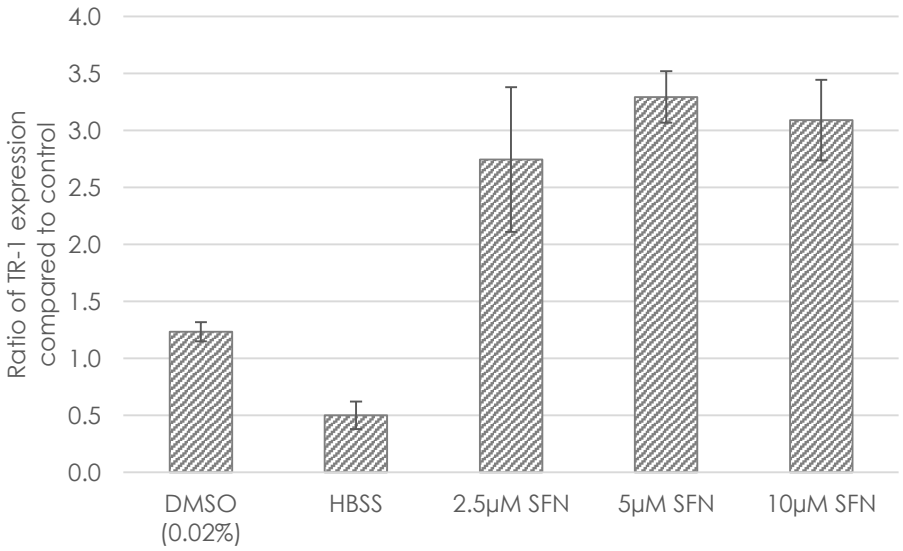

Figure 17: TR-1 expression in PC-12 cells after 4h SFN treatment as determined by qPCR.
Cells were treated with media alone, DMSO (0.02%), HBSS and different concentrations of SFN (2.5-10µM) for 4h. 18S rRNA was used as housekeeping gene. Bars show qPCR results as fold change compared to control samples. Each bar represents the average of two biological replicates carried out in 3 technical replicates (n=2).

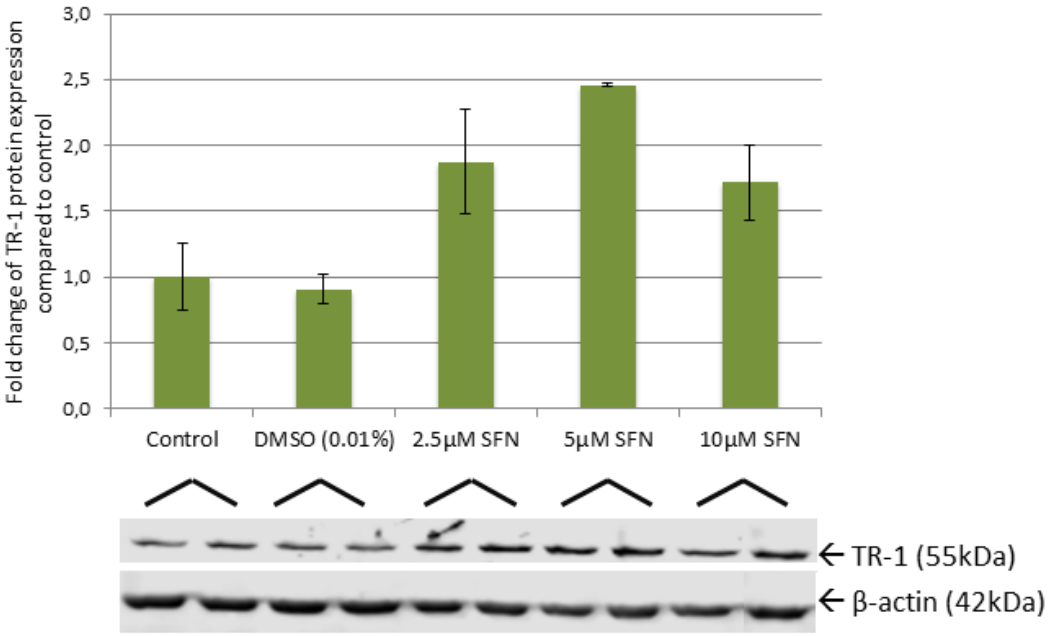

Figure 18: TR-1 expression in PC-12 cells after 24h SFN treatment as determined by western blot.
Cells were treated with media alone, DMSO (0.01%), or various concentrations of SFN (2.5-10µM) for 24h. The blots were imaged by Odyssey and show TR-1 bands at 55kDa and loading control β-actin at 42kDa. The bars represent the average of both biological replicates shown in the western blots (n=2, ±SD).

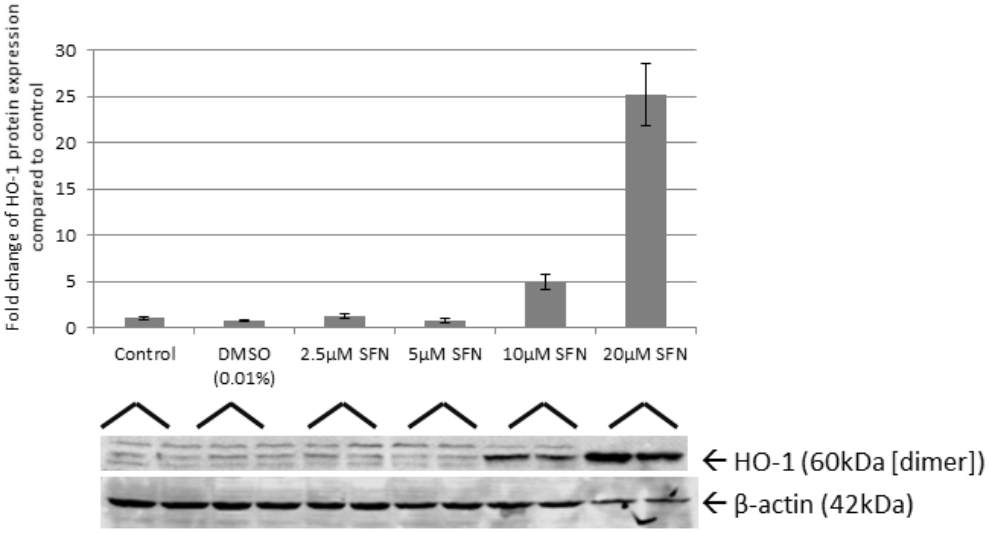

Figure 19: HO-1 expression in PC-12 cells after SFN treatment as determined by western blot.
Cells were treated with control media, DMSO (0,01%) or different SFN concentrations and incubated for 24h. The blots were imaged by Odyssey and show HO-1 bands at 60kDa and loading control β-actin at 42kDa. The bars represent the average of both biological replicates shown in the western blots (n=2; ±SD).

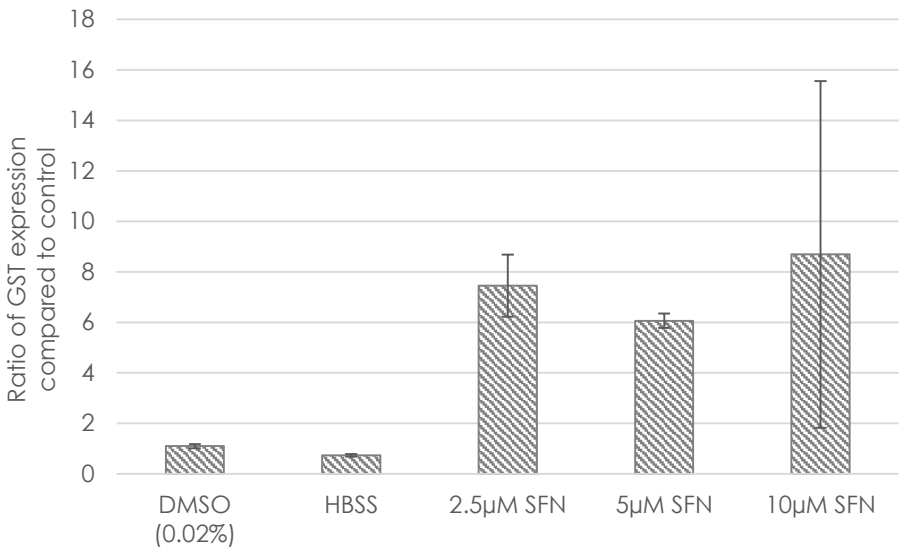

Figure 20: GST expression in PC-12 cells after 4h SFN treatment as determined by qPCR.
Cells were treated with media alone, DMSO (0.02%), HBSS or various concentrations of SFN (2.5-10µM) for 4h. 18S rRNA was used as housekeeping gene. Bars show qPCR results as fold change compared to control samples. Each bar represents the average of two biological replicates, carried out in 3 technical replicates (n=2; ±SD).

3.2.4 SULFORAPHANE AND AUTOPHAGY

Several experiments were carried out to investigate the effect of SFN on PC-12 and SH-SY5Y cells in relation to autophagy. For western blotting, a reliable method using the Odyssey imaging technique was developed (see page 53). The main target investigated is LC3-II, an autophagy related protein necessary for autophagosome formation. It is derived from LC3-I by the use of Atg7 and Atg3 (more detail on page 38). Also, transient transfections with various plasmids connected to autophagy were carried out.

Effect of SFN on LC3-II in PC-12 cells. SFN induced LC3-II protein levels in western blot experiments. The optimal dose, determined by a dose-response experiment was 10μM, which was taken further into a time-response experiment **(Figure 21)**. 20μM showed a greater effect (5 fold induction), however, at this concentration there is also the risk of reducing cell viability. The results of this experiment suggests that 3 hours was the most effective treatment time to observe LC3-II induction in PC-12 cells (data not shown).

Effect of SFN on p62 expression in PC-12 cells. Figure 22 shows a time-dependent induction of p62 protein levels after treatment with 5μM SFN. However, the positive controls for autophagy torin and HBSS reduce p62 levels, showing the opposite result to that observed in SFN-treated samples. This can be explained by the fact that p62 also interacts with Nrf2, another major target of SFN (explained in more detail on page 42). By taking into account the rise of p62 through the positive feedback loop with Nrf2 and SFN inducing Nrf2 however, one should expect p62 levels to rise in the presence of SFN. This makes it difficult to interpret the results on p62 levels, as it does not clearly state that autophagy is present.

Effect of SFN on LC3-II in SH-SY5Y cells. In **Figure 23**, a dose-dependent induction of LC3-II protein levels was observed. Even levels as low as 5μM SFN show a 3-fold increase, gradually rising to almost 23-fold (mean) activation in 20μM SFN samples.

Effect of SFN on p62 in SH-SY5Y cells. As explained above in PC-12 cells, SFN does not show the expected results in relation to autophagy. This can also be seen in **Figure 24**, as a clear dose-response from 2.5μM to 20μM SFN can be seen after 24h treatment, resulting in almost 25-fold increase compared to control samples. The high variability in the data within the 4 biological replicates means that the results

are not statistically important, although in one 20µM sample a 62-fold increase was observed compared to the control.

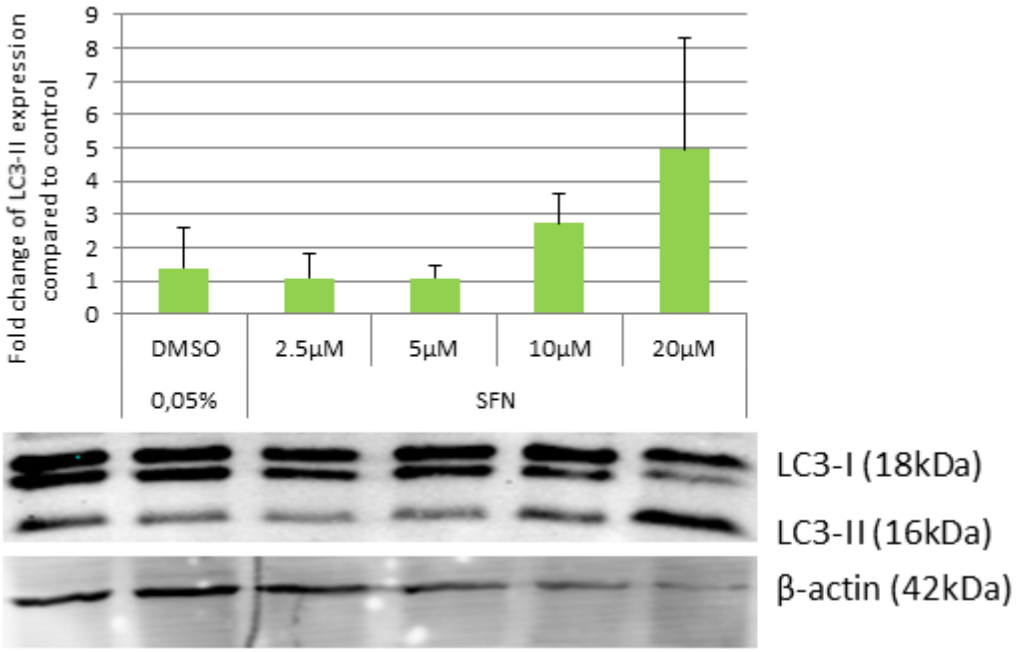

Figure 21: LC3-II expression in PC-12 cells as determined by western blot.
Cells were cultured either in media alone, in DMSO (0.05%) or in various concentrations of SFN (2.5-20µM) for 17h. The blots were imaged using Odyssey and show LC3-I bands at 18kDa, LC3-II at 16kDa and loading control β-actin at 42kDa.The graph shows the quantification of LC3-II after normalisation with β-actin expressed as fold change compared to control. The bars represent the average of 3 blots (n=3, ±SD).

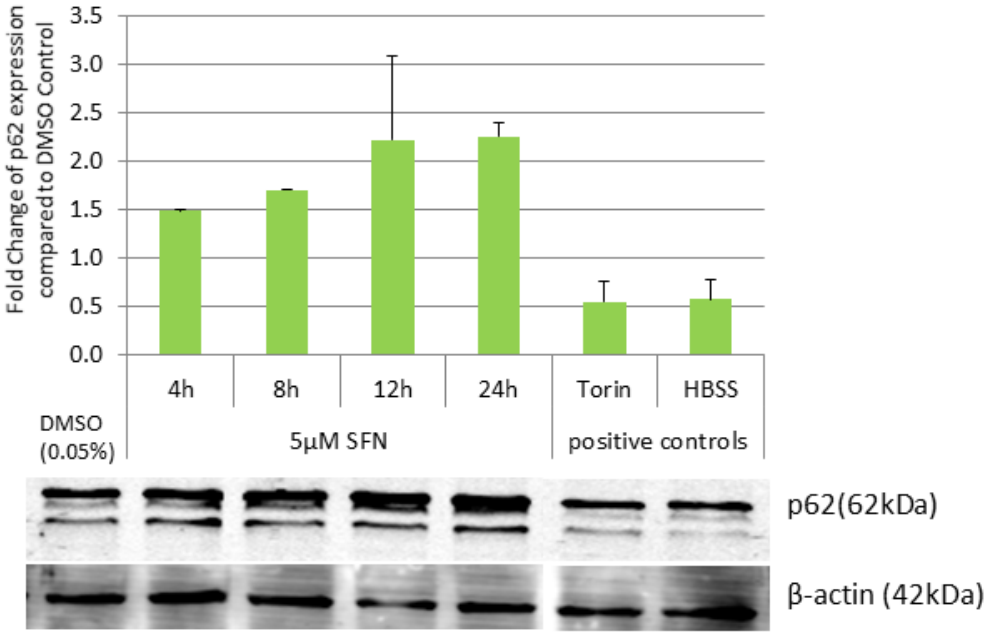

Figure 22: p62 expression in PC12 cells as determined by sestern blot.
Cells were cultured either in DMSO (0.05%), Torin (250nM), HBSS or 5µM SFN for 4, 8, 12 and 24h. The blots were imaged using Odyssey and show p62 bands at 62kDa and β-actin at 42kDa. The graph shows the quantification of p62 after normalisation with β-actin expressed as fold change compared to DMSO control. The bars represent the average of 2 blots (n=2, ±SD).

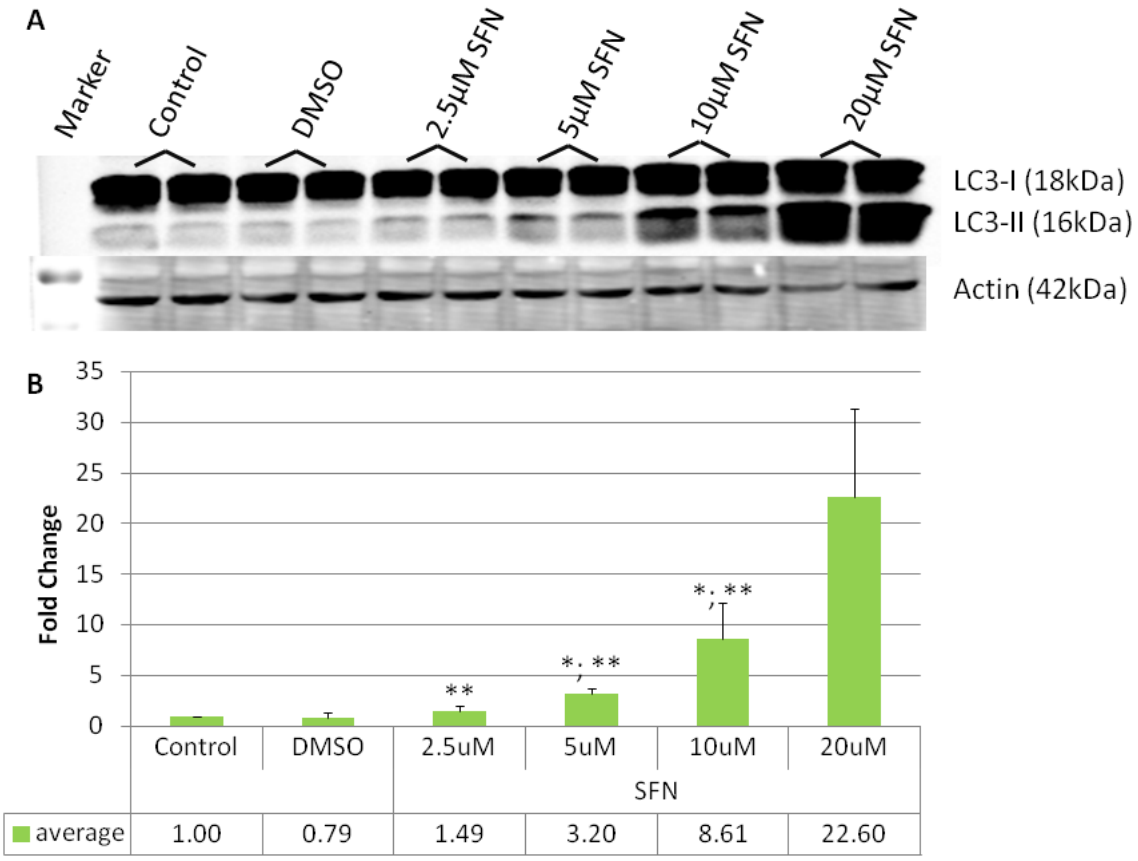

Figure 23: LC3-II expression in SH-SY5Y cells after a 24h treatment with SFN as determined by western blot.
A Cells were cultured in media, DMSO (0.02%) or various concentrations of SFN (2.5-20µM) for 24h. Appropriate amounts of DMSO were added to each SFN sample to adjust for equal amounts. The blots were imaged by Odyssey and show LC3-I bands at 18kDa, LC3-II at 16kDa and loading control β-actin at 42kDa.
B shows the quantification of LC3-II after normalisation against β-actin. Each bar represents the average of 4 biological replicates (n=4; ±SD). Statistical significance compared to control samples *, or to DMSO samples ** (P<0.05).

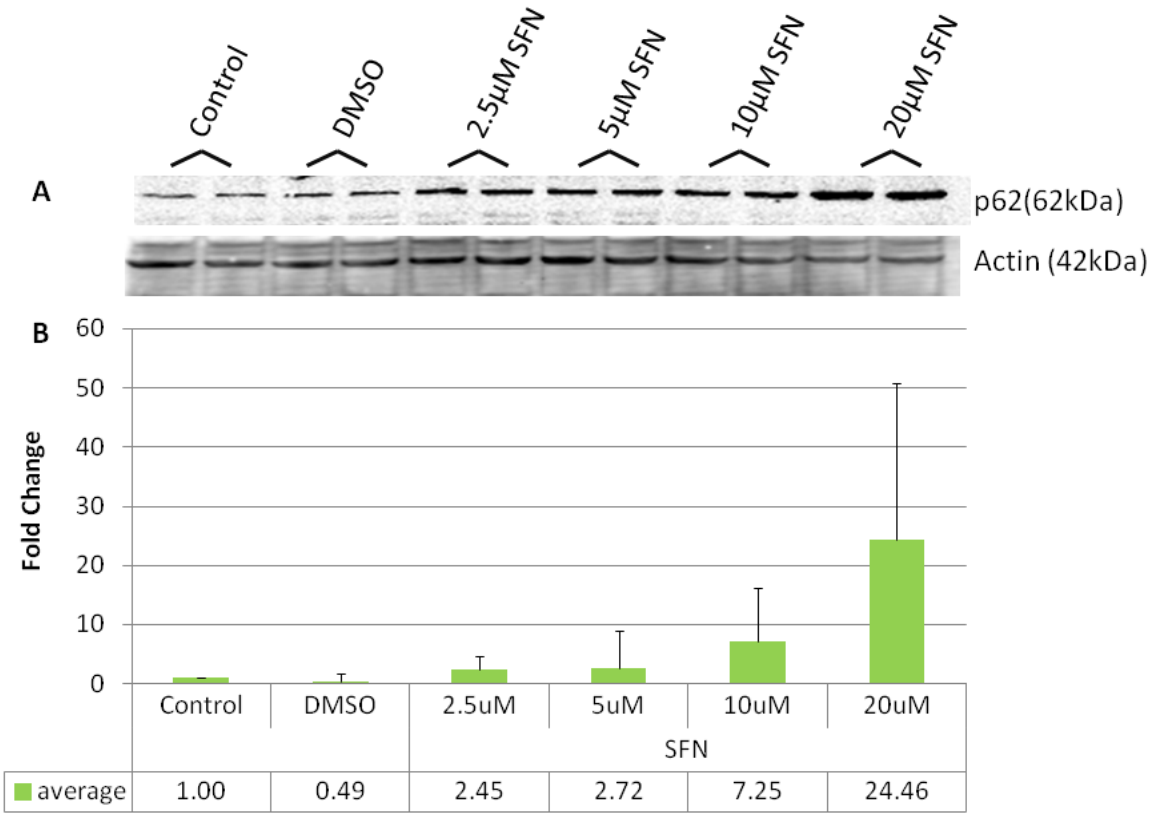

Figure 24: p62 expression in SH-SY5Y cells after a 24h treatment with SFN as determined by western blot.
A Cells were cultured in media, DMSO (0.02%) or various concentrations of SFN (2.5-20µM) for 24h. Appropriate amounts of DMSO were added for adjustment of equal DMSO amounts. The blots were imaged by Odyssey and present p62 bands at 62kDa and the loading control β-actin at 42kDa. **B** Each bar represents the average of 4 biological replicates after normalisation against β-actin (n=4; ±SD)

Bafilomycin experiment. To assess the autophagic flux, the lysosome-inhibitor bafilomycin (BAF) was added either alone or in combination with SFN. The results presented in **Figure 25** show that samples treated with BAF mostly induce LC3-II production. SFN on its own moderately increases LC3-II levels, while the combination of BAF and SFN can induce LC3-II bands between 4 and 12 fold in 4h and 8h treatments compared to control samples only treated with DMSO. These observations indicate that SFN mostly induces autophagy by enhancing autophagosome synthesis, but also increases autophagosome degradation, which explains the reduced or unchanged LC3-II levels after only SFN treatment. As these findings are simply momentary observations of the dynamic process autophagy, the results can only verify that SFN is inducing autophagy and suggest that increase of autophagosome synthesis plays the major role in the mechanism involved.

Transient transfections on PC-12 cells. The clearest results to visualize the autophagic process were obtained by the transfection with the p62-tomato red and mRFP/GFP-LC3 plasmids.

p62-transfected cells show increased punctae-formation from 2.5, 5 and 10µM SFN treated cells **Figure 26**. These punctae represent autophagosomes, in which p62 is present until degraded within the autolysosome. In this experiment, induced p62-levels are already present after 4 hours.

The tandem- or traffic light- plasmid mRFP/GFP-LC3 helps elucidate a time pattern for the autophagic process. **Figure 27** shows the images obtained after 4 hour treatment with media only, DMSO in media, HBSS or 2.5, 5 and 10µM SFN. As the punctae seen in this figure are all orange, and also the separate channels GFP and mRFP seem to overlap, there does not appear to be any autolysosome formation present.

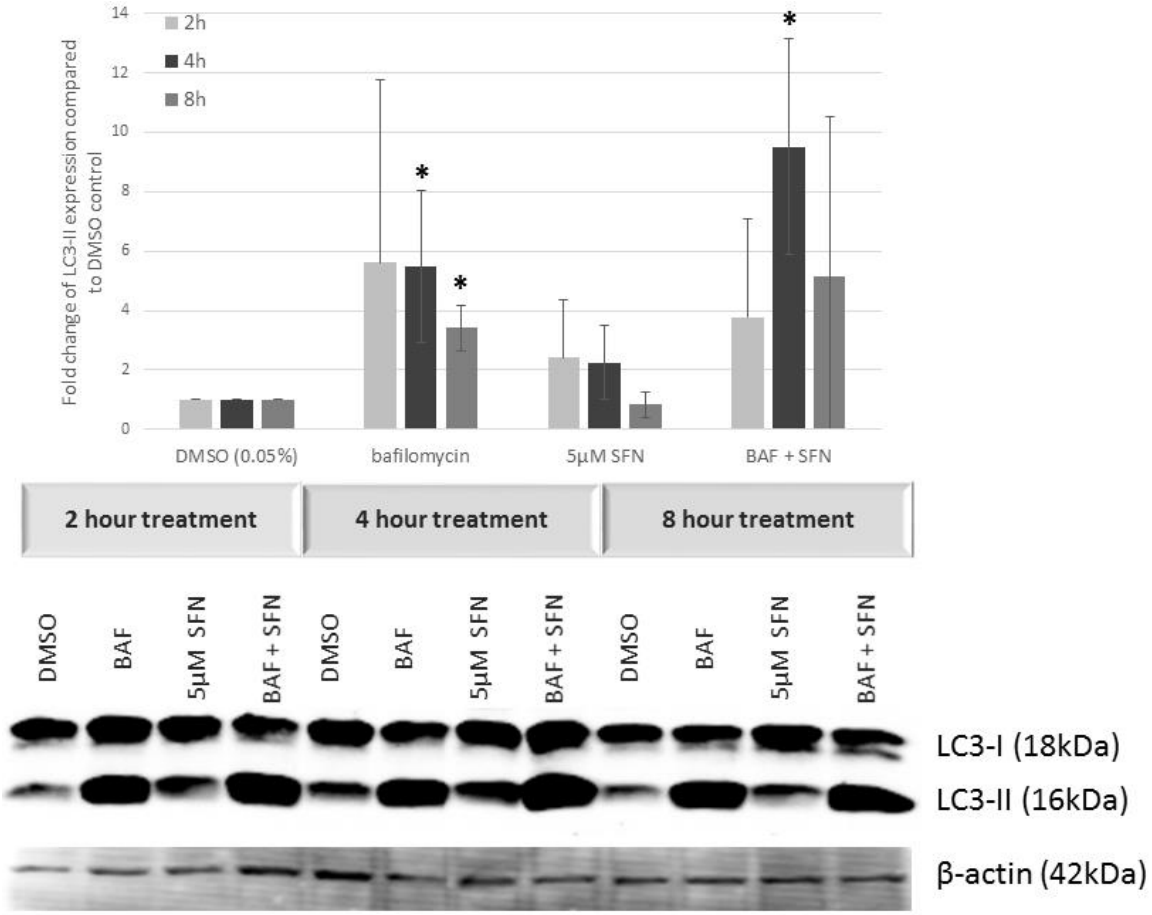

Figure 25: Bafilomycin (lysosome inhibitor) on PC-12 cells.
Cells were cultured in either DMSO (0.05%), 100nM bafilomycin (BAF; lysosome inhibitor), 5µM SFN or the combination of BAF and SFN for 2, 4 or 8 ours. The blots were imaged by Odyssey and show LC3-I bands at 18kDa, LC3-II at 16kDa and loading control β-actin at 42kDa. The graph shows the quantification of LC3-II after normalisation against β-actin expressed as fold change compared to vehicle control (0.05% DMSO). Each bar represents the average of 4 biological replicates (n=4; ±SD).

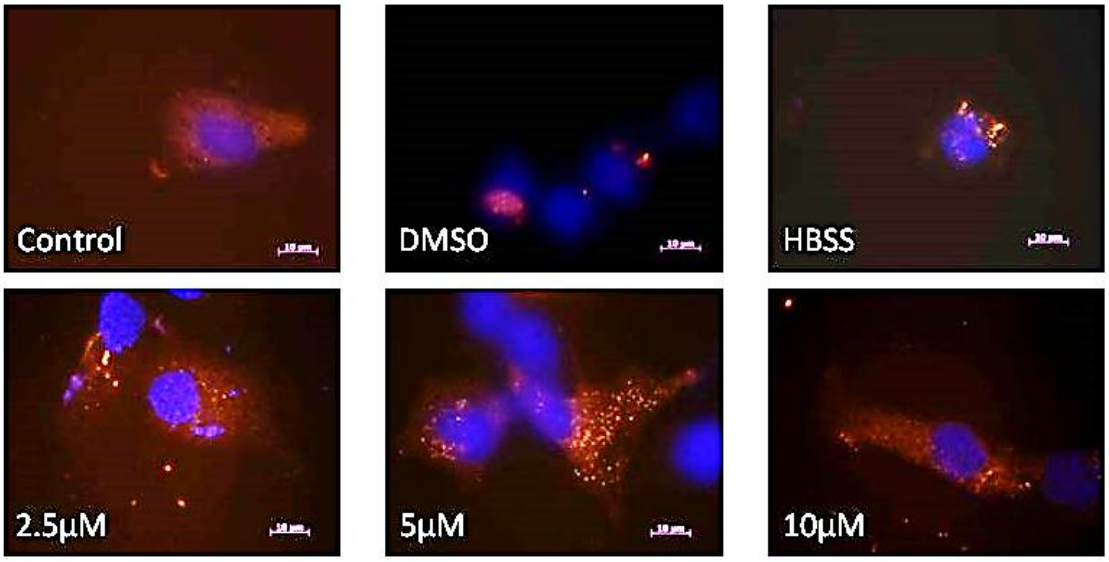

Figure 26: Transient Transfection of PC-12 cells with p62 tomato red plasmid. Cells were cultured for 4 hours in either media alone, DMSO (0.025%), HBSS or various concentrations of SFN (2.5-10µM). DMSO was added where necessary to reach equal amounts. The scale bar shows 10µm.

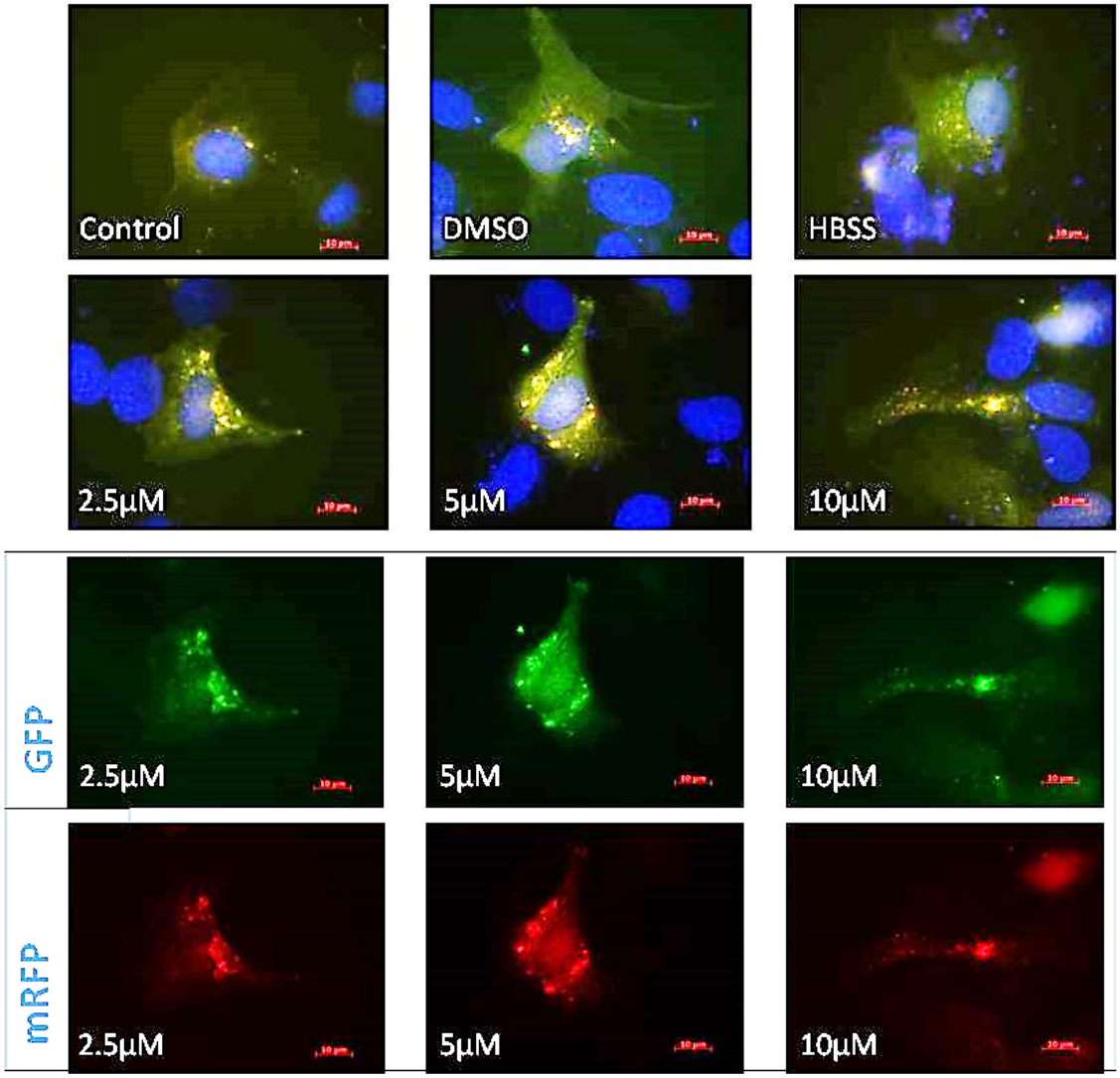

Figure 27: Transient transfection on PC-12 cells with mRFP/GFP-LC3 plasmid.
Cells were cultured for 4 hours in either media, DMSO (0.025%), HBSS, or various concentrations of SFN (2.5-10µM). DMSO was added to SFN samples when necessary to reach equal amounts. Pictures shown represent 100x magnification under the fluorescent microscope, scale bars show 10µm. The top 2 rows show merged images, while the nest two rows only present the green or red channel, as indicated.

3.2.5 NEUROPROTECTIVE EFFECTS OF SULFORAPHANE ON PC-12, DIFF PC-12 AND SH-SY5Y CELLS

3.2.5.1 SULFORAPHANE ON APOPTOSIS

Dose-dependent increase of apoptosis by SFN in PC-12 cells. A preliminary experiment was conducted to measure the effect of SFN on apoptosis in PC-12 cells and determine a concentration of SFN to use for further experiments. The AnnexinV/PI Flow Cytometry results **(see appendix Figure 60, p.147; gating see Figure 51, p.138)** show that 1.25, 2.5, 5 and 10µM SFN increases apoptosis in a dose-responsive manner. It was decided to use 2.5µM SFN in future experiments.

3.2.5.2 NEUROPROTECTIVE EFFECTS OF SULFORAPHANE ON PC-12 CELLS

Cell-protective effect of SFN against H_2O_2-induced apoptosis in PC-12 cells. H_2O_2 was used to induce apoptosis and investigate if SFN pre-treatment can protect these cells **(Figure 28; gating see Figure 49; p.136)**. 600µM H_2O_2 reduced cell viability to 40% and 800µM H_2O_2 to 35%, on average. SFN-pre-treated samples increased the numbers of viable cells to 63% and 61%, respectively. The average recovery rate was 25% for both 600 and 800µM H_2O_2 samples. However, the standard deviation hides the great differences that could be seen within individual data sets **(see appendix Figure 61, p.148)**, which can be explained by slightly different confluency stages at the start of the experiments. From this point onwards, experiments were seeded and treated at the exactly same time in the day to increase experiment reliability.

Cell-protective effect of SFN against 6-OHDA-induced apoptosis in PC-12 cells. Cells pre-treated with 2.5µM SFN show a higher resistance against 6-OHDA (another cytotoxin and ER-stress inducer) than untreated. **Figure 29** shows the percentage of events in the healthy cells gate (AnnexinV-/PI-) **(gating see Figure 50, p.137)**. 600µM 6-OHDA reduced the percentage to 34,97%, 800µM 6-OHDA even to 21,75%. Cells pre-treated with SFN however presented 50.99% (+600µM 6-OHDA) and 38.76% (+800µM 6-OHDA) in an average of 6 biological replicates, which is a recovery of 15,74% and 17,57% with $P<0,01$.

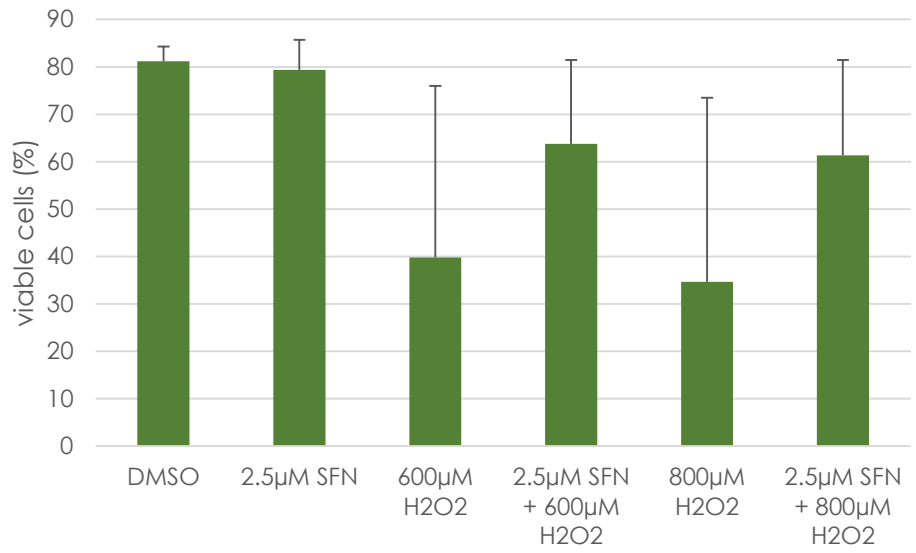

Figure 28: Effect of SFN on H_2O_2-induced apoptosis in PC-12 cells measured by flow cytometry.
Cells were pre-treated with either DMSO (0.025%) or 2.5µM SFN for 24h. Then these solutions were replaced with either serum-free media, 600µM or 800µM H_2O_2 for another 24h. The collected samples were analysed using the AnnexinV/PI kit and a flow cytometer. Bars are the average of 4 biological replicates with about 10.000 events each (n=4; ±SD).

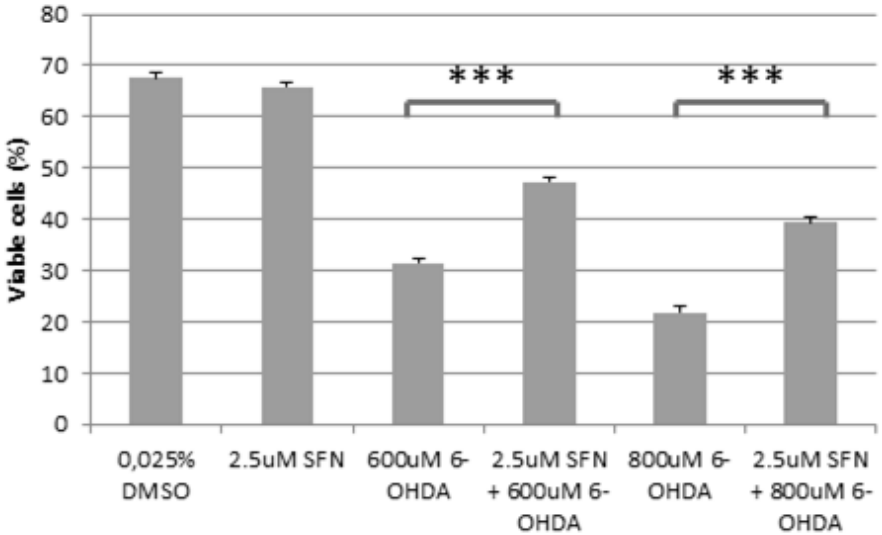

Figure 29: Effect of SFN on 6-OHDA-induced apoptosis in PC-12 cells measured by flow cytometry.
Cells were pre-treated with 0.025% DMSO or 2.5µM SFN for 24h and then treated with either serum-free media or 6-OHDA (600 and 800µM) in serum free media. Each bar shows the percentage of viable cells and represents the average of 6 biological replicates with 10.000 events each (n=6; ±SD; ***P<0.01).

3.2.5.3 NEUROPROTECTIVE EFFECTS OF SULFORAPHANE ON DIFF PC-12 CELLS

Cell-protective effect of SFN against H_2O_2-induced apoptosis in PC-12 cells. Cells pre-treated with 2.5µM SFN show a higher resistance against H_2O_2 than untreated. **Figure 30** shows the percentage of events in the healthy cells gate (AnnexinV-/PI-). Cells pre-treated with SFN reduced the percentage of apoptotic cells induced by 300µM H_2O_2 highly significantly (P<0.01), while SFN rescued cells exposed to 500µM H_2O_2 significantly (P<0.02).

3.2.5.4 NEUROPROTECTIVE EFFECTS OF SULFORAPHANE ON SH-SY5Y CELLS

Cell-protective effect of SFN against H_2O_2-induced apoptosis in SH-SY5Y cells. AnnexinV/PI assays have also been carried out on SH-SY5Y cells showing minor cytoprotection (data not shown).

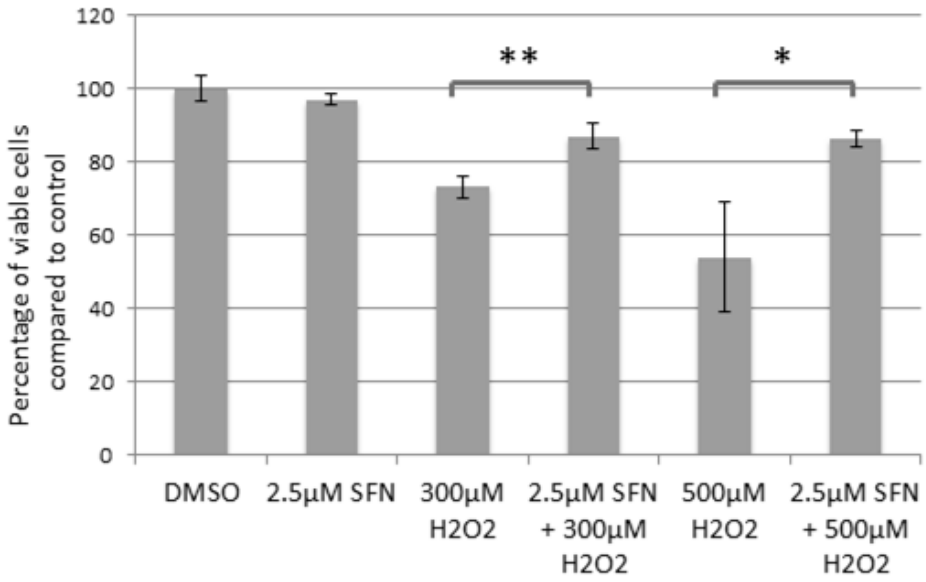

Figure 30: Effect of SFN on H_2O_2-induced apoptosis in DIFF PC-12 cells measured by Flow Cytometry.
Cells were pre-treated with media or 2.5µM SFN for 24 hours and then treated with either serum-free media, 300 or 500µM H_2O_2 in serum-free media. Each bar shows the percentage of gates of viable cells and represents an average of 4 biological replicates with 10.000 events investigated by AnnexinV/PI (n=4; **P<0,01; *P<0,02).

3.3 SUMMARY

The data presented in this chapter confirm that SFN has similar effects on neuronal cells as previously reported on other cell lines (see 1.1.5).

The effects of SFN on the cell cycle in PC-12 and SH-SY5Y cells suggest a dose-dependent increase in the S-phase of the cell cycle, while results in DIFF PC-12 could not be obtained due to polyploidy (data not shown). This however is an indirect confirmation that the PC-12 cells have actually differentiated (Ignatius et al. 1985).

In PC-12 cells SFN also increased nuclear protein levels of Nrf2 as well as the Nrf2/ARE driven enzymes GST and TR-1 at mRNA levels and HO-1 on protein level.

SFN dose-dependently induces autophagy and apoptosis in PC-12 and SH-SY5Y cells. Autophagy was measured by LC3-II and p62 formation at a protein level, transient transfections with autophagy-related plasmids as well as LC3 flux. A positive feedback loop between Nrf2 and p62 lead to an increase of p62 samples rather than a reduction. Torin and HBSS were used as positive autophagy controls. An experiment to assess autophagic flux assessed that SFN is likely increasing LC-II levels by enhanced autophagosome formation rather than by inhibition of its degradation.

Further, results of apoptosis assays have shown cell protective properties of SFN against H_2O_2- and 6-OHDA- induced apoptosis in all three cell lines at low dose.

4 EFFECT OF SULFORAPHANE ON THE EXPRESSION OF DJ-1 AND ER-STRESS

4.1 INTRODUCTION

DJ-1, or PARK7, is a multifunctional protein associated with Parkinson's disease (PD) pathogenesis. It contains 189 amino-acids and belongs to the Thi/PfpI protein superfamily (Gan et al. 2010). DJ-1 possesses antioxidant capabilities, but has also been associated with cancer. When mutated, it has been linked to recessively inherited Parkinson's Disease (PD), while wildtype DJ-1 has been shown to protect neuronal cells by removing H_2O_2 in response to oxidative stress (Rannikko et al. 2012; Bandopadhyay et al. 2004). The lack of DJ-1 has also been associated with COPD, which is a disease that presents a decline in Nrf2-regulated antioxidants (Malhotra et al. 2008). DJ-1 is highly expressed in human brain cells (Bandopadhyay et al. 2004).

Choi *et al.* (2006) observed that DJ-1 was irreversibly oxidised in brains of patients with idiopathic AD and PD. Brain tissues from five PD cases and five AD cases showed an increase in total DJ-1 protein compared to five healthy non-demented control subjects, especially in the acidic isoforms of the monomer of DJ-1. Also, cysteine and methionine oxidation of DJ-1 could be detected in PD and AD samples (Choi et al. 2006).

Studies on DJ-1-deficient mice have shown indistinct motor deficits and minor nigrostriatal dopaminergic dysfunctions as well as higher sensitivity towards some toxins, but interestingly none of the mice from these studies presented characteristics of PD such as loss of dopaminergic neurons, nor any major behavioural phenotype (Henchcliffe & Beal 2008; Pham et al. 2010). Possibly unknown mechanism take over the role of DJ-1 to protect healthy animals against the loss of DJ-1. Pham *et al.* (2010) undertook further research and found that DJ-1 knockout (KO) mice demonstrated a reduction in dopamine-producing neurons in the ventral tegmental area as well as minor changes in behaviour, for instance motivational and cognitive dysfunction. Lastly, this study also shows that these KO

mice exhibit different measures to compensate the lack of DJ-1, which may be the reason no more severe phenotypes were observed - supporting the hypothesis of PD being a multifactorial disease.

Many reports have found a correlation between the absence of DJ-1 and increased vulnerability to toxins. Lev *et al.* (2013) used DJ-1 KO mice to demonstrate enhanced sensitivity towards 6-OHDA insults compared to wild-type (WT) astrocytes. The DJ-1 KO showed a lower ability to counteract 6-OHDA-induced oxidative stress via the cellular mechanisms Nrf2 and HO-1. Also, the activation of the Nrf2 pathway appeared impaired in DJ-1 KO astrocytes compared to WT (Lev et al. 2013).

DJ-1 is understood to be an important stabiliser of Nrf2 after its dissociation from Keap1 (Clements et al. 2006). Another, more recent study has suggested the activation of Nrf2 to be downstream from DJ-1, and that the DJ-1/Nrf2/TR1 interplay is important in the cellular response to oxidative stress (Im et al. 2012). Contradictory to these reports, Gan *et al.* (2010) found the Nrf2/ARE pathway to be independent of DJ-1. They demonstrated that the Nrf2 activator tBHQ was able to protect primary cortical neurons from DJ-1 KO as well as WT mice. Yokota *et al.* (2003) investigated the mechanisms of neuronal cell death caused by absence or mutations of DJ-1 and found oxidative stress, ER stress and proteasome inhibition to be the inducers that can be influenced by DJ-1. Ziaei *et al.* (2013) showed that SFN could increase DJ-1 protein levels in primary corneal endothelial cells obtained from patients suffering from Fuchs endothelial corneal dystrophy. These cells demonstrated a lower expression of DJ-1 than regular corneal endothelial cells, however, after SFN treatment protein expression was improved. Their conclusion was that Nrf2 and DJ-1 were acting dependant of each other, but their results did not answer which of the two is the instigating part.

Although a few other research groups have briefly mentioned DJ-1 in context of SFN, none have investigated this relationship in depth. Our aim was therefore to investigate the influence SFN has on DJ-1, if it can protect PC-12 cells from ER-stress and if DJ-1 is connected to that.

Figure 31 shows the presumed relationship between SFN, DJ-1, Nrf2 and autophagy, based on several publications (Clements et al. 2006; Im et al. 2012).

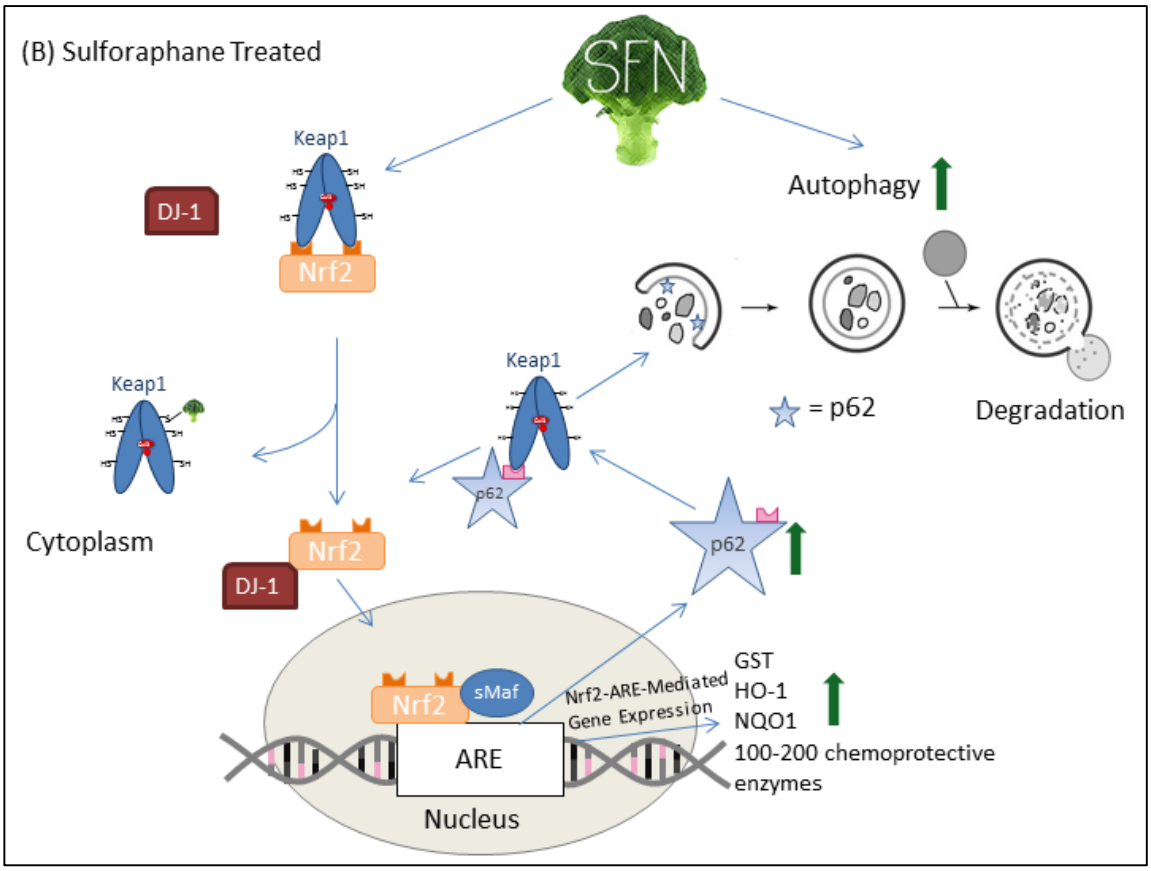

Figure 31: SFN/Nrf2/autophagy graph including DJ-1
This simplified graph shows how DJ-1 fits into the SFN/Nrf2/autophagy pathway. It only shows the SFN-triggered pathway. SFN can bind to Keap1 by interacting with the thiol groups of cysteine residing in Keap1 to impair the ubiquitination of Nrf2. With the assistance of DJ-1, Nrf2 then translocates into the nucleus, where it binds to the ARE of cytoprotective genes like GST and HO-1. SFN also increases autophagy, a process that degrades p62 as part of the protein degradation process. However, p62 can also be upregulated by Nrf2, thus binding more Keap1 and, by keeping Keap1 occupied, increasing the amount of free Nrf2 in the cytoplasm.

4.2 RESULTS

4.2.1 INDUCTION OF PROTEIN LEVELS OF DJ-1

Western Blots with total protein as well as cytosolic protein showed that SFN could increase DJ-1 expression in a dose dependent manner. Different SFN-treatment times were investigated to optimise future experiments **(Figure 32, more single replicate western blots can be found in the Appendices Figure 62)**.

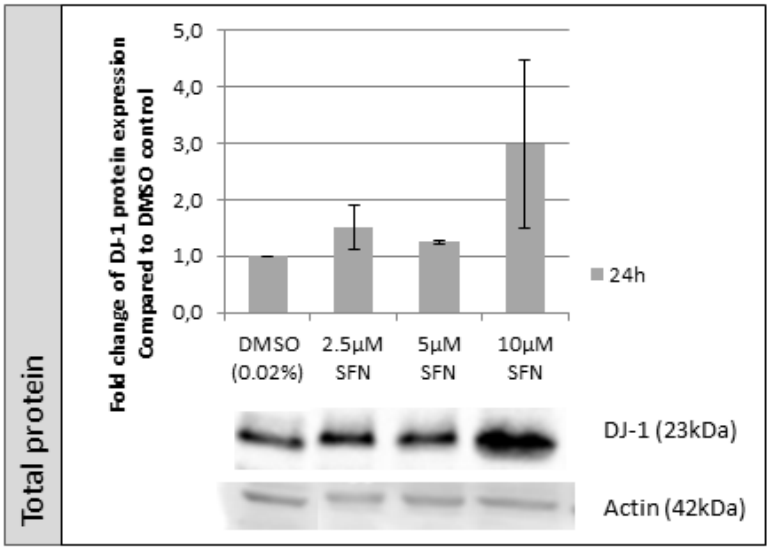

Figure 32: DJ-1 expression in PC-12 cells after SFN treatment as determined by western blot.
Cells were treated with 0.02% DMSO (vehicle control) or different SFN concentrations and incubated for 24h. The blots were imaged using Odyssey and data calculated from DJ-1 bands (23kDa) against β-actin (42kDa). The bars represent the average of two biological replicates, the western blot at the bottom shows one of them.

4.2.2 INFLUENCE OF SULFORAPHANE ON CHOP EXPRESSION UNDER ER-STRESS

First, the ideal concentration of tunicamycin, which is a mixture of homologous antibodies (containing uracil, N-acetyl glycosamine, tunicamine and a fatty acid) and a well-known ER-stress inducer, was ascertained by western blot against the antibody CHOP. CHOP (C/EBP homologous protein) is a protein expressed during ER-stress-mediated apoptosis and is therefore a good marker to measure ER-stress. SFN did not induce CHOP levels thus ER stress, but both 0.5 and 1µg/ml tunicamycin increased CHOP levels at 4h as well as 24h. As this was a basic assessment with sole intention to see if tunicamycin could in fact induce ER-stress and that SFN does not, a single biological replicate seemed adequate. It was determined that a 4h incubation with 1µl/mg tunicamycin is sufficient to increase CHOP levels considerably compared to tunicamycin-free samples **(Figure 33)**.

SFN did not change the tunicamycin-free levels, which were barely detectable, however, it was able to reduce the CHOP levels showing the tunicamycin induced ER-stress significantly. This could be seen for protein levels **(Figure 35)** as well as RNA levels **(Figure 35)**.

In addition, 6-OHDA was applied as an alternative ER-stress inducer, in which SFN also was able to reduce resulting CHOP levels significantly **(Figure 36)**.

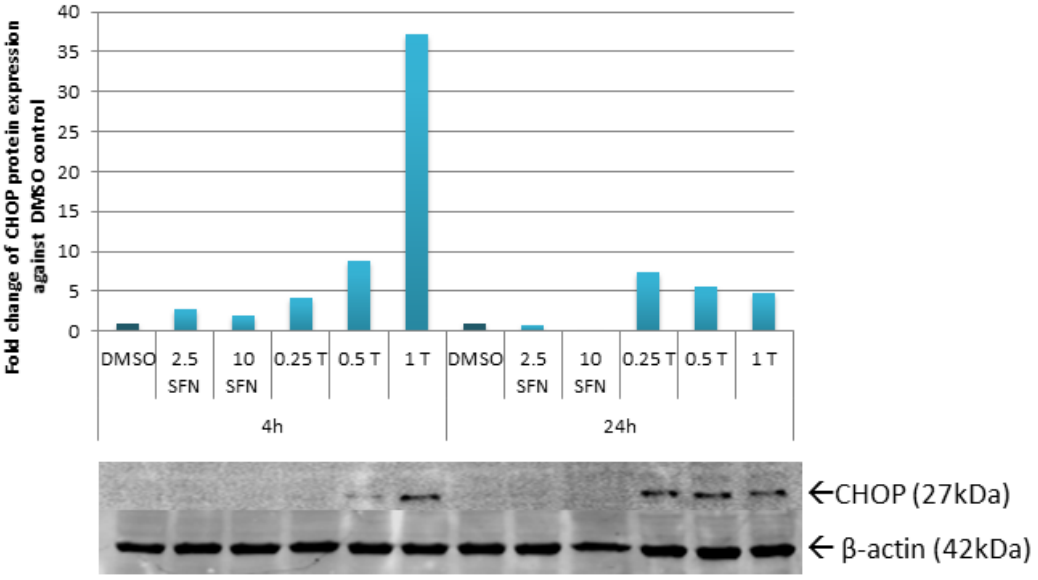

Figure 33: CHOP expression in PC-12 cells after SFN and tunicamycin treatment as determined by western blot.
PC-12 cells were treated with either 0.02% DMSO, 2.5 or 10μM SFN or 0.25, 0.5 and 1μl/mg tunicamycin for either 4h or 24h. The blots were imaged by Odyssey and show CHOP bands at 27kDa and actin at 42kDa. The graph shows the quantification of CHOP after normalisation with β-actin expressed as fold change compared to the vehicle control DMSO at each time point. Each bar represents the one biological replicate shown in the blot below.

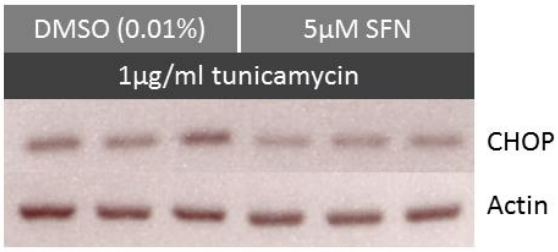

Figure 34: CHOP expression in PC-12 cells after SFN pre-treatment followed by tunicamycin exposure as determined by PCR.
PC-12 cells were treated with 0,02% DMSO or 5μM SFN for 24h prior to a 4h exposure to either DMSO or 1μg/ml tunicamycin. RNA extractions were transcribed into cDNA and then run on an agarose gel before being visualised under UV light.

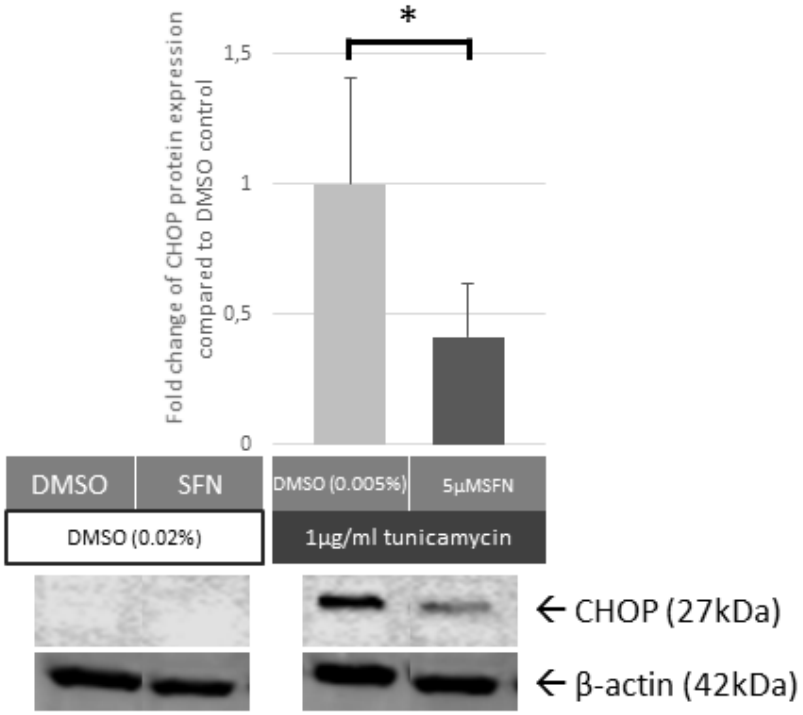

Figure 35: CHOP expression in PC-12 cells after SFN pre-treatment followed by tunicamycin exposure as determined by western blot.
PC-12 cells were treated with 0.02% DMSO or 5µM SFN for 24h. This was replaced 1µg/ml tunicamycin or DMSO for a further 4h exposure. The blots were imaged by Odyssey and show CHOP bands at 27kDa and actin at 42kDa. The graph shows the quantification of CHOP after normalisation with β-actin expressed as fold change compared to the vehicle control DMSO of tunicamycin treated cells. Each bar represents an average of 5 biological replicates.

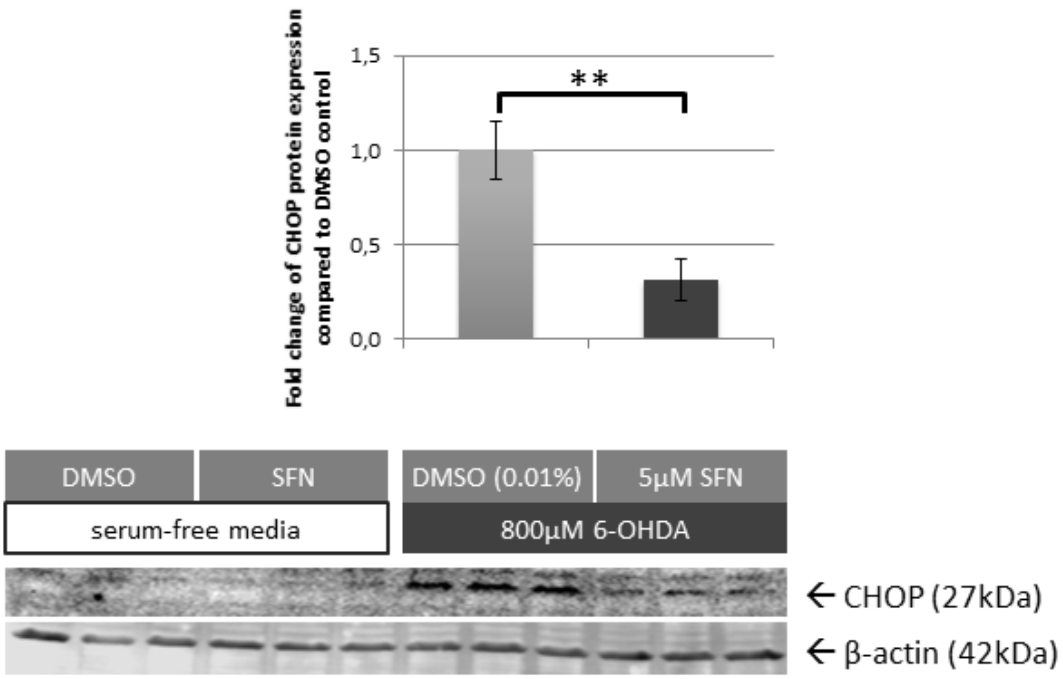

Figure 36: CHOP expression in PC-12 cells after SFN pre-treatment followed by 6-OHDA exposure as determined by western blot.
PC-12 cells were treated with 0.01% DMSO or 5µM SFN for 24h. This was replaced by 800µM 6-OHDA in serum-free media or just serum-free media for a further 4h exposure. The blots were imaged using the Odyssey and show CHOP bands at 27kDa and β-actin at 42kDa. The graph shows the quantification of CHOP after normalisation with β-actin expressed as fold change compared to the vehicle control DMSO. Each bar represents an average of 3 biological replicates. ** P<0.02%.

4.2.3 EFFICIANCY OF DJ-1 KNOCK DOWN USING SIRNA

siDJ-1 was used to simulate DJ-1 knock down in PC-12 cells. The efficiency of this siRNA was then tested with western blot **(Figure 37, B)**. Although the blot shown indicates that siDJ-1 can reduce DJ-1 levels in SFN-treated tunicamycin-free as well as in DMSO-treated tunicamycin samples, this is not the case in any of the others within this data set. This inconsistency could be observed in follow-up experiments. The graph **(Figure 37, A)** shows that overall (n=4) no knock down could be established.

10µM SFN might have been a better choice of concentration to see a proper induction of DJ-1. 3 of these experiments have been carried out on a lower passage number of PC-12 cells, which might be less sensitive to SFN. Due to time constraints these assay optimisation ideas could not be addressed.

The protein collected from the siRNA experiments was also blotted against CHOP to see if DJ-1 is involved in the protective effects of SFN. However, due to the siRNA not showing a consistent knock down, these results are mere speculation. At least they confirm that SFN can significantly reduce tunicamycin-induced ER-stress **(see Appendices Figure 64, graph only showing siRNA-free samples see Figure 35)**.

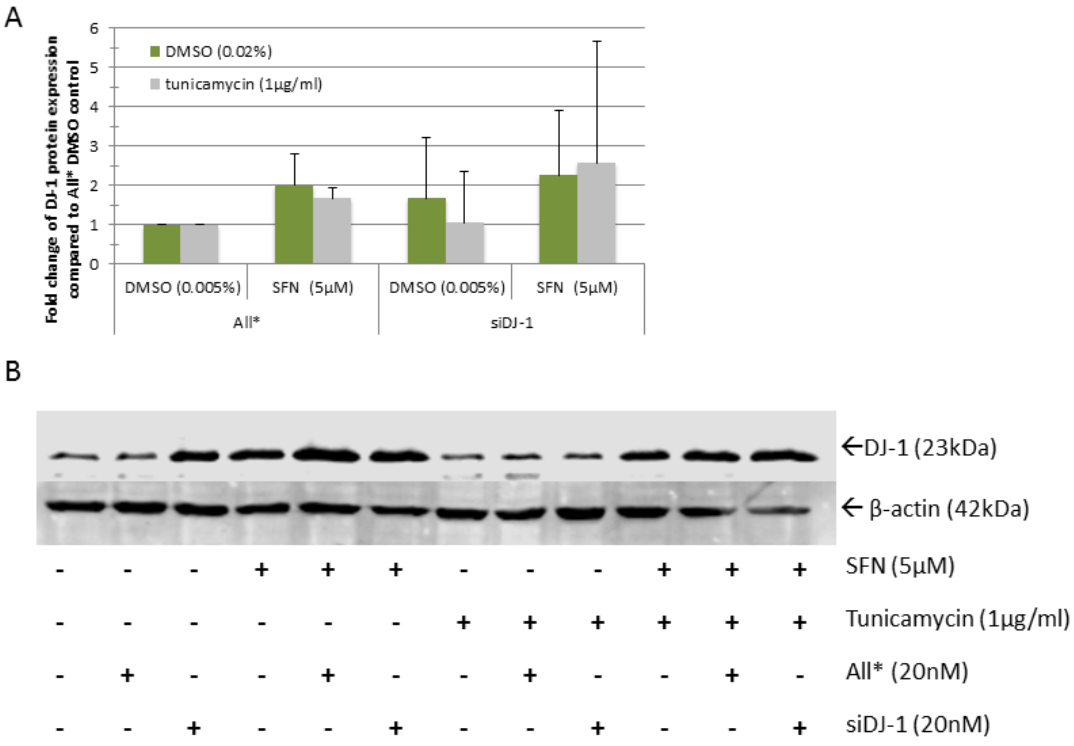

Figure 37: DJ-1 expression in PC-12 cells in siRNA knockdown conditions as determined by western blot.
PC-12 cells were treated with siDJ-1 before starting a 24h incubation with 5µM SFN. This was replaced by 1µg/ml tunicamycin for another 4h, followed by protein extraction. **A** Blots were imaged using Odyssey and show DJ-1 bands at 23kDa and β-actin bands at 42kDa. **B** shows the fold change of normalised DJ-1 protein levels compared to All* DMSO controls. Each bar represents an average of 4 biological replicates.

4.3 SUMMARY

DJ-1 protein levels were elevated after 24h SFN treatment.

ER-stress levels could successfully be induced by 1µg/ml tunicamycin at 4h. SFN did not cause ER-stress, but in fact reduce ER-stress levels created by tunicamycin. This could be shown by investigating CHOP protein levels as well as RNA levels. The western blot results show a highly significant reduction in CHOP levels, while PCR gel results are clearly visible, but were not quantified.

siDJ-1 results were inconclusive. DJ-1 was silenced to investigate any correlation DJ-1 has with ER-stress, and if SFN can still protect PC-12 cells when DJ-1 levels are diminished. Since none of the blots on DJ-1 to review the effectiveness of the siDJ-1 showed consistent results, any changes observed when blotting against CHOP are negated. Thus, this experiment model needs improving.

5 THE ROLE OF AUTOPHAGY IN CELL PROTECTIVE MECHANISMS OF SULFORAPHANE

5.1 BACKGROUND & AIMS

Autophagy has become a popular research field in the recent years. This complex process, which is described in more detail on page 37, is responsible for the organised degradation of proteins and organelles through lysosomes as a response to nutrient limitation to maintain the homeostasis of the cell (Jo et al. 2014). Amongst others illnesses, impaired autophagy has also been connected to neurodegenerative diseases (Metcalf et al. 2012). Autophagy-inducing agents have already shown to have a beneficial therapeutic impact in various mouse models of different neurodegenerative diseases (Nixon 2013).

First reports of SFN on autophagy were carried out in cancer cell lines. Herman-Antosiewicz *et al.* (2006) investigated SFN on pancreatic cancer cell lines PC-3 and LNCaP. They found that SFN could upregulate autophagosome formation and the recruitment of LC3 while also inhibiting the cytosolic release of cytochrome c and apoptotic cell death. When autophagy inhibitor 3-MA was added, LC3 production was reduced and apoptosis upregulated. As cell death of cancer cells by apoptosis is one approach to eliminate cancer, this study focused on the enhancement of apoptosis by adding 3-MA. In the previous chapter 3 (page 65) we could show that SFN is able to induce autophagy in PC-12 and SH-SY5Y cells. This chapter investigates the possibility of autophagy being another important player in the protective effects of SFN. By knocking down or out a gene in autophagy, the effect of SFN cell survival can be tested in an autophagy-deficient or inhibited cell.

First, the efficiency of the two autophagy inhibitors, 3-MA and wortmannin, are assessed. They both block the autophagosome formation by inhibiting PI3K (Triola 2015). However, when knocking down pathways with chemical reagents, this pathway might find substitute routes to restore its activation. Does chemically induced autophagy deficiency reduce the protective effects of SFN against

apoptosis? The development of Atg16L1 KO mice enabled an alternative methodology to chemical inhibition.

The protective effects or SFN was shown in many different scenarios and has mostly been linked to the activation of Nrf2 (Guerrero-Beltrán et al. 2012; Tarozzi et al. 2013). Through the liberation of phase II enzymes as a reaction to oxidative stress, the cell can break down the harmful intruders like H_2O_2, 6-OHDA or other cytotoxins. In the absence of Nrf2-driven enzymes, SFN is still able to protect cells, to an extent, from toxin-induced cell death, suggesting the involvement of other pathways, such as autophagy.

5.2 RESULTS

5.2.1 NEUROPROTECTIVE EFFECTS OF SULFORAPHANE WITH PART INHIBITION OF AUTOPHAGY

3-MA and wortmannin did not significantly inhibit autophagy in PC-12 cells.

Western blots were carried out to investigate the inhibition efficiency of the autophagy inhibitors wortmannin and 3-MA **(Figure 38 and Figure 39)**. Wortmannin was blotted against the autophagy marker LC3-II. 5µM SFN on its own increased LC3-II levels. However, when paired with wortmannin (100nM), it still showed a minor increase in LC3-II protein levels, meaning that autophagosome formation was still possible.

A similar result could be observed with 3-MA (5mM). LC3-II levels were still significantly increased when 3-MA was given together with SFN.

With both inhibitors, a wide variation occurred, which also suggests unreliability. Therefore, alternative methods might be more suitable to study the protective effects of SFN in an autophagy-free environment.

SFN decreased H_2O_2-induced apoptosis in presence of 3-MA. Results suggest that SFN cannot rescue as many cells from H_2O_2-induced apoptosis in the presence of 3-MA. Instead of increasing the number of healthy cells up to almost 90%, only 80% healthy cells could be measured **(see Appendix Figure 65, p.153)** However, due to the fact that autophagy could not be fully suppressed **(as seen in Figure 39)**, these results were not explored further.

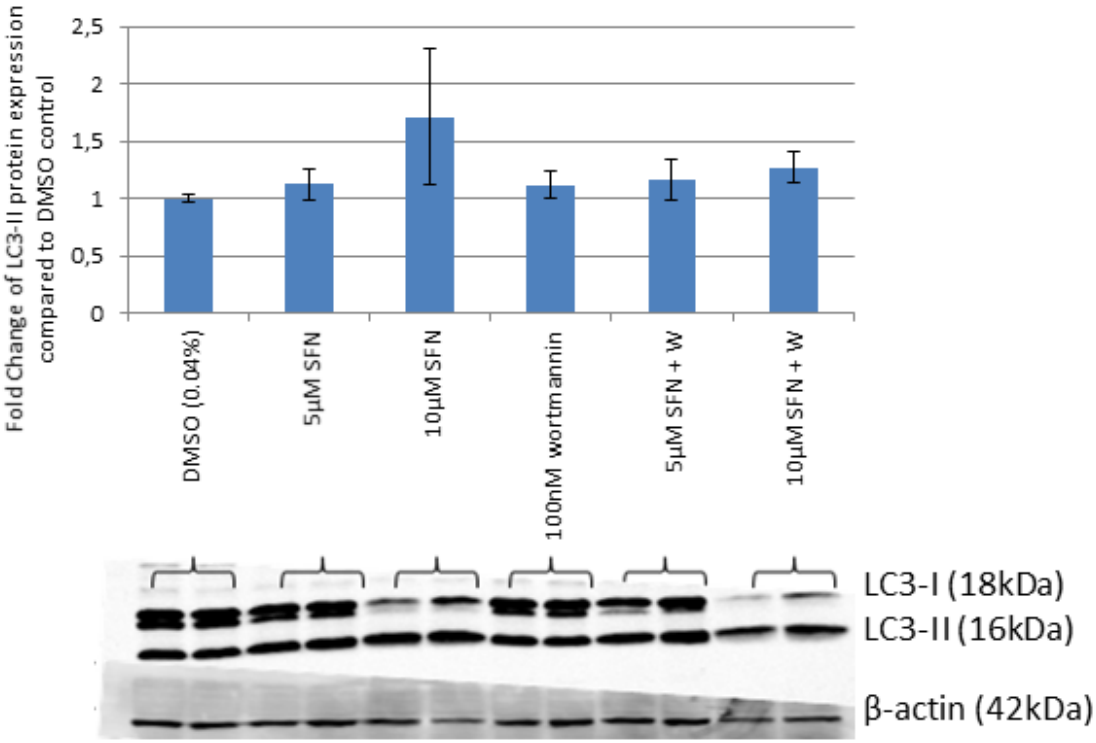

Figure 38: LC3-II expression in PC-12 cells after 24h treatment with SFN in presence of wortmannin.
Cells were cultured in 0.04% DMSO, 5µM and 10µM SFN and/or 100nM wortmannin. The blots were imaged by Odyssey and present the LC3-I bands at 18kDa, LC3-II at 16kDa and β-actin at 42kDa. The graph shows the quantification of LC3-II after normalisation against β-actin. Each bar represents the average of the bands of 2 biological replicates (error bars = SD; n =2)).

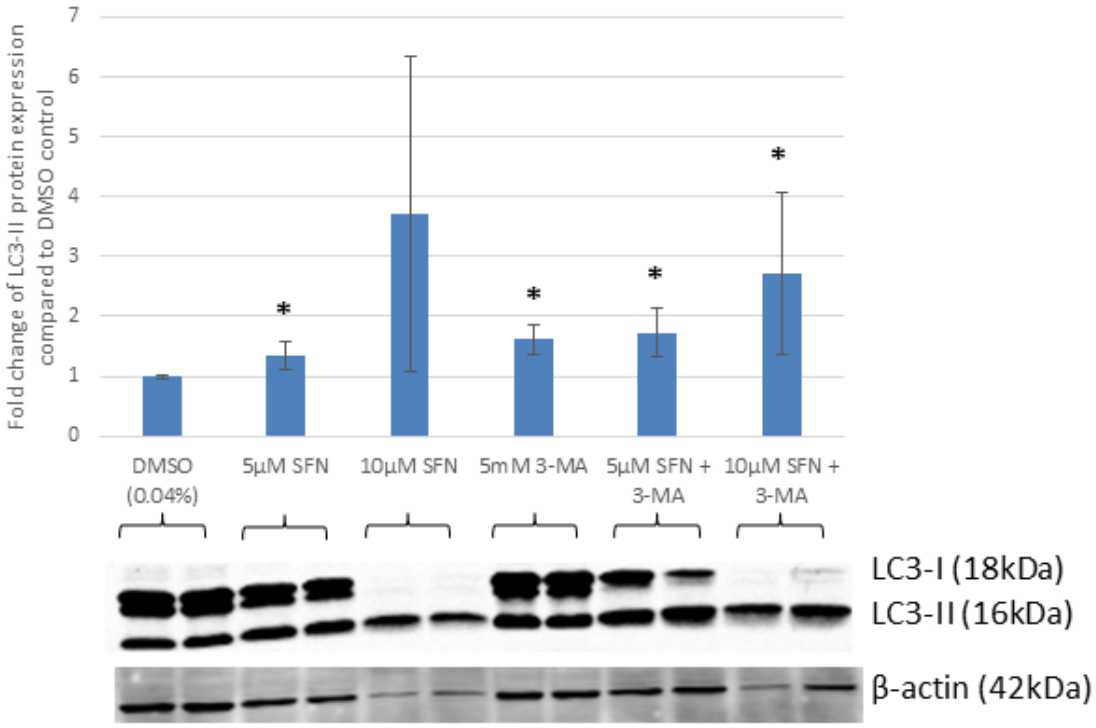

Figure 39: LC3-II expression in PC-12 cells after 24h treatment with SFN in presence of 3-MA

Cells were cultured in DMSO, 5µM and 10µM SFN and/or 5mM 3-MA. The blots were imaged by Odyssey and present the LC3-I bands at 18kDa, LC3-II at 16kDa and β-actin at 43kDa. The diagram shows the quantification of LC3-II after normalisation against β-actin. Each bar represents the average of 5 biological replicates (error bars = SD; n =5; *P<0.05).

5.2.2 ATG16L1 KO PRIMARY NEURONAL CELLS FROM MOUSE EMBRYOS

Number of KO samples. The Mendelian ratio estimates a 1:4 chance to receive an Atg16L1 KO mouse from two Atg16L1 +/- mice **(Figure 40)**.

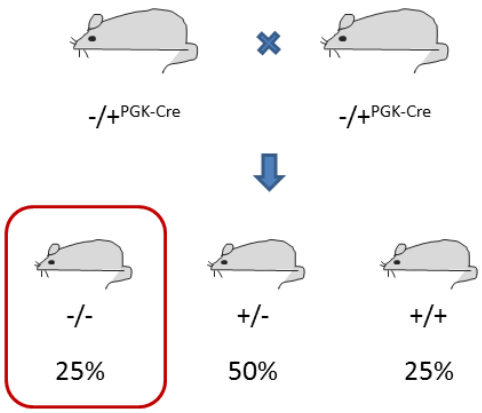

Figure 40 Simple schematics of the breeding scheme for generating Atg16L1 KO mice.
The red block indicates Atg16L1 KO mouse. The percentage under each mouse presents the Mendelian ratio expected. For simplicity, the PGK-Cre inheritance has not been shown in the second generation.

Method development and optimisation. The technique had not been previously established in our lab, therefore, through a number of experiments, cell retrieval and plating as well as treatment conditions were optimised to minimise waste and produce the highest number of viable PNCs per experiment. Since Atg16L1 mice have only a small chance of surviving, and that only for a short number of days or weeks, it was considered unethical to grow them until birth (Arasteh 2012). Hence, primary neuronal cells had to be derived from embryos (E14-16) rather than pups. This limited the choices of methods as well as experimental settings, since cell numbers were low. Since embryos had to be collected and dissected individually to prohibit cell contamination, there was not sufficient time to count the cells before plating. Thus, PNCs of each embryo were simply plated in equal parts following a protocol sketched out in **Figure 41**, which resulted in a great data variation between embryos.

Primary neuronal cells were grown as described in the methods. After 7-9 days, full differentiation was achieved **(Figure 42)**.

Immunostainings of Atg16L1 KO and WT PNCs. In WT PNCs punctae can be seen in SFN samples, depicted in red (Alexafluor 594 **(Figure 43)**). These punctae seen are

LC3 positive autophagosomes and therefore resemble activation of autophagy. In KO cells, stimulation with SFN did not show the same effect, suggesting that autophagy is not present in these cells. The p62-Alexa488 staining presented inconclusive, which could again be explained by the positive feedback loop between p62 and Nrf2.

A vehicle control and a positive control for autophagy were added to strengthen these findings. HBSS and SFN samples both showed punctae formation, while they were absent in KO samples **(Figure 44)**. Quantification of autophagosomes punctae could be carried out using IMARIS software. Thus, a comparison of ratios autophagosomes/cells was carried out to calculate significant increase in LC3 punctae of HBSS- and SFN-treated samples compared to controls **(Figure 45)**. These findings confirmed that autophagy was heavily impaired in Atg16L1 KO samples.

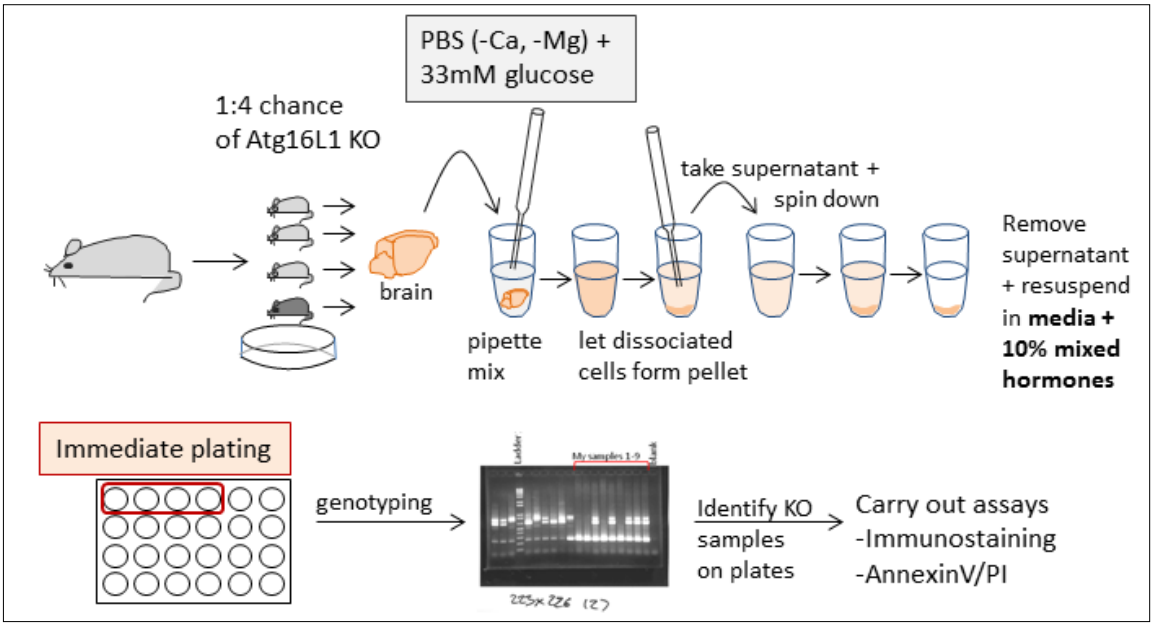

Figure 41 This graph shows a sketch of the retrieval of PNCs.
First, the pregnant mouse was dissected. Next, the embryos were placed into PBS in individual wells. The brain was carefully removed and pipette mixed. After letting cells rest, the supernatant was removed, spun down and resuspended in media + 10% hormones. Cells had to be plated immediately. After genotyping to identify Atg16L1 KO samples, experiments were carried out.

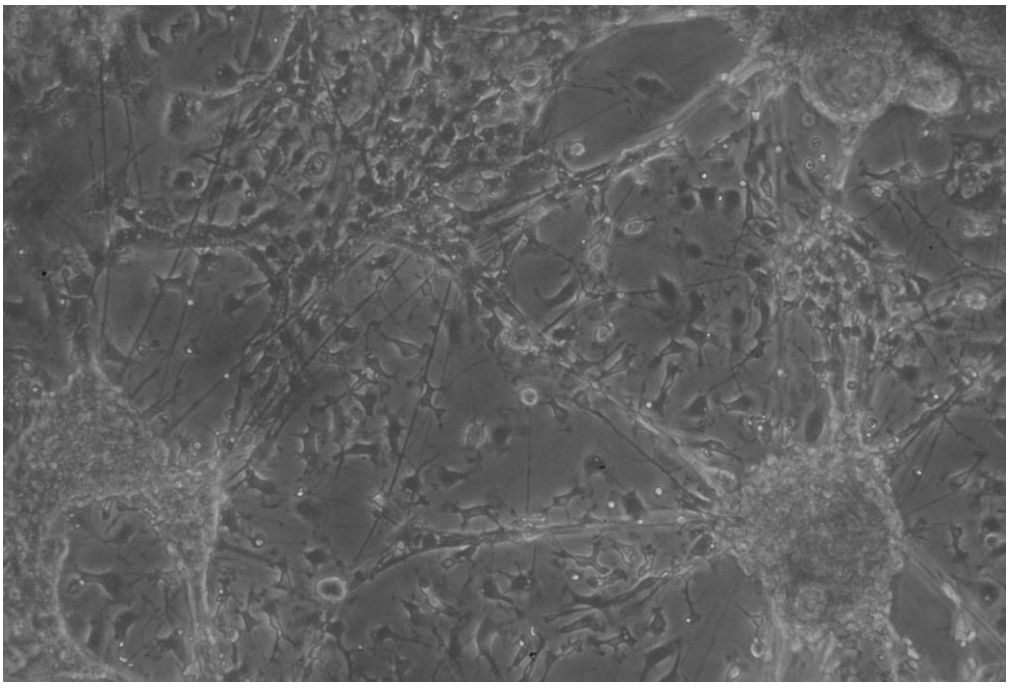

Figure 42: Example picture of PNCs after 7 growth days.

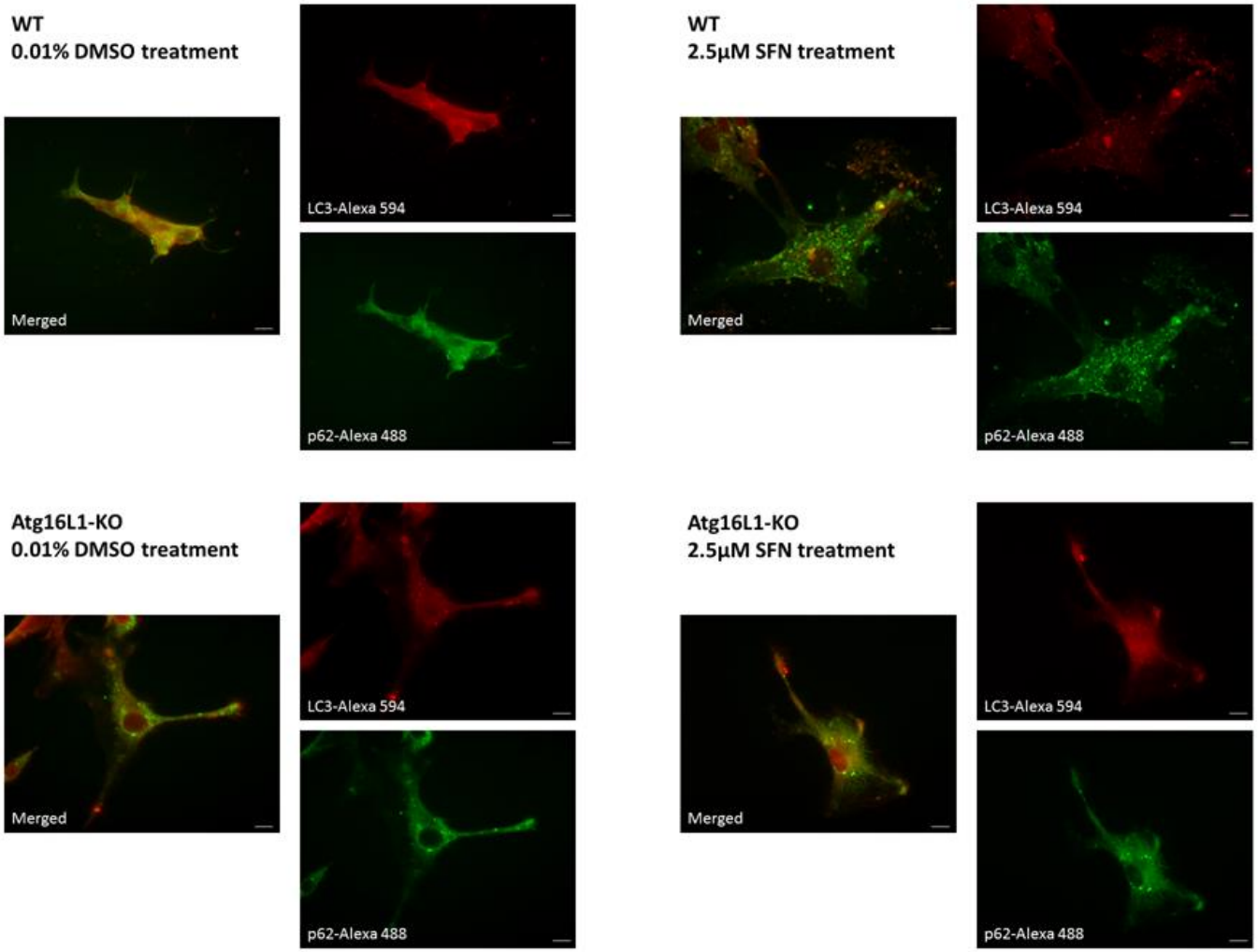

Figure 43: Images of stained PNCs against LC3-Alexa594 and p62-Alexa488.
Atg16L1 KO and WT PNCs were plated for immunostainings. They were treated with 0.01% DMSO or 2.5µM SFN for 4h. Then they were stained for LC3 (Alexafluor 594, red) and p62 (Alexafluor 488, green).

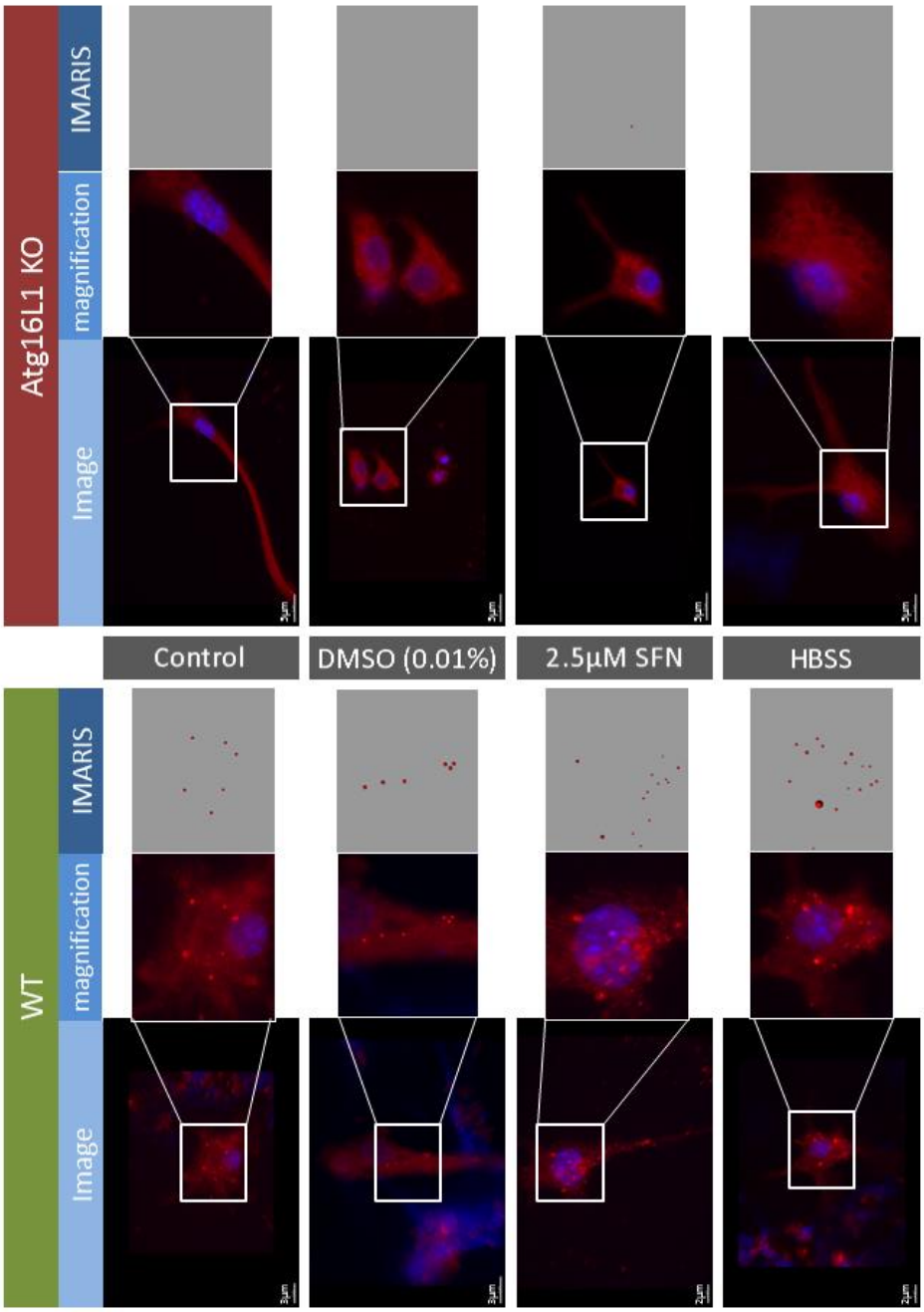

Figure 44: Images of stained PNCs against LC3-Alexa594 and DAPI.
Atg16L1 KO and WT PNCs were plated for immunostainings. They were treated with regular media (+10% hormones), 0.01% DMSO, 2.5µM SFN or HBSS, a positive control for autophagy, for 4h. Then they were stained with DAPI (nuclear stain, blue) and LC3 (Alexafluor 594, red). Images taken on the microscope were then analysed using the IMARIS software, which detects and quantifies punctae (see red dots on grey background).

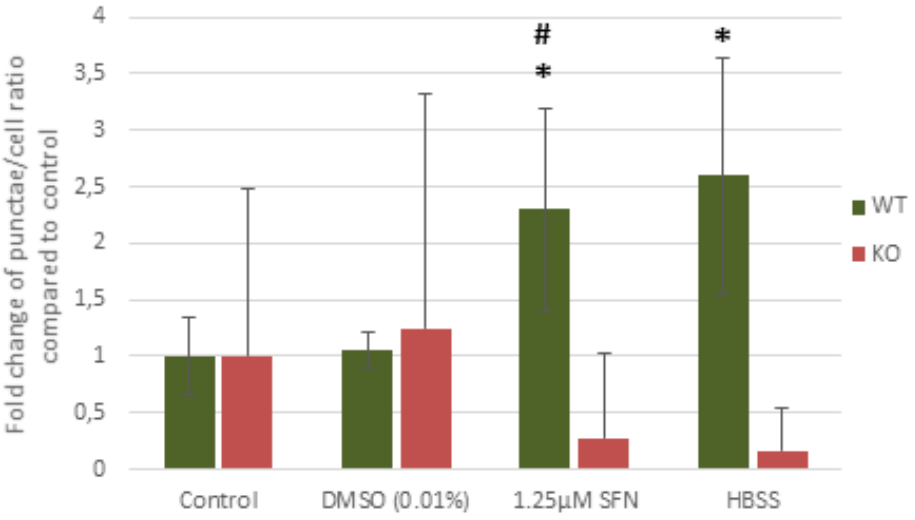

		total no. of cells	average punctae/cell ratio
WT	Control	6	5,10
	DMSO	7	5,40
	1.25µM SFN	10	11,73
	HBSS	6	13,25
KO	Control	5	0,60
	DMSO	16	0,75
	1.25µM SFN	18	0,17
	HBSS	16	0,10

Figure 45: Quantification of LC3 punctae with IMARIS.
Atg16L1 KO and WT PNCs were plated on coverslips for immunostainings. They were treated with only media (+10% hormones), 0.01% DMSO, 1.25µM SFN or HBSS, a positive control for autophagy, for 4h. Then they were stained for LC3 (Alexafluor 594, red) and DAPI (nuclear stain, blue). Images were quantified using IMARIS software. Bars represent the average of 5 or 6 images analysed (For the WT HBSS sample only 4 images could be taken into account because of an extremely high outlier). * P<0.05 compared to Control; # P<0.05 compared to DMSO.

5.2.3 NEUROPROTECTIVE EFFECTS OF SULFORAPHANE IN ATG16L1 KO PRIMARY NEURONAL CELLS

Finally, PNCs were set up for AnnexinV/PI flow cytometry. This method was first optimised. Results show that in WT samples, SFN is able to significantly increase cell survival of cells against H_2O_2-induced cell death. In KO samples, however, this protective effect could not be observed, as SFN could only marginally rescue the H_2O_2-treated cells **(Figure 46A)**. As the cells of each PNC source were plated individually to separate WT and KO cells, some variation between different data sets could be expected. The standard deviation shown as error bars in the diagram does therefor not accurately reflect the change observed within a data set, so a table was added to present those numbers **(Figure 46B)**. SFN can recover an average of 18.18% of cells in WT samples, compared to only 2.94% in KO PNCs.

During data collection, two different populations could be detected, thus, the gating strategy for the AnnexinV/PI experiments in PNCs needed to be assessed differently than for the other cell lines that have been used for this project. For better quantification, they were not only calculated as one, but also separately **(Gating graphs see appendix Figure 66, Figure 67, Figure 68, p.154f).** Unfortunately we did not have the time nor the tools to investigate this further. However, it could indicate that another cell type other than neuronal cells is also present.

A

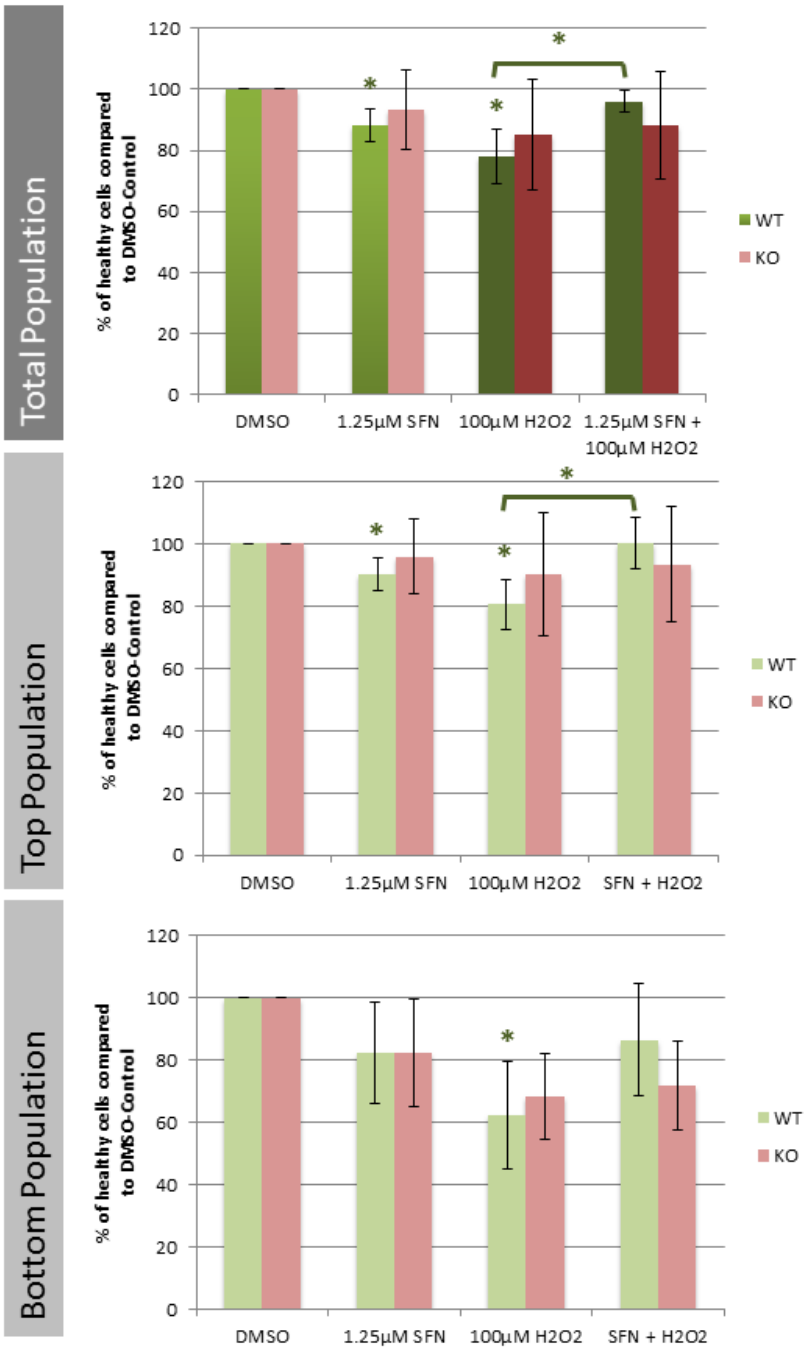

B

Total Population	WT	KO
Average difference in % of healthy cells between H_2O_2 samples and SFN+H_2O_2 samples within one data set	18,18	2,94
STDEV	9,89	3,88

Figure 46: Effect of SFN on H_2O_2-induced apoptosis in Atg16L1 KO and WT PNCs measured by Flow Cytometry

A Cells were pre-treated with 0.01% DMSO or 1.25µM SFN for 24h and then treated with serum-free media or 100µM H_2O_2. The treatment was removed after 4h and replaced with regular medium. Samples were measured by flow cytometry. Each bar represents an average of 4 (KO) and 5 (WT) biological replicates with 5000 events investigated by AnnexinV/PI (*P<0.05 compared to DMSO control, unless otherwise shown; ANOVA and post-hoc t-test/Bonferroni corrected).

B This table shows the average of the difference in % of healthy cells between H_2O_2 and SFN+H_2O_2 samples within individual biological samples (total population).

5.3 SUMMARY

The autophagy inhibitors 3-MA and wortmannin showed reduced protective effects of SFN when given in combination with H_2O_2. However, western blots to assess the efficiency of these inhibitors depicted only partly suppression of the autophagosome formation and thus the autophagic pathway. Therefore, as an alternative method with most likely a better outcome, PNCs were plated from WT or Atg16L1 KO mouse embryos.

After several optimisation steps, these PNCs were successfully grown. In addition, I was able to confirm absence of LC3 positive autophagosomes in Atg16L1 KO cells compared to WT when induced by either SFN or HBSS. This could be observed by immunostaining. Furthermore, AV/PI experiments indicate the involvement of autophagy in the neuroprotective effects of SFN in H_2O_2 induced cell death.

AnnexinV/PI results showed two faintly different populations during event collection. Therefore the experiment was plotted as was, but also separated in those two groups of events. The top population resembled the result of the total population almost 1:1.

Atg16L1 KO samples did not show any significant difference between controls and SFN pre-treated samples. Although presented with a low sample number, and although the carefully selected concentration of 100µM H_2O_2 only reduced the percentage of viable cells to 80%, WT samples did show that SFN could rescue PNCs from H_2O_2-induced cell death a significant amount. Due to the timely and costly procedure as well as availability of KO embryos, these findings could not be confirmed during the time at hand.

6 DISCUSSION AND FUTURE PERSPECTIVES

6.1 EFFECT OF SFN ON CELL VIABILITY OF PC-12 CELLS

To assess the bioactivity of SFN in neuronal cells, PC-12 and SH-SY5Y cells were selected as cell models. As PC-12 cells represented a novel target for SFN activity, cell viability of SFN on PC-12 cells was assessed and an IC50 of 36.9µM following 24h exposure to SFN was determined.

Several recent publications have also reported the effect of SFN on PC-12 cells. Exposure to 1µM and 5µM SFN for 24h resulted in reduction of 6-OHDA induced cytotoxicity, and a dose- and time-dependent increase HO-1 and Nrf2 protein levels (C Deng et al. 2012). Deng et al (2012) also reported that 6h pre-treatment with 5µM SFN decreased 6-OHDA induced ER-stress (Chang Deng et al. 2012).

In a study described by Izumi et al. (2012), SFN was used as a positive ARE-activating control, at a dose of 3µM SFN applied for 9h. Their preliminary results have shown that exposure to ≥10µM SFN over a period of 48h elicited cytotoxicity.

Throughout the course of the research described in this thesis, doses of 0.625-20µM SFN have been used for varying periods of cellular exposure, as followed.

6.2 EXPRESSION OF NRF2 AND NRF2/ARE-REGULATED ENZYMES IN PC-12 AND SH-SY5Y CELLS AFTER TREATMENT WITH SULFORAPHANE

Experiments investigating the effect of SFN on PC-12 and SH-SY5Y demonstrated that SFN can induce the expression of Nrf2 and Nrf2/ARE regulated enzymes in both cell lines (see 3.2.3, p.70). This was quantified at the protein level by immunoblotting, and at the level of RNA by qPCR. These findings are in agreement with several previously (see introduction) or simultaneously conducted studies (C Deng et al. 2012; Morroni et al. 2013).

More recently, PC-12 cells have been used as a neuronal model to demonstrate the protective effects of SFN against 6-OHDA-induced cytotoxicity (C Deng et al. 2012). Further experimental work reported in this thesis, and conducted in order to

understand the underlying mechanism by which SFN protects against 6-OHDA-induced cell death, demonstrated that SFN could significantly reduce caspase-3 activation and subsequent cell death, increase HO-1 expression, induce the translocation of Nrf2 into the nucleus, and activate PI3K/Akt. SFN has also been reported to enhance HO-1 expression in BV2 microglial cells at a concentration of 5-20μM when applied for 24h (Foresti et al. 2013). As noted previously, SFN protected SH-SY5Y cells against H_2O_2 and 6-OHDA-induced cytotoxicity, which was attributed to observed increases in NQO1, GST and GR (glutathione reductase) (Tarozzi et al. 2009).

The application of SFN in a PD mouse model demonstrated protective effects against 6-OHDA induced neurotoxicity (Morroni et al. 2013). Mice were fed with 5mg/kg SFN twice weekly for four weeks after a unilateral intrastriatal injection of 6-OHDA, inducing PD-like symptoms. The reduction in motor and coordination functions as well as degeneration in dopaminergic neurons was ameliorated significantly by SFN. The authors hypothesised that expression of GST was involved in mediating these effects, as increases in GST protein levels were observed.

The research presented in this thesis demonstrates that exposure to SFN can induce expression of Nrf2, GST, HO-1 and TR-1 in PC-12 and SH-SY5Y cells, as reported in other cell lines (Brooks et al. 2001; Dinkova-Kostova & Talalay 2008; Fimognari et al. 2008).

6.3 THE EFFECT OF SULFORAPHANE ON AUTOPHAGY MARKERS IN PC-12 AND SH-SY5Y CELLS

As described in chapter 3.2.4 (p. 75), an induction of autophagic markers could be observed in all cell lines using several different methods. Immunoblotting data indicated increased LC3-II protein levels following treatment with SFN, while the effect on p62 expression was unclear. Levels of p62 usually decreased following exposure to SFN for up to x hours, as it is degraded during the autophagy pathway. However, treatment with SFN for up to 24h resulted in a clear increase of p62 levels. This could reflect a positive feedback loop between Nrf2 and p62. p62 is degraded during autolysosome formation and therefore decreased levels of p62 protein would be expected when autophagy is activated. However, p62 can also bind to Keap1, thus disrupting the association between Keap1 and Nrf2 and releasing Nrf2

into the cytosol. Subsequent translocation of Nrf2 into the nucleus results in Nrf2/ARE-driven gene expression, including the expression of p62 since the ARE is present in the p62 promotor (Jain et al. 2010). A diagram of the proposed molecular pathways is presented on page 44.

SFN has been shown to increase LC3-II protein levels in previous studies, although to date none were conducted in PC-12 cells. Most experiments were performed using cells, where induction of apoptosis by SFN was the main focus of investigation. It was found several reported studies that by adding an autophagy inhibitor (3-MA or BAF), SFN-induced apoptosis could be increased in human prostate cancer, and breast cancer colon cancer cells (Herman-Antosiewicz et al. 2006; Kanematsu et al. 2010; Nishikawa, Tsuno, Okaji, Shuno, et al. 2010).

In this thesis, an experiment using BAF to block the fusion and thus degradation of autophagosomes was used to assess whether SFN increased autophagosome formation or elicited inhibition of fusion and subsequent degradation (see chapter 3.2.4, p. 81). This experiment was based on methodology proposed by Rubinsztein *et al.* (2009) by measuring LC3-II protein levels following cell treatment with a test compound, or with BAF, or with both combined; although a chemical may both enhance synthesis and decrease degradation simultaneously. In our study SFN appeared to primarily induce autophagy by increasing autophagosome synthesis, but SFN also activated autophagosome degradation. However, autophagy is a dynamic process and the methodology described in this thesis only examines single observations; future investigations should utilise live imaging to address this issue.

Increased autophagosome formation following exposure to SFN was also observed after transient transfection of PC-12 cells with p62-tomato red and mRFP/GFP LC3 plasmids (monomeric red fluorescence protein/green fluorescence protein; see p. 82f). GFP-LC3 fluorescence decreases in the acidic lysosomal environment, whilst mRFP-LC3 fluorescence does not (Kimura et al. 2007). By using tandem fluorescent-tagged LC3, the observed punctae, which correspond with the number of autophagosomes, can be separated to differentiate between autophagosomes before fusion (showing both mRFP-LC3 and GFP-LC3) and after fusion (showing only the mRFP signal). In the experiments described in Chapter 3.2.4 (p. 83), only overlapping red and green signals were detected, suggesting that at the time of measurement no autolysosome formation had occurred.

By combining live imaging with the tandem fluorescent tagged mRFP/GFP-LC3, the dynamic process of autophagy could similarly be divided into stages of pre- and post-lysosome fusion.

6.4 THE EFFECT OF SULFORAPHANE ON CELL CYCLE ARREST IN PC-12 AND SH-SY5Y CELLS

Cultured PC-12 or SH-SY5Y cells treated with various amounts of SFN (0.625µM-5µM SFN in PC-12 and 2.5µM-20µM in SH-SY5Y cells) were harvested and analysed by flow cytometry to examine the effects of SFN on the cell cycle (see Chapter 3.2.2, p.68). A significant dose dependent cell cycle arrest in the S-stage was observed in PC-12 cells, and this was also observed in one experiment conducted in SH-SY5Y cells.

To date, SFN-modulated cell cycle arrest in either PC-12 or SH-SY5Y cells has not been reported in scientific literature. Previous reports of SFN-induced cell cycle arrest have described arrest mainly in the G2/M-phase, and occasionally in the S-stage, but these experiments were conducted using cancer cell lines (Herman-Antosiewicz et al. 2006; Matsui et al. 2007; Kanematsu et al. 2010; Pawlik et al. 2013). In cancer cells, cell cycle arrest often results in subsequent p53-mediated cell death (Vermeulen et al. 2003). In neuronal cells however, neurodegeneration is associated with the activation of the cell cycle, and inhibition of cell cycle proteins such as cyclin-dependent kinases can increase neuroprotective effects (Kruman et al. 2004). Thus, SFN-induced cell cycle arrest as described in Chapter X could be interpreted as a protective effect I for cell function. This could be analysed further by examining the effect of SFN upon expression of cell-cycle related proteins such as cyclin-dependent kinases.

6.5 NEUROPROTECTIVE EFFECTS OF SULFORAPHANE IN PC-12, DIFF PC-12 AND SH-SY5Y CELLS

The protective effects of SFN against H_2O_2 and 6-OHDA-induced cell death was assessed by Annexin V/PI flow cytometry, as well as MTT assays (data not shown). In all cell lines, increased cell survival was detected, which in PC-12 and DIFF PC-12 cells was highly significant (see Chapter 3.2.5, p.84).

Mitochondrial membrane potential has been reported to regulate a cytochrome c induction in apoptosis (Gottlieb et al. 2003). To investigate if a reduction in depolarisation of mitochondrial membranes was involved in the cytoprotective

effect of SFN, a JC-1 experiment was conducted as described in Chapter X. JC-1 is a fluorescent probe, which emits a green-orange fluorescence in cells with normal polarised mitochondrial membranes, while in depolarised mitochondrial membranes it emits only green fluorescence. This can be observed in a fluorescence plot by a shift from the FL-1^+/FL-2^+ to right to the FL-1^+/FL-2^- bottom right. This has previously been observed for SFN in the human myeloid leukaemia cell line, amongst other cell lines, however not to a very strong extent (Jana Jakubikova et al. 2005). The results described in the appendix (p. 139) did not reveal the expected shift towards the green fluorescence, so it could not be determined whether SFN modulated the mitochondrial membrane potential. However, protective effects could be observed (p.139; Raw data not shown).

Other studies have also described a positive effect of SFN on neuronal cell function (Guerrero-Beltrán et al. 2010). Vauzour *et al.* (2010) demonstrated that cortical neurons had an increased rate of cell survival against 5-S-cysteinyl-induced toxicity when pre-treated with SFN. These authors also reported that expression of NQO1 and other detoxification enzymes was induced by SFN.

However, most reported studies have examined the effect of SFN on Nrf2 regulated genes, but have not investigated the complexity of potential SFN bioactivity.

6.6 INDUCTION OF DJ-1 BY SULFORAPHANE IN PC-12 CELLS

Research presented in Chapter 4.2.1 (p.91) of this thesis demonstrates that SFN is able to increase DJ-1 protein levels after a 24h exposure to 2.5, 5 and 10µM SFN. DJ-1 is a multifunctional protein, and mutations of DJ-1 have been associated with the development of PD. To date, only a few research groups have investigated DJ-1 in context of SFN bioactivity, for example as an agent to stimulate Nrf2 activity (Malhotra et al. 2008; Beal 2009).

DJ-1 may represent a novel target mediating bioactivity of SFN. This multi-functional protein is thought to be important for neuronal cell health, as mutations or absence of DJ-1 have been associated with PD (Clements et al. 2006; Rannikko et al. 2012).

6.7 REDUCTION OF ER-STRESS BY SFN IN PC-12 CELLS

The endoplasmic reticulum (ER) is an important cell organelle involved in the process of synthesis, folding and processing of proteins, amongst others (Loeffler G.

2003). DJ-1 transcription is controlled by ER-stress through the transcription factor XBP-1 (Duplan et al. 2013). Since DJ-1 has been connected to ER-stress, the current thesis assessed whether SFN could protect PC12 cells from tunicamycin-induced ER-stress. After optimising experimental conditions for tunicamycin, a significant reduction of ER-stress could be observed by measuring RNA and protein levels of the ER-stress marker CHOP. While PC-12 cells do not display an ER-stress response under normal culture conditions, treatment with tunicamycin for 4 hours resulted in increased CHOP protein levels. 24 hour pre-treatment of PC-12 cells with SFN, which did not modulate CHOP expression alone, significantly reduced the increase in CHOP levels induced by tunicamycin. A similar effect was observed when tunicamycin was replaced by 6-OHDA.

This observation is consistent with the findings of Chang Deng *et al.* (2012) in a similar experimental model. Moreover, 6h pre-treatment of PC-12 cells with 5µM SFN reduced the cytotoxicity generated by a 24h exposure to 80µM 6-OHDA. SFN was also able to reduce homocysteine-induced ER-stress in immortalised human hepatocytes (He et al. 2014). That study could show that TR-1 and NQO1 were involved in the protective effect of SFN.

6.8 EFFICIENCY OF DJ-1 KNOCK DOWN USING SIRNA

In order to investigate whether the ER-stress reduction induced by SFN is DJ-1 dependent, a knock- down DJ-1 model was created using siRNA, as detailed in Chapter 4.2.3 (p.96). Although DJ-1 protein levels were reduced in cells affected by siDJ-1, consistent results could not be obtained, and immunoblotting data obtained using this model cannot be viewed as informative.

DJ-1 has been reported to stabilise Nrf2 on its way to the nucleus (Clements et al. 2006). As mentioned above, Chang Deng *et al.* (2012) have investigated the inhibition of 6-OHDA-induced ER-stress by SFN in PC-12 cells, in addition to underlying mechanisms including possible involvement of Nrf2. The protective effects of SFN were reduced in the presence of Nrf2 siRNA, suggesting the activity of SFN is at least partly mediated by Nrf2. Although 5µM SFN was sufficient to enhance Nrf2 protein expression in the cited paper, 10µM SFN may represent an optimal dose to induce DJ-1 expression in our experiment model. Alternatively, a

higher concentration of siRNA could be used, relative to 50nM Nrf2 siRNA in the cited study.

Yokota *et al.* (2003) investigated the relationship between DJ-1 and ER-stress in mouse Neruo2a cells by silencing DJ-1 using siRNA. This resulted in increased levels of oxidative stress-, ER stress-, and proteasome-inhibition-related cell death. We would have expected a similar result in our experiment model.

While exploring the activity of SFN on DJ-1, it should be mentioned that mutations in Parkin and PINK1 (pten-induced putative kinase 1) have equally been associated with the early onset familial form of PD, (Wilhelmus et al. 2012). Parkin is an E3 ubiquitin-protein ligase that plays a vital part in the ubiquitin-proteasome system, while PINK1 is important in the regulation of mitochondrial and cellular redox balance (Wilhelmus et al. 2012). In order to promote ubiquitination and degradation of Parkin substrates, a complex composed of all three proteins is formed (PPD complex). All three proteins are involved in mitochondrial dysfunction, oxidative injury and faulty functioning of the ubiquitin-proteasome system (UPS) (Wilhelmus et al. 2012). Including Parkin and PINK1 in further investigations of ER-stress, in the presence or absence of DJ-1, might indicate a potential role for DJ-1 in the development of PD.

6.9 REDUCING AUTOPHAGY BY USE OF CHEMICAL INHIBITORS

Although Nrf2 is probably the most important target of SFN, other mechanisms need to be considered when investigating the potential protective effects of this molecule. To examine the importance of autophagy in the neuroprotective activity of SFN, autophagy inhibitors were introduced into a PC-12 cell model as described in Chapter 5.2.1 (p.101). By suppressing autophagy, the current thesis aimed to determine whether neuroprotection induced by SFN was ablated in these experimental conditions. 3-MA and wortmannin prevent autophagosome formation by inhibiting class III phosphatidylinositol 3-kinases (PI3K III), which form a complex with Beclin1 and other components during the process of autophagy; and both 3-MA and wortmannin are considered useful experimental tools (Triola 2015).

As detailed in Chapter 5.2.1 (p.101), PC-12 cells were treated with 5μM SFN together with 3-MA or wortmannin for 24 hours and LC3-II protein expression was analysed. While SFN induced, as expected, an increase in LC3-II levels, both autophagy

inhibitors surprisingly either elicited no change relative to control or induced a minor increase in LC3-II levels. Therefor an alternative method to inhibit autophagy was selected, as described in Chapter 5.2.2 (p.104).

Zhang *et al.* (2015) applied 3-MA to PC-12 cells in their investigation of autophagy as a regulator of colistin-induced apoptosis. These authors also analysed the protein expression of LC3-II relative to 3-MA and only observed a minor decrease in LC3-II expression compared to control, but a clear decrease compared to colistin or rapamycin was recorded. 3-MA has been utilised in several studies in cancer cells in conjunction with SFN; however, SFN and 3-MA were investigated in a different context, as these study groups did not demonstrate any immunoblotting data using 3-MA against LC3 (Herman-Antosiewicz et al. 2006; Kanematsu et al. 2010; Nishikawa, Tsuno, Okaji, Sunami, et al. 2010).

Wu *et al.* (2010) suggested that 3-MA should be used with caution, it may transiently block class III PI3K, while inhibiting class I PI3K permanently; wortmannin has been reported to show the opposite binding affinity.

6.10 GENERATING ATG16L1 KO PRIMARY NEURONAL CELLS AND ASSESSING THE PRESENCE OF AUTOPHAGY IN AGA16L1 KO AND WT PNCS

To study the role of autophagy in SFN-mediated cytoprotective effects, WT and Atg16L1 KO PNCs were generated (see Chapter 5.2.2, p.104). We hypothesised that the loss of Atg16L1 leads to the loss of autophagy, which could serve as a suitable cell model to investigate the neuroprotective effects of SFN in relation to the autophagic pathway. Atg16L1 KO PNCs did not show any morphological difference to WT cells.

By investigating the number of LC3-II punctae by immunostaining, it was determined that Atg16L1 KO PNCs, unlike their WT counterpart, did not show any enhanced autophagosome formation after SFN treatment or starvation with HBSS (Chapter X). Thus, autophagy was indeed suppressed in this model.

Since Atg16L1 is associated with the development of Crohn's disease, a type of inflammatory bowel disease, a number of studies in Atg16L1 mice models have generated different gut-related primary cells to study this condition (Stappenbeck

et al. 2011). However, to the best of the author's knowledge, Atg16L1 KO PNCs have not yet been studied.

6.11 NEUROPROTECTIVE EFFECTS OF SULFORAPHANE IN ATG16L1 KO PRIMARY NEURONAL CELLS

H_2O_2-induced cell death was reduced by SFN significantly in WT PNCs, but not in Atg16L1 KO as detailed in Chapter 5.2.3 (p.110). PNCs were pre-treated with SFN for 24h before H_2O_2 was added for 4h. Analysis via Annexin V/PI flow cytometry detected a significant increase in cell survival following pre-treatment with SFN compared to untreated cells, in WT PNCs. However, in Atg16L1 KO cells no significant protective effect of SFN was observed, suggesting that autophagy is partly involved in the observed protective effects of SFN.

Only recently, Wang *et al.* (2015) demonstrated for the first time that SFN can protect cells from lipotoxicity through activation of autophagy, and not the Nrf2 pathway. Umbilical vein endothelial cells (EA.hy926) were pre-treated with 20μM SFN for 1h followed by exposure to palmitate (600μM) for 9h, which resulted in reduced caspase-3 protein levels in SFN pre-treated cells compared to palmitate treatment alone. Although analysis of Nrf2 and HO-1 levels demonstrated a dose-dependent induction by SFN, inhibiting the Nrf2 pathway via siRNA did not reduce the protective effects of SFN. It was also determined that the protective effect of SFN was independent of the ERK, Akt and ER-stress pathways. By blocking autophagy using BAF or chloroquine (both of which inhibit autophagosome-lysosome fusion), or alternatively by silencing AMPK, SFN did not induce any protective effects. Therefore SFN may protect EA.hy926 cells from palmitate-induced lipotoxicity via AMPK-dependent autophagy. It is unusual and surprising that the Nrf2 pathway was not involved in meditating the protective effects of SFN, so these findings may be specific to EA.hy926 cells.

In future studies of the neuroprotective effects of SFN, Nrf2 could be knocked down in PNCs (WT) to assess the involvement of Nrf2 in mediating SFN activity. Moreover, cytoprotection of SFN against toxin-induced cell death could be examined in relation to both pathways simultaneously by silencing Nrf2 with siRNA in Atg16L1 KO and WT PNCs.

The aim of research presented in Chapter 5.2.3 (p.110) was to assess if autophagy was an alternative mechanism involved in the protective effects of SFN, possibly in conjunction with the role of Nrf2. However, the findings of Wang *et al.* (2015) suggest that autophagy may play an even greater role in cytoprotection than so far established.

6.12 FUTURE PERSPECTIVES

Based on the data presented in this thesis, the two most intriguing observations that should be further investigated are the SFN/DJ-1/Nrf2/ER-stress interaction as well as the role of autophagy in the neuroprotective effects of SFN.

By using a knock down DJ-1 model, the effect of this protein on the cytoprotective effects of SFN in ER-stress could be assessed, perhaps in conjunction with silencing of Nrf2. Since DJ-1, Parkin and PINK1 have all previously been associated with PD (B et al. 2009; Wilhelmus et al. 2012), it would be of particular interest to investigate if the expression of Parkin and PINK1 can also be modulated by SFN.

Further examination into the involvement of autophagy in the neuroprotective effects of SFN is an exciting field with many possibilities. Autophagy is a complex mechanism that has not fully been established. Owing to its dual role of providing energy as well as removing organelles, any impairment of this sensitive system can have a detrimental impact. As already described, several neurodegenerative diseases have been linked to dysfunctional autophagy (Sanchez-Perez et al. 2012; Sarkar 2011).

The Atg16L1 KO system described in this thesis warrants a more detailed assessment, including the effect SFN on Nrf2-regulated enzymes, which can now be studied in an autophagy-suppressed environment.

In addition to investigating the mechanisms underlying the cytoprotective effects of SFN, SFN could be studied in human intervention studies, to attempt to correlate identified cellular activities of SFN with neurodegenerative disease development and outcome. Based on evidence from animal models, Shah & Duda (2015) have hypothesised that phytochemicals, such as SFN, may contribute to neuroprotection in PD and that adopting a plant-based diet may alter disease progression and provide improvement in the symptomatic of PD (Shah & Duda 2015).

Apart from the many reports on the beneficial effects of SFN, hormetic effects of ITCs have been described (Bao et al. 2014). Low doses of ITCs may have the potential to be either beneficial or harmful, and as the relevant molecular mechanisms are not fully elucidated, these should be addressed in future research. However, consumption of broccoli is still considered to be a dietary intervention which may help to prevent many types of cancers. Several epidemiological studies have been performed to examine links between dietary intake of isothiocyanates and reduced cancer risk (Verhoeven et al. 1996; Kristal & Lampe 2002), but, to the author's knowledge, no epidemiological research has been undertaken to investigate the association of an isothiocyanate-rich diet and neurodegenerative diseases.

In conclusion, this thesis has contributed to the current understanding of the biological activity of SFN in neuronal cells. However, further research is required to explain fully the mechanisms underlying the observed neuroprotective effects of SFN. Increased dietary intake of SFN-containing food sources could represent a simple way to reduce the risk of neurodegenerative diseases, which is of a particular interest in today's increasingly aging society.

7 REFERENCES

Abbott, N.J. et al., 2010. Structure and function of the blood-brain barrier. *Neurobiology of Disease*, 37(1), pp.13–25.

Albert-Puleo, M., 1983. Physiological effects of cabbage with reference to its potential as a dietary cancer-inhibitor and its use in ancient medicine. *J Ethnopharmacol*, 9(2-3), pp.261–272.

alzheimers.org.uk, 2012. Demography. , 2012(01.03.2012), p.Alzheimer's Society is a membership organisation. Available at: http://alzheimers.org.uk/site/scripts/document_pdf.php?documentID=412.

Arasteh, M., 2012. *Generation of mouse models to study the role of Atg16l1 in Inflammatory Bowel Disease (IBD)*. University of East Anglia.

Aykin-Burns, N., Franklin, E.A. & Ercal, N., 2005. Effects of N-acetylcysteine on lead-exposed PC-12 cells. *Arch Environ Contam Toxicol*, 49(1), pp.119–123.

Azarenko, O. et al., 2008. Suppression of microtubule dynamic instability and turnover in MCF7 breast cancer cells by sulforaphane. *Carcinogenesis*, 29(12), pp.2360–2368.

B, B.O.E.G. et al., 2009. Parkin, PINK1, and DJ-1 form a ubiquitin E3 ligase complex promoting unfolded protein degradation. *The Journal of Clinical Investigation*, 119(3).

Bandopadhyay, R. et al., 2004. The expression of DJ-1 (PARK7) in normal human CNS and idiopathic Parkinson's disease. *Brain*, 127(Pt 2), pp.420–430.

Bao, Y. et al., 2014. Benefits and risks of the hormetic effects of dietary isothiocyanates on cancer prevention. *PLoS ONE*, 9(12), pp.1–19.

Beal, M.F., 2009. Therapeutic approaches to mitochondrial dysfunction in Parkinson's disease. *Parkinsonism Relat Disord*, 15 Suppl 3, pp.S189–94.

Benedict, A.L. et al., 2012. Neuroprotective effects of sulforaphane after contusive spinal cord injury. *Journal of neurotrauma*, 29(16), pp.2576–86.

Biedler, J.L., Helson, L. & Spengler, B.A., 1973. Morphology and growth, tumorigenicity, and cytogenetics of human neuroblastoma cells in continuous culture. *Cancer Res*, 33(11), pp.2643–2652.

Bjorkoy, G. et al., 2009. Monitoring autophagic degradation of p62/SQSTM1. *Methods Enzymol*, 452, pp.181–197.

Bricker, G. V. et al., 2014. Isothiocyanate metabolism, distribution, and interconversion in mice following consumption of thermally processed broccoli sprouts or purified sulforaphane. *Molecular Nutrition and Food Research*, 58(10), pp.1991–2000.

Brooks, J.D. et al., 2001. Potent Induction of Phase 2 Enzymes in Human Prostate Cells by Sulforaphane Potent Induction of Phase 2 Enzymes in Human Prostate. *Cancer Epidemiology, Biomarkers & Prevention*, 10(September), pp.949–954.

Chen, Y. & Klionsky, D.J., 2011. The regulation of autophagy - unanswered questions. *J Cell Sci*, 124(Pt 2), pp.161–170.

Cherra 3rd, S.J. et al., 2010. Regulation of the autophagy protein LC3 by phosphorylation. *J Cell Biol*, 190(4), pp.533–539.

Cheung, K.L. & Kong, A.N., 2009. Molecular targets of dietary phenethyl isothiocyanate and sulforaphane for cancer chemoprevention. *AAPS J*, 12(1), pp.87–97.

Cheung, Y.T. et al., 2009. Effects of all-trans-retinoic acid on human SH-SY5Y neuroblastoma as in vitro model in neurotoxicity research. *NeuroToxicology*, 30(1), pp.127–135.

Cheung, Z.H. & Ip, N.Y., 2011. Autophagy deregulation in neurodegenerative diseases -

recent advances and future perspectives. *J Neurochem*, 118(3), pp.317–325.

Choi, J. et al., 2006. Oxidative damage of DJ-1 is linked to sporadic Parkinson and Alzheimer diseases. *J Biol Chem*, 281(16), pp.10816–10824.

Ciccarone, V. et al., 1989. Phenotypic diversification in human neuroblastoma cells: expression of distinct neural crest lineages. *Cancer Res*, 49(1), pp.219–225.

Clarke, J.D. et al., 2011. Bioavailability and inter-conversion of sulforaphane and erucin in human subjects consuming broccoli sprouts or broccoli supplement in a cross-over study design. *Pharmacol Res*.

Clements, C.M. et al., 2006. DJ-1, a cancer- and Parkinson's disease-associated protein, stabilizes the antioxidant transcriptional master regulator Nrf2. *Proc Natl Acad Sci U S A*, 103(41), pp.15091–15096.

Das, K.P., Freudenrich, T.M. & Mundy, W.R., 2004. Assessment of PC12 cell differentiation and neurite growth: a comparison of morphological and neurochemical measures. *Neurotoxicol Teratol*, 26(3), pp.397–406.

Deng, C. et al., 2012. Inhibition of 6-hydroxydopamine-induced endoplasmic reticulum stress by sulforaphane through the activation of Nrf2 nuclear translocation. *Molecular medicine reports*, 6(1), pp.215–9.

Deng, C. et al., 2012. Sulforaphane protects against 6-hydroxydopamine-induced cytotoxicity by increasing expression of heme oxygenase-1 in a PI3K/Akt-dependent manner. *Mol Med Report*, 5(3), pp.847–851.

Dinkova-Kostova, A.T. et al., 2002. Direct evidence that sulfhydryl groups of Keap1 are the sensors regulating induction of phase 2 enzymes that protect against carcinogens and oxidants. *Proc Natl Acad Sci U S A*, 99(18), pp.11908–11913.

Dinkova-Kostova, A.T. et al., 2007. Induction of the phase 2 response in mouse and human skin by sulforaphane-containing broccoli sprout extracts. *Cancer Epidemiol Biomarkers Prev*, 16(4), pp.847–851.

Dinkova-Kostova, A.T. & Kostov, R. V, 2012. Glucosinolates and isothiocyanates in health and disease. *Trends Mol Med*.

Dinkova-Kostova, A.T. & Talalay, P., 2008. Direct and indirect antioxidant properties of inducers of cytoprotective proteins. *Mol Nutr Food Res*, 52 Suppl 1, pp.S128–38.

Duplan, E. et al., 2013. ER-stress-associated functional link between Parkin and DJ-1 via a transcriptional cascade involving the tumor suppressor p53 and the spliced X-box binding protein XBP-1. *Journal of cell science*, 126(Pt 9), pp.2124–33.

Efeyan, A., Comb, W.C. & Sabatini, D.M., 2015. Nutrient-sensing mechanisms and pathways. *Nature*, 517(7534), pp.302–310.

EuroPa, 2014. Parkinson's Disease. *EuroPa*. Available at: http://www.europarkinson.net/html/5/5a/fs_5a.html.

Europe, A., 2014. Amyotrophic Lateral Sclerosis (ALS). *Alzheimer Europe*. Available at: http://www.alzheimer-europe.org/Dementia/Other-forms-of-dementia/Neuro-Degenerative-Diseases/Amyotrophic-Lateral-Sclerosis-ALS?#fragment-1.

European Brain Council, 2011. *Parkinson ' s d isease Fact Sheet*, Available at: http://www.europeanbraincouncil.org/pdfs/Documents/Parkinson's fact sheet July 2011.pdf.

Fahey, J.W. et al., 2002. Sulforaphane inhibits extracellular, intracellular, and antibiotic-resistant strains of Helicobacter pylori and prevents benzo[a]pyrene-induced stomach tumors. *Proc Natl Acad Sci U S A*, 99(11), pp.7610–7615.

Fahey, J.W., Zalcmann, A.T. & Talalay, P., 2001. The chemical diversity and distribution of glucosinolates and isothiocyanates among plants. *Phytochemistry*, 56(1), pp.5–51.

Ferrari, N. et al., 2010. Diet-Derived Phytochemicals: From Cancer Chemoprevention to Cardio-Oncological Prevention. *Curr Drug Targets*.

Fimognari, C., Lenzi, M. & Hrelia, P., 2008. Interaction of the isothiocyanate sulforaphane with drug disposition and metabolism: pharmacological and toxicological implications. *Curr Drug Metab*, 9(7), pp.668–678.

Foresti, R. et al., 2013. Small molecule activators of the Nrf2-HO-1 antioxidant axis modulate heme metabolism and inflammation in BV2 microglia cells. *Pharmacological Research*, 76, pp.132–148.

Fujii, D.K. et al., 1982. Neurite outgrowth and protein synthesis by PC12 cells as a function of substratum and nerve growth factor. *J Neurosci*, 2(8), pp.1157–1175.

Gan, L., Johnson, D.A. & Johnson, J.A., 2010. Keap1-Nrf2 activation in the presence and absence of DJ-1. *Eur J Neurosci*, 31(6), pp.967–977.

Gasper, A. V et al., 2005. Glutathione S-transferase M1 polymorphism and metabolism of sulforaphane from standard and high-glucosinolate broccoli. *Am J Clin Nutr*, 82(6), pp.1283–1291.

Gennaro Giordano and Lucio G Costa, 2011. primary neurons in culture and neuronal cell lines for in vitro neurotoxicological studies. *In Vitro Neurotoxicology: Methods and Protocols*. Springer, pp. 13–27.

Ghawi, S.K. et al., 2012. Thermal and high hydrostatic pressure inactivation of myrosinase from green cabbage: A kinetic study. *Food Chemistry*, 131(4), pp.1240–1247.

Golde, T.E., 2009. The therapeutic importance of understanding mechanisms of neuronal cell death in neurodegenerative disease. *Mol Neurodegener*, 4, p.8.

Gottlieb, E. et al., 2003. Mitochondrial membrane potential regulates matrix configuration and cytochrome c release during apoptosis. *Cell Death and Differentiation*, 10, pp.709–717.

Gottlieb, R.A. & Carreira, R.S., 2010. Autophagy in health and disease. 5. Mitophagy as a way of life. *Am J Physiol Cell Physiol*, 299(2), pp.C203–10.

Green, S.H., 1995. The Use of PC12 Cells for the Study of the Mechanism of Action of Neurotrophic Factors: Signal Transduction and Programmed Cell Death. In I. Academic Press, ed. *A Companion to Methods in Enzymology*. pp. 222–237.

Greene, L.A., 1978. Nerve growth factor prevents the death and stimulates the neuronal differentiation of clonal PC12 pheochromocytoma cells in serum-free medium. *J Cell Biol*, 78(3), pp.747–755.

Greene, L.A. & Tischler, A.S., 1976. Establishment of a noradrenergic clonal line of rat adrenal pheochromocytoma cells which respond to nerve growth factor. *Proc Natl Acad Sci U S A*, 73(7), pp.2424–2428.

Griffiths, D.W., Birch, A.N.E. & Hillman, J.R., 1998. Antinutritional compounds in the Brassicaceae - Analysis, biosynthesis, chemistry and dietary effects. *Journal of Horticultural Science & Biotechnology*, 13(1), pp.1–18.

Gross-Steinmeyer, K. et al., 2010. Sulforaphane- and phenethyl isothiocyanate-induced inhibition of aflatoxin B1-mediated genotoxicity in human hepatocytes: role of GSTM1 genotype and CYP3A4 gene expression. *Toxicol Sci*, 116(2), pp.422–432.

Grubb, C.D. & Abel, S., 2006. Glucosinolate metabolism and its control. *Trends Plant Sci*, 11(2), pp.89–100.

Guerrero-Beltrán, C.E. et al., 2010. Protective effect of sulforaphane against oxidative stress: Recent advances. *Exp Toxicol Pathol*, 64(5), pp.503–8.

Guerrero-Beltrán, C.E. et al., 2012. Protective effect of sulforaphane against oxidative stress: recent advances. *Experimental and toxicologic pathology : official journal of the Gesellschaft für Toxikologische Pathologie*, 64(5), pp.503–8.

Han, J.M. et al., 2007. Protective effect of sulforaphane against dopaminergic cell death. *J Pharmacol Exp Ther*, 321(1), pp.249–256.

Haristoy, X. et al., 2003. Efficacy of sulforaphane in eradicating Helicobacter pylori in human gastric xenografts implanted in nude mice. *Antimicrob Agents Chemother*, 47(12), pp.3982–3984.

Harris, K.E. & Jeffery, E.H., 2008. Sulforaphane and erucin increase MRP1 and MRP2 in human carcinoma cell lines. *J Nutr Biochem*, 19(4), pp.246–254.

He, C. et al., 2014. Sulforaphane attenuates homocysteine-induced endoplasmic reticulum stress through Nrf-2-driven enzymes in immortalized human hepatocytes. *Journal of Agricultural and Food Chemistry*, 62(30), pp.7477–7485.

He, C. & Klionsky, D.J., 2009. Regulation mechanisms and signaling pathways of autophagy. *Annual review of genetics*, 43, pp.67–93.

Henchcliffe, C. & Beal, M.F., 2008. Mitochondrial biology and oxidative stress in Parkinson disease pathogenesis. *Nature clinical practice. Neurology*, 4(11), pp.600–609.

Herman-Antosiewicz, A., Johnson, D.E. & Singh, S. V, 2006. Sulforaphane causes autophagy to inhibit release of cytochrome C and apoptosis in human prostate cancer cells. *Cancer Res*, 66(11), pp.5828–5835.

Holst, B. & Williamson, G., 2004. A critical review of the bioavailability of glucosinolates and related compounds. *Nat Prod Rep*, 21(3), pp.425–447.

Hwang, H.W. et al., 2009. Oligomerization is crucial for the stability and function of heme oxygenase-1 in the endoplasmic reticulum. *Journal of Biological Chemistry*, 284(34), pp.22672–22679.

Ignatius, M.J., Chandler, C.R. & Shooter, E.M., 1985. Nerve growth factor-treated, neurite-bearing PC12 cells continue to synthesize DNA. *J Neurosci*, 5(2), pp.343–351.

Im, J.Y. et al., 2012. DJ-1 induces thioredoxin 1 expression through the Nrf2 pathway. *Hum Mol Genet*, 21(13), pp.3013–3024.

Innamorato, N.G. et al., 2008. The transcription factor Nrf2 is a therapeutic target against brain inflammation. *J Immunol*, 181(1), pp.680–689.

Izumi, Y. et al., 2012. Isolation, identification, and biological evaluation of Nrf2-ARE activator from the leaves of green perilla (Perilla frutescens var. crispa f. viridis). *Free Radical Biology and Medicine*, 53(4), pp.669–679.

Jaeger, P.A. & Wyss-Coray, T., 2009. All-you-can-eat: autophagy in neurodegeneration and neuroprotection. *Mol Neurodegener*, 4, p.16.

Jain, A. et al., 2010. p62/SQSTM1 is a target gene for transcription factor NRF2 and creates a positive feedback loop by inducing antioxidant response element-driven gene transcription. *J Biol Chem*, 285(29), pp.22576–22591.

Jakubikova, J. et al., 2005. Role of PI3K/Akt and MEK/ERK signaling pathways in sulforaphane- and erucin-induced phase II enzymes and MRP2 transcription, G2/M arrest and cell death in Caco-2 cells. *Biochem Pharmacol*, 69(11), pp.1543–1552.

Jakubikova, J., Bao, Y. & Sedlak, J., 2005. Isothiocyanates induce cell cycle arrest, apoptosis and mitochondrial potential depolarization in HL-60 and multidrug-resistant cell lines. *Anticancer Research*, 25(5), pp.3375–3386.

James, D. et al., 2012. Novel concepts of broccoli sulforaphanes and disease: induction of phase II antioxidant and detoxification enzymes by enhanced-glucoraphanin broccoli. *Nutr Rev*, 70(11), pp.654–665.

Jo, C. et al., 2014. Sulforaphane induces autophagy through ERK activation in neuronal cells. *FEBS Lett*, 588(17), pp.3081–3088.

Juge, N., Mithen, R.F. & Traka, M., 2007. Molecular basis for chemoprevention by

sulforaphane: a comprehensive review. *Cell Mol Life Sci*, 64(9), pp.1105–1127.

Kanematsu, S. et al., 2010. Autophagy inhibition enhances sulforaphane-induced apoptosis in human breast cancer cells. *Anticancer Res*, 30(9), pp.3381–3390.

Kimura, S., Noda, T. & Yoshimori, T., 2007. Dissection of the autophagosome maturation process by a novel reporter protein, tandem fluorescent-tagged LC3. *Autophagy*, 3(5), pp.452–460.

Kissen, R., Rossiter, J.T. & Bones, A.M., 2009. The "mustard oil bomb": Not so easy to assemble?! Localization, expression and distribution of the components of the myrosinase enzyme system. *Phytochemistry Reviews*, 8(1), pp.69–86.

Klionsky, D.J. et al., 2011. A comprehensive glossary of autophagy-related molecules and processes (2nd edition). *Autophagy*, 7(November), pp.1273–1294.

Klionsky, D.J. et al., 2008. Guidelines for the use and interpretation of assays for monitoring autophagy in higher eukaryotes. *Autophagy*, 4(2), pp.151–175.

Komatsu, M. & Ichimura, Y., 2010. Physiological significance of selective degradation of p62 by autophagy. *FEBS Lett*, 584(7), pp.1374–1378.

Kristal, A.R. & Lampe, J.W., 2002. Brassica vegetables and prostate cancer risk: a review of the epidemiological evidence. *Nutr Cancer*, 42(1), pp.1–9.

Krobitsch, S. & Kazantsev, A.G., 2011. Huntington's disease: From molecular basis to therapeutic advances. *International Journal of Biochemistry and Cell Biology*, 43(1), pp.20–24.

Kroemer, G., Mario, G. & Levine, B., 2010. Autophagy and the Integrated Stress Response. *Molecular Cell*, 40(2), pp.280–293.

Kruman, I.I. et al., 2004. Cell Cycle Activation Linked to Neuronal Cell Death Initiated by DNA Damage. *Neuron*, 41(4), pp.549–561.

Lamark, T. et al., 2009. NBR1 and p62 as cargo receptors for selective autophagy of ubiquitinated targets. *Cell Cycle*, 8(13), pp.1986–1990.

Lampe, J.W., 2009. Interindividual differences in response to plant-based diets : implications for cancer risk 1 – 4. *American Journal of Clinical Nutrition*, 89, pp.1553–1557.

Lampe, J.W. & Peterson, S., 2002. Brassica, biotransformation and cancer risk: genetic polymorphisms alter the preventive effects of cruciferous vegetables. *J Nutr*, 132(10), pp.2991–2994.

Lee, C. et al., 2013. Attenuation of beta-Amyloid-Induced Oxidative Cell Death by Sulforaphane via Activation of NF-E2-Related Factor 2. *Oxid Med Cell Longev*, 2013, p.313510.

Lees, A.J., Hardy, J. & Revesz, T., 2009. Parkinson's Disease. *Lancet*, 373(9680), pp.2055–66.

Lev, N. et al., 2013. Knocking Out DJ-1 Attenuates Astrocytes Neuroprotection Against 6-Hydroxydopamine Toxicity. *J Mol Neurosci*.

Li, Y. et al., 2010. Sulforaphane, a dietary component of broccoli/broccoli sprouts, inhibits breast cancer stem cells. *Clin Cancer Res*, 16(9), pp.2580–2590.

Loeffler G., P.P., 2003. *Biochemie und Pathobiochemie* 7th ed., Springer-Verlag.

Lopes, F.M. et al., 2010. Comparison between proliferative and neuron-like SH-SY5Y cells as an in vitro model for Parkinson disease studies. *Brain Res*, 1337, pp.85–94.

Ludikhuyze, L. et al., 1999. Kinetic study of the irreversible thermal and pressure inactivation of myrosinase from broccoli (Brassica oleracea L. Cv. Italica). *Journal of Agricultural and Food Chemistry*, 47(5), pp.1794–1800.

Malhotra, D. et al., 2008. Decline in NRF2-regulated antioxidants in chronic obstructive pulmonary disease lungs due to loss of its positive regulator, DJ-1. *Am J Respir Crit*

Care Med, 178(6), pp.592–604.

Mastrangelo, L. et al., 2008. Serotonin receptors, novel targets of sulforaphane identified by proteomic analysis in Caco-2 cells. *Cancer Res*, 68(13), pp.5487–5491.

Matsui, T.-A. et al., 2007. Sulforaphane induces cell cycle arrest and apoptosis in murine osteosarcoma cells in vitro and inhibits tumor growth in vivo. *Oncology reports*, 18(5), pp.1263–8.

Matusheski, N. V., Juvik, J.A. & Jeffery, E.H., 2004. Heating decreases epithiospecifier protein activity and increases sulforaphane formation in broccoli. *Phytochemistry*, 65(9), pp.1273–1281.

McNaughton, S.A. & Marks, G.C., 2003. Development of a food composition database for the estimation of dietary intakes of glucosinolates, the biologically active constituents of cruciferous vegetables. *Br J Nutr*, 90(3), pp.687–697.

Melo, A. et al., 2011. Oxidative stress in neurodegenerative diseases: mechanisms and therapeutic perspectives. *Oxid Med Cell Longev*, 2011, p.467180.

Metcalf, D.J. et al., 2012. Autophagy and misfolded proteins in neurodegeneration. *Exp Neurol*, 238(1), pp.22–28.

Millet, L.J. & Gillette, M.U., 2012. Over a Century of Neuron Culture : From the Hanging Drop to Microfluidic devices. , 85, pp.501–521.

Mizushima, N., 2007. Autophagy: process and function. *Genes Dev*, 21(22), pp.2861–2873.

Mizushima, N. & Yoshimori, T., 2007. How to interpret LC3 immunoblotting. *Autophagy*, 3(6), pp.542–545.

Mizushima, N., Yoshimori, T. & Levine, B., 2010. Methods in mammalian autophagy research. *Cell*, 140(3), pp.313–326.

Morroni, F. et al., 2013. Neuroprotective effect of sulforaphane in 6-hydroxydopamine-lesioned mouse model of Parkinson's disease. *NeuroToxicology*, 36C, pp.63–71.

Nishikawa, T., Tsuno, N.H., Okaji, Y., Shuno, Y., et al., 2010. Inhibition of autophagy potentiates sulforaphane-induced apoptosis in human colon cancer cells. *Ann Surg Oncol*, 17(2), pp.592–602.

Nishikawa, T., Tsuno, N.H., Okaji, Y., Sunami, E., et al., 2010. The inhibition of autophagy potentiates anti-angiogenic effects of sulforaphane by inducing apoptosis. *Angiogenesis*, 13(3), pp.227–238.

Nixon, R.A., 2013. The role of autophagy in neurodegenerative disease. *Nature Medicine*, 19(8), pp.983–997.

Oliviero, T. et al., 2014. Effect of water content and temperature on inactivation kinetics of myrosinase in broccoli (Brassica oleracea var. italica). *Food Chemistry*, 163, pp.197–201.

Pan, T. et al., 2008. The role of autophagy-lysosome pathway in neurodegeneration associated with Parkinson's disease. *Brain*, 131(8), pp.1969–1978.

Parnaud, G. et al., 2004. Mechanism of sulforaphane-induced cell cycle arrest and apoptosis in human colon cancer cells. *Nutr Cancer*, 48(2), pp.198–206.

Pawlik, A. et al., 2013. Sulforaphane inhibits growth of phenotypically different breast cancer cells. *European Journal of Nutrition*, 52(8), pp.1949–1958.

Pham, T.T. et al., 2010. DJ-1-deficient mice show less TH-positive neurons in the ventral tegmental area and exhibit non-motoric behavioural impairments. *Genes, Brain and Behavior*, 9(3), pp.305–317.

Pledgie-Tracy, A., Sobolewski, M.D. & Davidson, N.E., 2007. Sulforaphane induces cell type-specific apoptosis in human breast cancer cell lines. *Mol Cancer Ther*, 6(3), pp.1013–1021.

Querfurt, H.W.. & LaFerla, F.M., 2010. Alzheimer's Disease. *The New England Journal of Medicine*, 362(4), pp.329–344.

Rannikko, E.H. et al., 2012. Loss of DJ-1 protein stability and cytoprotective function by Parkinson's disease-associated proline-158 deletion. *J Neurochem*.

Ravikumar, B. et al., 2008. Rab5 modulates aggregation and toxicity of mutant huntingtin through macroautophagy in cell and fly models of Huntington disease. *Journal of cell science*, 121(Pt 10), pp.1649–1660.

Robinson, D. & McGee Jr., R., 1985. Agonist-induced regulation of the neuronal nicotinic acetylcholine receptor of PC12 cells. *Mol Pharmacol*, 27(4), pp.409–417.

Ross, C.A. & Tabrizi, S.J., 2010. Huntington's disease: from molecular pathogenesis to clinical treatment. *The Lancet Neurology*, pp.83–98.

Rubinsztein, D.C. et al., 2005. Autophagy and its possible roles in nervous system diseases, damage and repair. *Autophagy*, 1(1), pp.11–22.

Rubinsztein, D.C. et al., 2009. In search of an "autophagomometer." *Autophagy*, 5(5), pp.585–589.

Rubinsztein, D.C. et al., 2007. Potential therapeutic applications of autophagy. *Nat Rev Drug Discov*, 6(4), pp.304–312.

Rubinsztein, D.C., 2006. The roles of intracellular protein-degradation pathways in neurodegeneration. *Nature*, 443(7113), pp.780–786.

Rungapamestry, V. et al., 2007. Effect of meal composition and cooking duration on the fate of sulforaphane following consumption of broccoli by healthy human subjects. *Br J Nutr*, 97(4), pp.644–652.

Rusten, T.E. & Stenmark, H., 2010. p62, an autophagy hero or culprit? *Nat Cell Biol*, 12(3), pp.207–209.

Sadasivan, S. et al., 2006. Amino acid starvation induced autophagic cell death in PC-12 cells: evidence for activation of caspase-3 but not calpain-1. *Apoptosis*, 11(9), pp.1573–1582.

Saha, S. et al., 2012. Isothiocyanate concentrations and interconversion of sulforaphane to erucin in human subjects after consumption of commercial frozen broccoli compared to fresh broccoli. *Mol Nutr Food Res*, 56(12), pp.1906–1916.

Salminen, A. et al., 2012. Emerging role of p62/sequestosome-1 in the pathogenesis of Alzheimer's disease. *Prog Neurobiol*, 96(1), pp.87–95.

Sanchez-Perez, A.M. et al., 2012. Parkinson's disease and autophagy. *Parkinsons Dis*, 2012, p.429524.

Sarkar, S., 2011. Role of autophagy in neurodegenerative diseases. *Current Science*, 101(04), pp.514–519.

Selkoe, D.J., 2001. Alzheimer ' s Disease : Genes , Proteins , and Therapy. , 81(2), pp.741–766.

Shah, S.P. & Duda, J.E., 2015. Dietary modifications in Parkinson's disease: A neuroprotective intervention? *Medical Hypotheses*, 85(6), pp.1002–1005.

Shan, Y. et al., 2006. Effect of sulforaphane on cell growth, G(0)/G(1) phase cell progression and apoptosis in human bladder cancer T24 cells. *Int J Oncol*, 29(4), pp.883–888..

Shan, Y. et al., 2009. Sulforaphane down-regulates COX-2 expression by activating p38 and inhibiting NF-kappaB-DNA-binding activity in human bladder T24 cells. *Int J Oncol*, 34(4), pp.1129–1134.

Shapiro, T.A. et al., 2001. Chemoprotective glucosinolates and isothiocyanates of broccoli sprouts: metabolism and excretion in humans. *Cancer Epidemiol Biomarkers Prev*,

10(5), pp.501–508.

Shavali, S. & Sens, D.A., 2008. Synergistic neurotoxic effects of arsenic and dopamine in human dopaminergic neuroblastoma SH-SY5Y cells. *Toxicol Sci*, 102(2), pp.254–261.

Shibata, T. et al., 2008. A food-derived synergist of NGF signaling: identification of protein tyrosine phosphatase 1B as a key regulator of NGF receptor-initiated signal transduction. *J Neurochem*, 107(5), pp.1248–1260.

Singh, S. V. et al., 2005. Sulforaphane-induced cell death in human prostate cancer cells is initiated by reactive oxygen species. *Journal of Biological Chemistry*, 280(20), pp.19911–19924.

Skupinska, K. et al., 2009. The effect of isothiocyanates on CYP1A1 and CYP1A2 activities induced by polycyclic aromatic hydrocarbons in Mcf7 cells. *Toxicol In Vitro*, 23(5), pp.763–771.

Soane, L. et al., 2010. Sulforaphane protects immature hippocampal neurons against death caused by exposure to hemin or to oxygen and glucose deprivation. *J Neurosci Res*, 88(6), pp.1355–1363.

Spencer, P.S. et al., 1987. Guam amyotrophic lateral sclerosis-parkinsonism-dementia linked to a plant excitant neurotoxin. *Science (New York, N.Y.)*, 237(4814), pp.517–522.

Stappenbeck, T.S. et al., 2011. Crohn disease: A current perspective on genetics, autophagy and immunity. *Autophagy*, 7(4), pp.355–374.

Surh, Y., 2003. Cancer Chemoprevention With Dietary Phytochemicals. , 3(October), pp.768–780.

Talalay, P. & Fahey, J.W., 2001. Phytochemicals from cruciferous plants protect against cancer by modulating carcinogen metabolism. *J Nutr*, 131(11 Suppl), p.3027S–33S.

Tang, L. et al., 2006. Potent activation of mitochondria-mediated apoptosis and arrest in S and M phases of cancer cells by a broccoli sprout extract. *Mol Cancer Ther*, 5(4), pp.935–944.

Tarozzi, A. et al., 2013. Sulforaphane as a Potential protective phytochemical against neurodegenerative diseases. *Oxidative Medicine and Cellular Longevity*, 2013.

Tarozzi, A. et al., 2009. Sulforaphane as an inducer of glutathione prevents oxidative stress-induced cell death in a dopaminergic-like neuroblastoma cell line. *J Neurochem*, 111(5), pp.1161–1171.

Triola, G., 2015. Chemical tools for modulating autophagy. *Tetrahedron*, 71(3), pp.387–406.

Tsatsanis, C. et al., 2006. Signalling networks regulating cyclooxygenase-2. *Int J Biochem Cell Biol*, 38(10), pp.1654–1661.

Tufekci, K.U. et al., 2011. The Nrf2/ARE Pathway: A Promising Target to Counteract Mitochondrial Dysfunction in Parkinson's Disease. *Parkinsons Dis*, 2011, p.314082.

Vauzour, D. et al., 2010. Sulforaphane protects cortical neurons against 5-S-cysteinyl-dopamine-induced toxicity through the activation of ERK1/2, Nrf-2 and the upregulation of detoxification enzymes. *Mol Nutr Food Res*, 54(4), pp.532–542.

Verhoeven, D.T. et al., 1996. Epidemiological studies on brassica vegetables and cancer risk. *Cancer Epidemiol Biomarkers Prev*, 5(9), pp.733–748.

Verkerk, R. et al., 2009. Glucosinolates in Brassica vegetables: the influence of the food supply chain on intake, bioavailability and human health. *Mol Nutr Food Res*, 53 Suppl 2, p.S219.

Vermeulen, K., Van Bockstaele, D.R. & Berneman, Z.N., 2003. The cell cycle: a review of regulation, deregulation and therapeutic targets in cancer. *Cell Prolif*, 36(3), pp.131–149.

Vermeulen, M. et al., 2006. Association between consumption of cruciferous vegetables

and condiments and excretion in urine of isothiocyanate mercapturic acids. *J Agric Food Chem*, 54(15), pp.5350–5358.

Vermeulen, M. et al., 2008. Bioavailability and kinetics of sulforaphane in humans after consumption of cooked versus raw broccoli. *J Agric Food Chem*, 56(22), pp.10505–10509.

Walker, F.O., 2007. Huntington's disease. *Lancet*, 369(9557), pp.218–228.

Wang, N. et al., 2015. Sulforaphane protects human umbilical vein cells against lipotoxicity by stimulating autophagy via an AMPK-mediated pathway. *Journal of Functional Foods*, 15, pp.23–34.

Wilhelmus, M.M. et al., 2012. Involvement and interplay of Parkin, PINK1, and DJ1 in neurodegenerative and neuroinflammatory disorders. *Free Radic Biol Med*, 53(4), pp.983–992.

Wu, Y.T. et al., 2010. Dual role of 3-methyladenine in modulation of autophagy via different temporal patterns of inhibition on class I and III phosphoinositide 3-kinase. *Journal of Biological Chemistry*, 285(14), pp.10850–10861.

www.nhs.uk, 2011. No Title. , 2012(01.03.2012). Available at: http://www.nhs.uk/conditions/huntingtons-disease/Pages/Introduction.aspx.

www.parkinsonsawareness.eu.com, 2012. Prevalence of Parkinson's Disease. , 2012(01.03.2012). Available at: http://www.parkinsonsawareness.eu.com/en/campaign-literature/prevalence-of-parkinsons-disease/.

Xiao, D. et al., 2009. Cellular responses to cancer chemopreventive agent D,L-sulforaphane in human prostate cancer cells are initiated by mitochondrial reactive oxygen species. *Pharmaceutical research*, 26(7), pp.1729–38.

Xie, H.R., Hu, L.S. & Li, G.Y., 2010. SH-SY5Y human neuroblastoma cell line: in vitro cell model of dopaminergic neurons in Parkinson's disease. *Chin Med J (Engl)*, 123(8), pp.1086–1092.

Yanaka, A. et al., 2009. Dietary sulforaphane-rich broccoli sprouts reduce colonization and attenuate gastritis in Helicobacter pylori-infected mice and humans. *Cancer Prev Res (Phila)*, 2(4), pp.353–360.

Yang, G. et al., 2010. Isothiocyanate exposure, glutathione S-transferase polymorphisms, and colorectal cancer risk. *Am J Clin Nutr*, 91(3), pp.704–711.

Yang, Z. & Klionsky, D.J., 2009. An overview of the molecular mechanism of autophagy. *Curr Top Microbiol Immunol*, 335, pp.1–32.

Yang, Z. & Klionsky, D.J., 2010. Mammalian autophagy: Core molecular machinery and signaling regulation. *Current Opinion in Cell Biology*, 22(2), pp.124–131.

Ye, L. et al., 2002. Quantitative determination of dithiocarbamates in human plasma, serum, erythrocytes and urine: pharmacokinetics of broccoli sprout isothiocyanates in humans. *Clin Chim Acta*, 316(1-2), pp.43–53.

Yokota, T. et al., 2003. Down regulation of DJ-1 enhances cell death by oxidative stress, ER stress, and proteasome inhibition. *Biochem Biophys Res Commun*, 312(4), pp.1342–1348.

Zanichelli, F. et al., 2011. Dose-dependent effects of R-sulforaphane isothiocyanate on the biology of human mesenchymal stem cells, at dietary amounts, it promotes cell proliferation and reduces senescence and apoptosis, while at anti-cancer drug doses, it has a cytotoxic effect. *Age (Dordr)*.

Zhang, L. et al., 2015. Autophagy regulates colistin-induced apoptosis in PC-12 cells. *Antimicrobial Agents and Chemotherapy*, 59(4), pp.2189–2197.

Zhang, Y. et al., 1992. A major inducer of anticarcinogenic protective enzymes from

broccoli: isolation and elucidation of structure. *Proc Natl Acad Sci U S A*, 89(6), pp.2399–2403.

Zhang, Y. et al., 1994. Anticarcinogenic activities of sulforaphane and structurally related synthetic norbornyl isothiocyanates. *Proc Natl Acad Sci U S A*, 91(8), pp.3147–3150.

Zhang, Y. & Tang, L., 2007. Discovery and development of sulforaphane as a cancer chemopreventive phytochemical. *Acta Pharmacol Sin*, 28(9), pp.1343–1354.

Zhao, J. et al., 2007. Enhancing expression of Nrf2-driven genes protects the blood brain barrier after brain injury. *J Neurosci*, 27(38), pp.10240–10248.

Ziaei, A. et al., 2013. Sulforaphane decreases endothelial cell apoptosis in fuchs endothelial corneal dystrophy: a novel treatment. *Investigative ophthalmology & visual science*, 54(10), pp.6724–34.

Zlokovic, B. V., 2008. The Blood-Brain Barrier in Health and Chronic Neurodegenerative Disorders. *Neuron*, 57(2), pp.178–201.

8 APPENDICES

8.1 FREQUENTLY USED BUFFERS AND SOLUTIONS

5x Loading buffer

0.625M Tris base (Ultrapure)	3.78g
2% SDS (Sodium Doecyl Sulphate)	1g
10% Glcerol	5ml

10x PBS buffer (stock solution)

NaCl	80g
KCl	2g
Na_2HPO_4	11.1g pH 7.4
KH_2PO_4	2g add 1L ddH_2O, mix well.

Lysis buffer (NP40) **for 500ml**

20mM Tris-EDTA/HCl pH 8 for 500ml (add 10ml of this solution) [2mM EDTA]

150mM NaCl	4.35g
10% Glycerol	50ml
1% Nonidet P40	5ml

Complete volume up to 500ml with ddH2O and MIX WELL

PBST (Phosphate Buffered Saline Tween-20)

PBS pH 7.4 containing 0.1% Tween 20

Transfer Buffer **for 500ml**

10% Bio-Rad transfer buffer 10x	50ml
20% methanol	100ml
70% H_2O	350ml

REAGENTS TO PREPARE	COMPONENTS	60MM PLATE OR $3.2X10^6$ CELLS	100MM PLATE OR $8.8X10^6$ CELLS
PBS/PHOSPHATASE INHIBITOR	10x PBS	0.4ml	0.8ml
	Distilled water	3.4ml	6.8ml
	Phosphatase Inhibitor	0.2ml	0.4ml
	TOTAL REQUIRED	**4.0ml**	**8.0ml**
1X HYPOTONIC BUFFER	10x Hypotonic Buffer	25.0µl	50.0µl
	Distilled water	225.0µl	450.0µl
	TOTAL REQUIRED	**250.0µl**	**500.0µl**
COMPLETE LYSIS BUFFER	10mM DTT	2.5µl	5µl
	Lysis Buffer AMI	22.25µl	44.5µl
	Protease Inhibitor Cocktail	0.25µl	0.5µl
	TOTAL REQUIRED	**25.0µl**	**50.0µl**

Table 8: Composition of solutions necessary for nuclear protein extraction
The nuclear extract kit was purchased from Active Motif (Cat.No. 40010). It did not provide the information on concentrations of the phosphatase inhibitor, lysis buffer AMI or protease inhibitor cocktail.

8.2 METHOD OPTIMISATION TABLES AND PROTOCOLS

8.2.1 CELL CYCLE METHOD OPTIMISATION TABLE

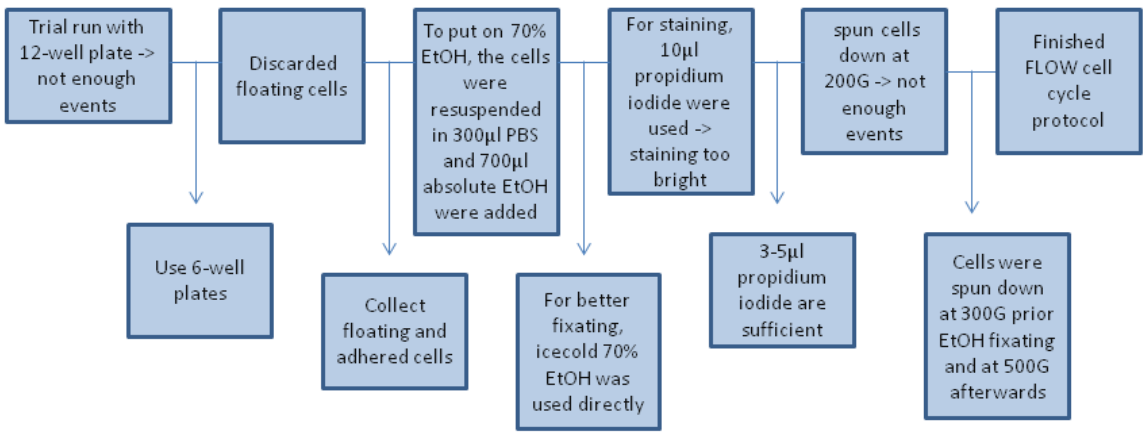

Figure 47: Cell cycle assay optimisation

8.2.2 ANNEXINV/PI METHOD OPTIMISATION TABLE AND GATING

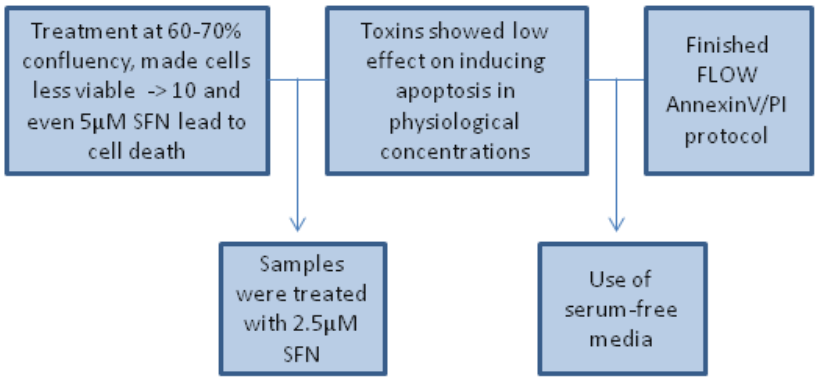

Figure 48: AnnexinV/PI assay optimisation table

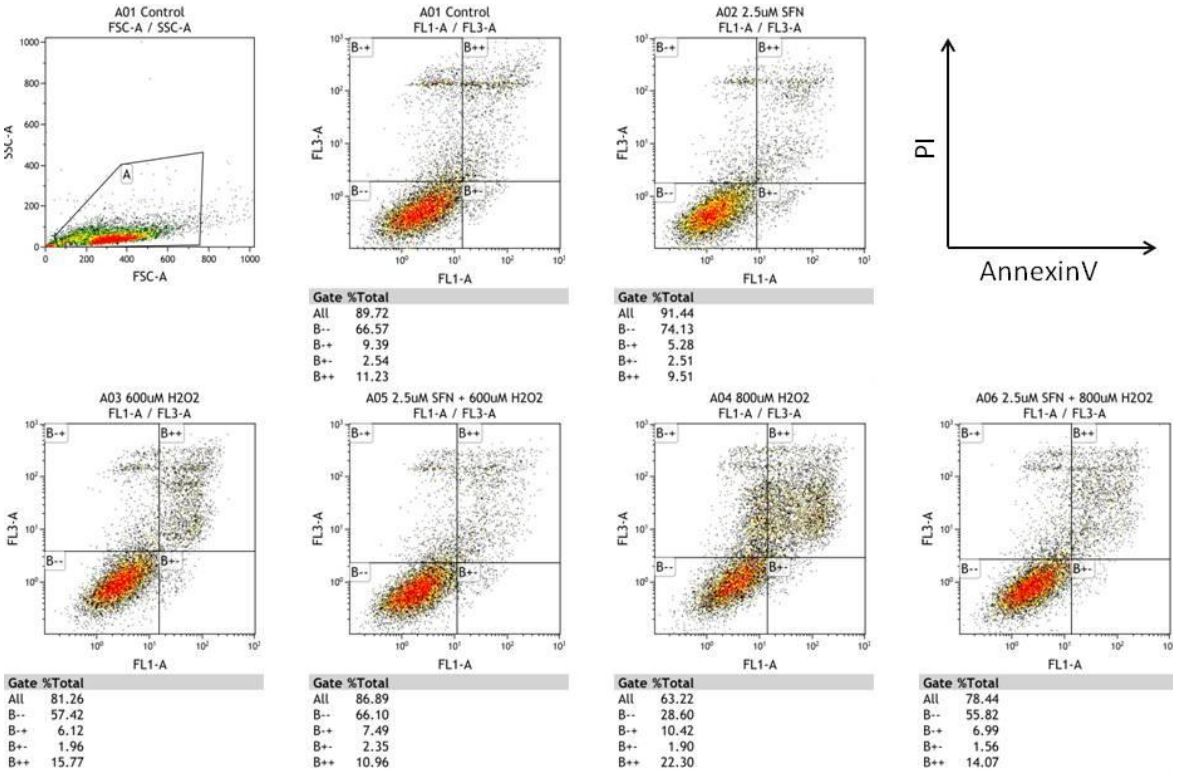

Figure 49: Flow cytometry AnnexinV/PI gating for results in Figure 28, p.85.
SFN protects PC-12 cells from H_2O_2-induced cell death.

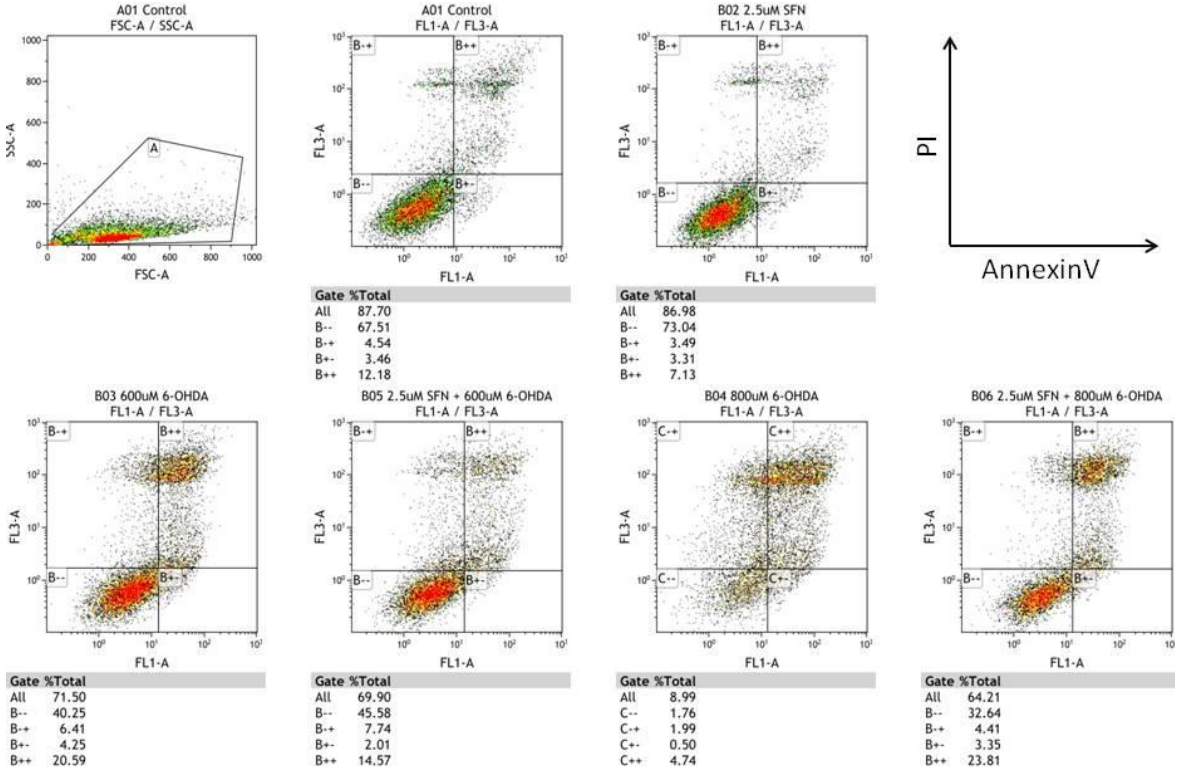

Figure 50: Flow cytometry AnnexinV/PI gating for results shown in Figure 29, p.85.
SFN protects PC-12 cells from 6-OHDA induced cell death.

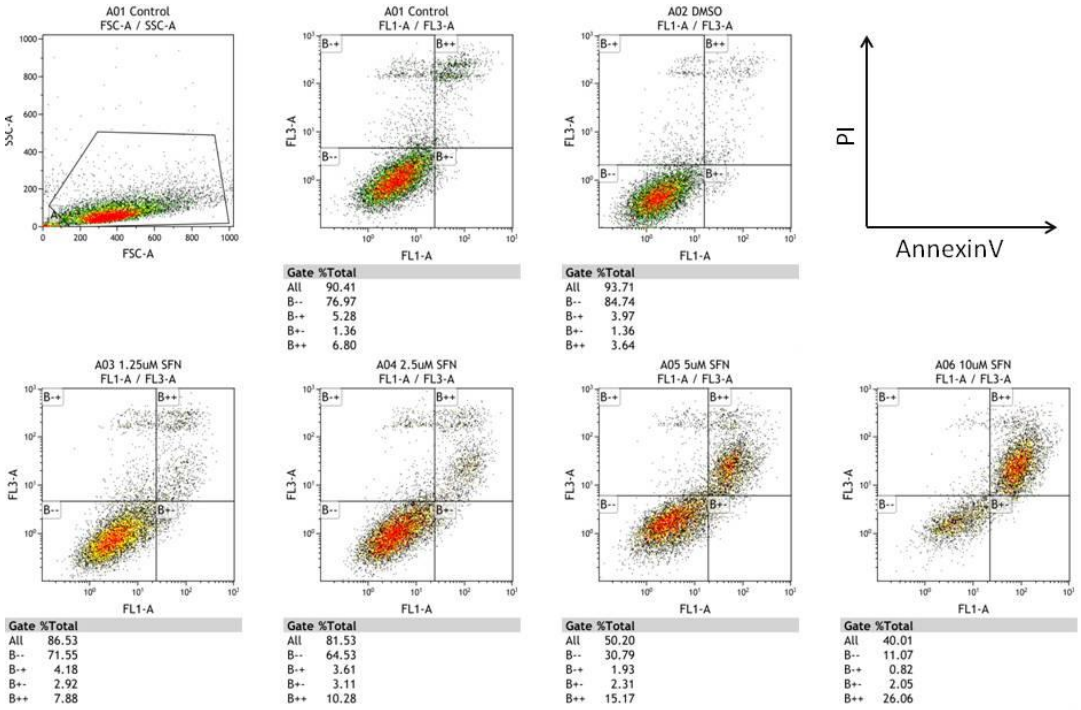

Figure 51: Flow cytometry AnnexinV/PI gating for results in Figure 65, p.153.
A dose responsive induction of apoptosis by SFN

8.2.3 PLATING OF CELLS

Experiment	Size of plate	PC-12	DIFF PC-12	SH-SY5Y
Western Blot	6 wells	$1x10^6$/plate	20.000/well	$1.5x10^6$/plate
MTT assay	96 wells	$1x10^6$/plate	1000/well	$2x10^6$/plate
RNA extraction	6 wells	$1,2x10^6$/plate	-	$1,5x10^6$/plate
AV/PI	12 wells	70.000-140.000 / well/ml	10.000-20.000 / well/ml	150.000-300.000 / well/ml
Cell cycle	6 wells	$1.2x10^6$/plate	10.000/well (12-well plate)	$1.5x10^6$/plate
JC-1	12 wells	80.000/well	-	-
siRNA	96 wells	$0.5x10^6$/plate	-	-
	12 wells	80.000-160.000 / well/ml	-	-
	6 wells	$1x10^6$/plate	-	-

Table 9: Seeding density chart

8.2.4 JC-1

PC-12 cells were seeded in 12 well plates at a concentration of 80.000 cells/well. On day 3, treatment with SFN or DMSO control is started. After 24h, the treatment media is replaced by H_2O_2 containing media and incubated for another 24h. On day 5 the staining with JC-1 is started. Treatment media is replaced by 400µl JC-1 at working concentration (2µM). The plate is then placed on a rocker for 30 mins. Then the media is removed and placed into allocated tubes and spun down. 50µl trypsin is added to the remaining cells and after a minute is joined by 250µl of media. The media of the previously spun down cells is removed and the 250µl media containing the attached cells are added. The pellet is resuspended and put into allocated 1.5ml Eppendorf tubes, in which the samples are then read on the flow cytometer.

Results did not show the expected shift towards the right if plotted against FL-1 on x and FL-2 on y axis, so the involvement of SFN in change of membrane potential could not be determined. However, protective effects could also be observed **(Figure 52)**.

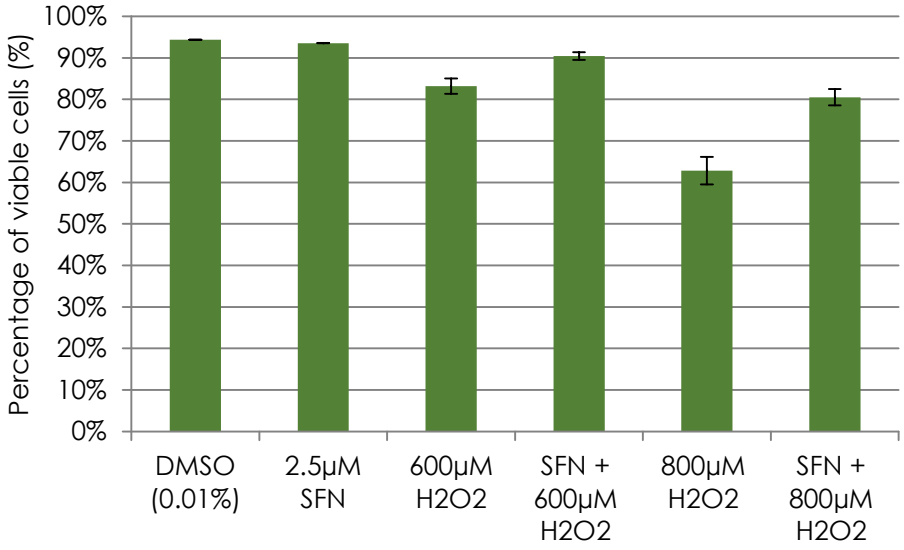

Figure 52: JC-1 experiment
PC-12 cells were treated with 0.01% DMSO or 2.5µM SFN for 24h. This was replaced by 600 or 800µM H_2O_2 for another 24h. After 30mins incubation with JC-1, samples were analysed using flow cytometry. Each bar represents the average of 2 biological replicates.

8.3 ADDITIONS TO CHAPTER 3

8.3.1 SULFORAPHANE AND CELL CYCLE IN SH-SY5Y CELLS

SFN on cell cycle in SH-SY5Y cells. The data collected from SFN treatment on SH-SY5Y cells presented a stronger indication of S phase arrest **(Figure 53).** However, as control samples could not be collected due to low recovery numbers, no direct comparison can be made. Still, looking at SFN-treated samples alone, an increase of percentage of cells can be seen in 10 and 20µM SFN (26.94% and 41.22%) compared to 2.5µM (22.92). This increase was followed by a corresponding decrease in G1 phase cell percentage. G2 phase did not change between SFN treatment samples.

Cell cycle was also assessed in DIFF PC-12 cells, however they showed polyploidy and therefore could not be quantified properly. This result however confirms previous reports of DIFF PC-12 cells demonstrating this phenomenon, which confirms also on cellular level that PC-12 have indeed been differentiated **(example graphs shown in Figure 54).**

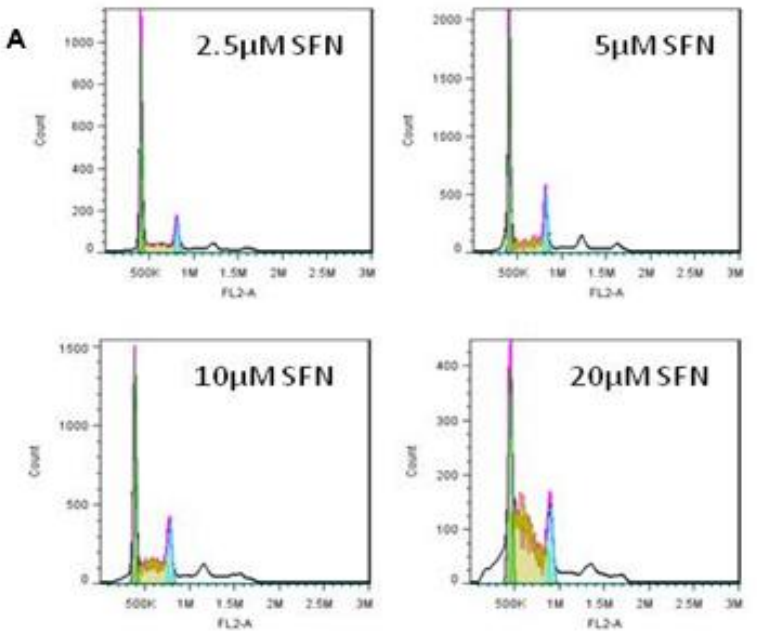

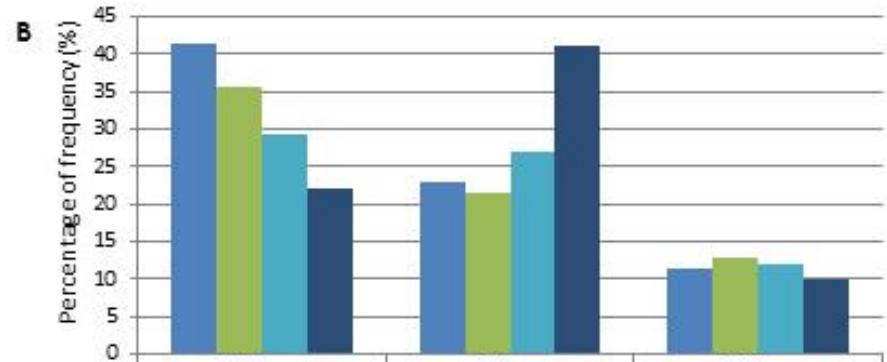

	G1 phase	S phase	G2 Phase
2.5µM SFN	41.49	22.92	11.27
5µM SFN	35.7	21.46	12.84
10µM SFN	29.28	26.94	12.09
20µM SFN	21.91	41.22	9.81

Figure 53: Cell cycle assay of SFN in SH-SY5Y cells.
Cells were exposed to media alone, DMSO (0.05%) or different SFN concentrations (2.5µM-20µM) for 24h. The distributions of cells in different cell cycle stages was obtained using flow cytometry and FlowJo software (n=1).

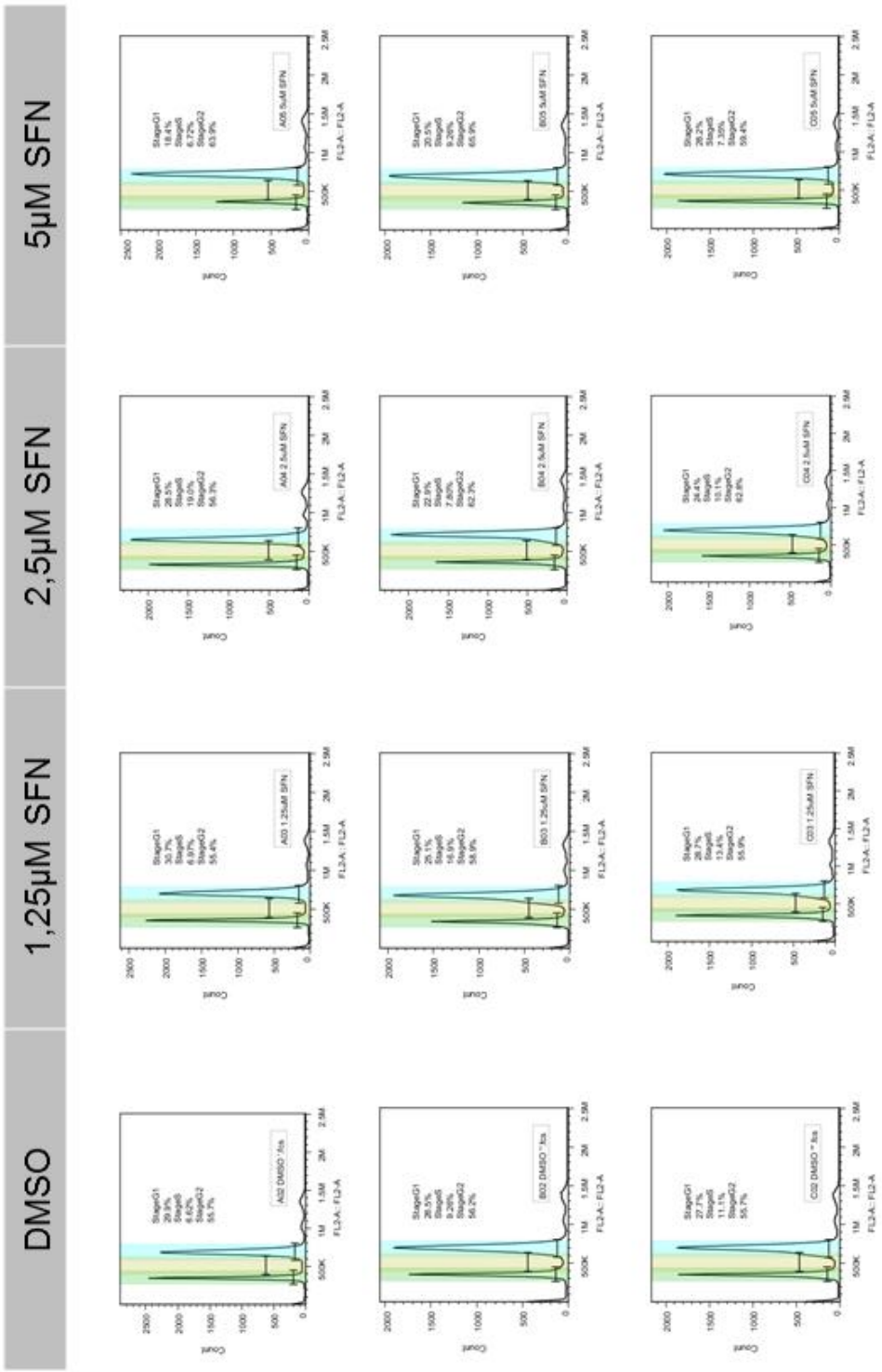

Figure 54: Cell cycle assay of SFN in DIFF PC-12 cells.
Cells were exposed to media alone, DMSO (0.02%), or various concentrations of SFN (1.25-5µM) for 24h. The distribution of cells in different cell cycle stages was obtained by flow cytometry and FlowJo software. (n=1)

8.3.2 EFFECT OF SFN ON PHASE II AND ANTIOXIDANT ENZYME EXPRESSION

SFN on Nrf2 in nuclear protein of PC-12 cells

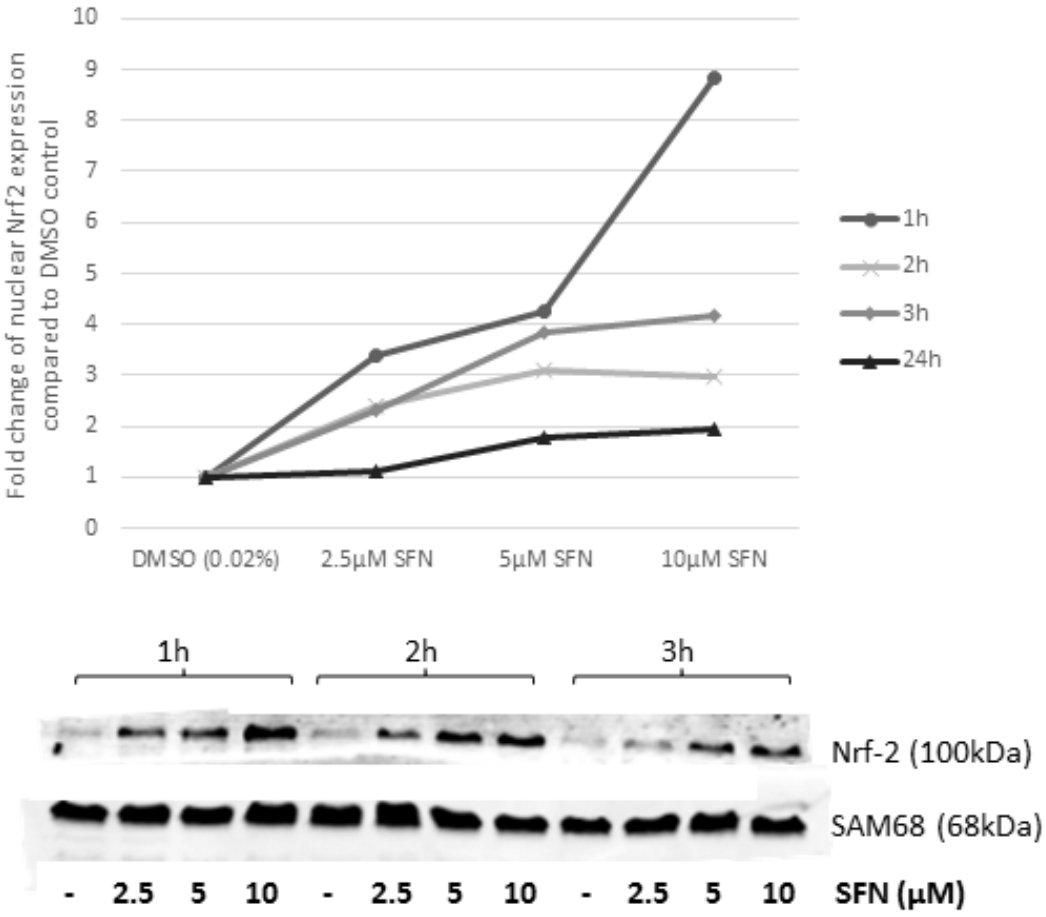

Figure 55: Nrf2 expression in PC-12 cells after SFN treatment as determined by western blot.
PC-12 cells were treated with DMSO (0.02%) or various concentrations of SFN (2.5-10µM) for 1h, 2h, 3h or 24h. Nuclear protein was collected and blots were imaged using Odyssey. The graph shows the trend of the individual time points (2h: n=2; all others: n=1).

SFN on TR-1 gene expression in PC-12. 2h and 6h RNA samples were quantified with qPCR. SFN-treated samples show a fold change of up to 3 fold, as seen in the 6h 5µM SFN sample. These results **(Figure 56)** show a single biological replicate carried out in 3 technical replicates.

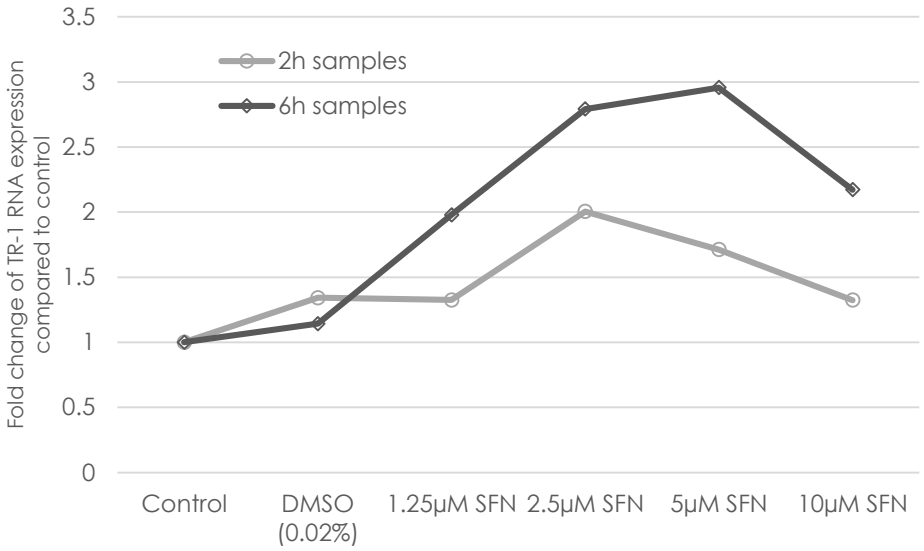

Figure 56: TR-1 expression in PC-12 cells after 2h or 6h SFN treatment as determined by qPCR.
Cells were treated with media alone, DMSO (0.02%), or various concentrations of SFN (1.25-10µM) for 2h or 6h. 18S rRNA was used as housekeeping gene. Bars show qPCR results as fold change compared to control samples. Each bar represents a single biological replicate carried out in 3 technical replicates (n=1).

SFN on GST gene expression in PC-12. 2h and 6h RNA samples were quantified with qPCR. SFN treatment samples show an increase in GST expression of up to 2-fold in 2h and 4.5-fold in 6h samples, with the lower SFN concentrations showing the greatest induction **(Figure 57)**. However, this result only shows one biological replicate, hence more repeats are necessary for a significant conclusion.

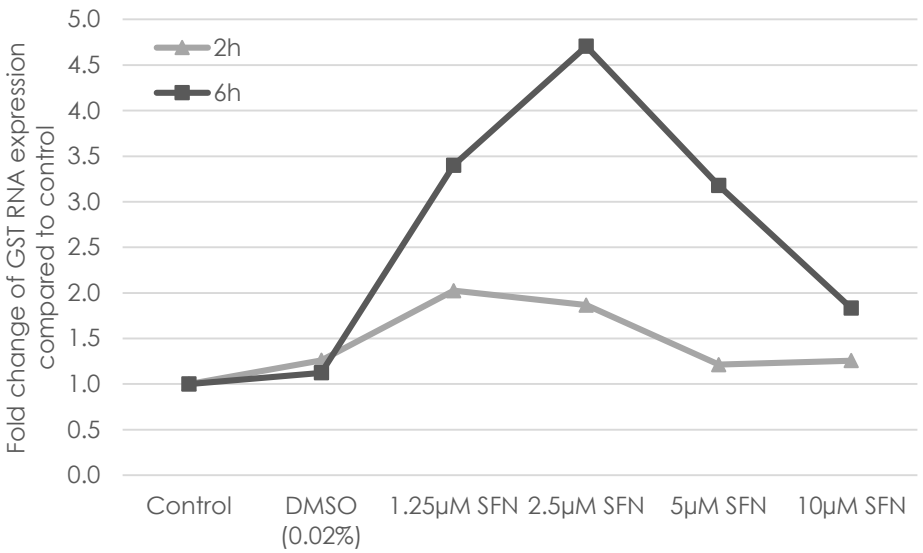

Figure 57: GST expression in PC-12 cells after 2h or 6h SFN treatment as determined by qPCR.
Cells were treated with media alone, DMSO (0.02%), or various concentrations of SFN (1.25-10µM) for 2h or 6h. 18S rRNA was used as housekeeping gene. Bars show qPCR results as fold change compared to control samples. Each bar represents a single biological replicate carried out in 3 technical replicates (n=1).

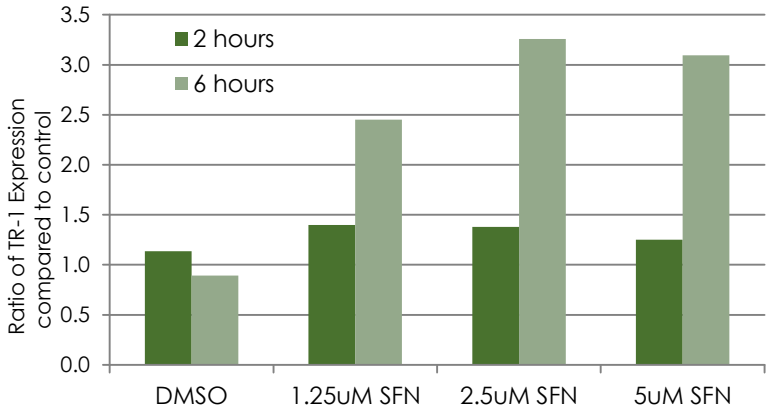

Figure 58: TR-1 expression in SH-SY5Y cells after 2h and 6h SFN treatment as determined by qPCR.
Cells were treated with media alone, DMSO (0.02%) or various concentrations of SFN for 2h and 6h. 18S rRNA was used as housekeeping gene. Bars show qPCR results as fold change compared to vehicle control samples (media only). Each bar represents one biological replicate carried out in 3 technical replicates (n=1).

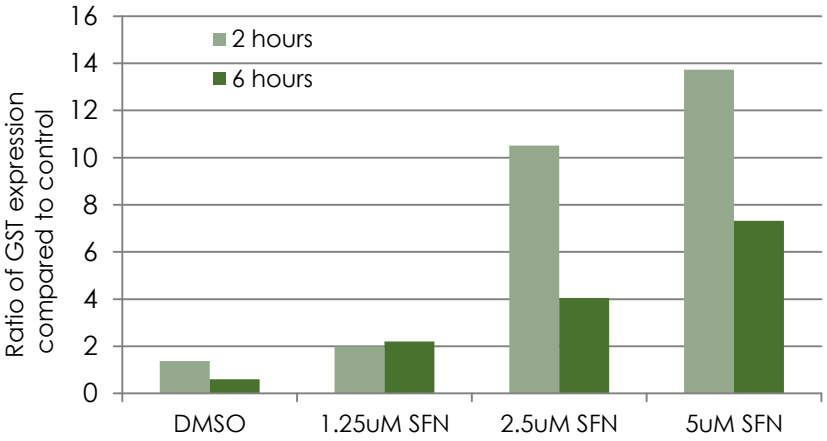

Figure 59: GST expression in SH-SY5Y cells after 2h and 6h SFN treatment as determined by qPCR.
Cells were treated with media alone, DMSO (0.02%) or various concentrations of SFN (1.25-2.5µM) for 2h or 6h. 18S rRNA was used as housekeeping gene. Bars show qPCR results of 2h and 6h experiments as fold change compared to vehicle control samples (media only). Each bar represents one biological replicate carried out in 3 technical replicates (n=1).

8.3.3 NEUROPROTECTIVE EFFECTS OF SULFORAPHANE ON PC-12, DIFF PC-12 AND SH-SY5Y CELLS

Dose-dependent increase of apoptosis by SFN in PC-12 cells. The AnnexinV/PI Flow Cytometry results **(see Figure 60)** show that 1.25, 2.5, 5 and 10µM SFN increases apoptosis in a dose-responsive manner. From 8.16% cell death in control cells, 1.25µM already presents 10.8% apoptotic cells, increasing to 28.11% in 10µM SFN samples. The cell number in "gate 1" decreased with higher concentrations of SFN most likely due to a higher occurrence of debris within the sample.

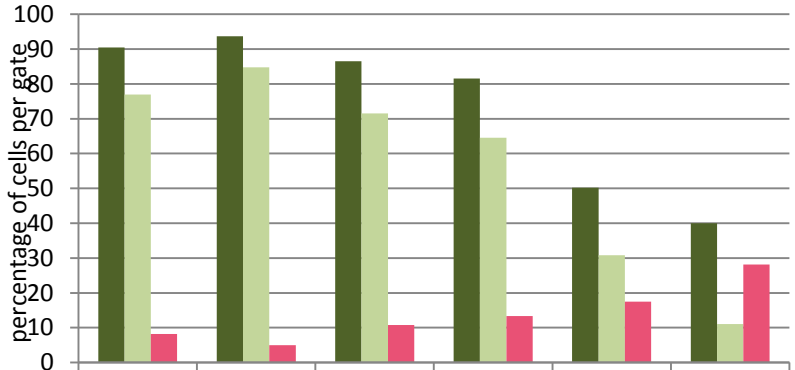

	Control	DMSO	1.25uM SFN	2.5uM SFN	5uM SFN	10uM SFN
all cells (gate 1)	90.41	93.71	86.53	81.53	50.2	40.01
healthy cells	76.97	84.74	71.55	64.53	30.79	11.07
sum of apoptotic cells	8.16	5	10.8	13.39	17.48	28.11

Figure 60: Apoptosis of SFN on PC-12 cells measured by flow cytometry.
Cells were cultured in 6-well plates (200.000 cells/well) and treated with media, DMSO (0.05%) or various concentrations of SFN (1.25-10µM) for 24 hours at ~70% confluency. Collected samples were used with the AnnexinV/PI kit and analysed on the flow cytometer. Each bar represents a single biological replicate of 10.000 events.

Cell-protective effect of SFN against H_2O_2-induced apoptosis in PC-12 cells. This graph shows two individual experiments consisting of two biological replicates each **(see Figure 61)**. By plotting them individually, the in some cases great recovery of up to 40% can be seen more clearly.

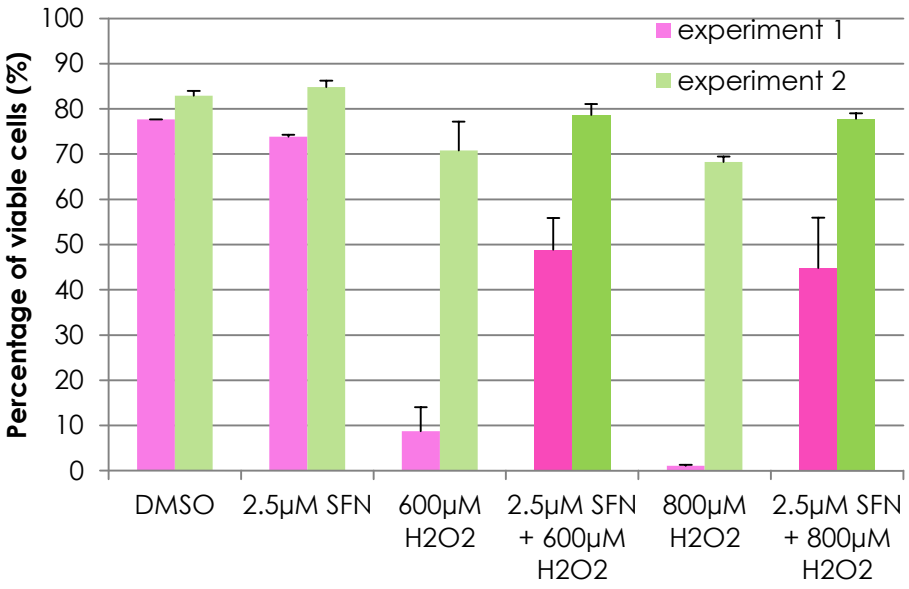

Figure 61: Effect of SFN on H_2O_2-induced apoptosis in PC-12 cells measured by flow cytometry – individual experiments.
Cells were pre-treated with either DMSO (0.025%) or 2.5µM SFN for 24h. Then these solutions were replaced with either serum-free media, 600µM or 800µM H_2O_2 for another 24h. The collected samples were analysed using the AnnexinV/PI kit and a flow cytometer. Bars are the average of 2 biological replicates with about 10.000 events each (n=2; ±SD).

8.4 ADDITIONS TO CHAPTER 4

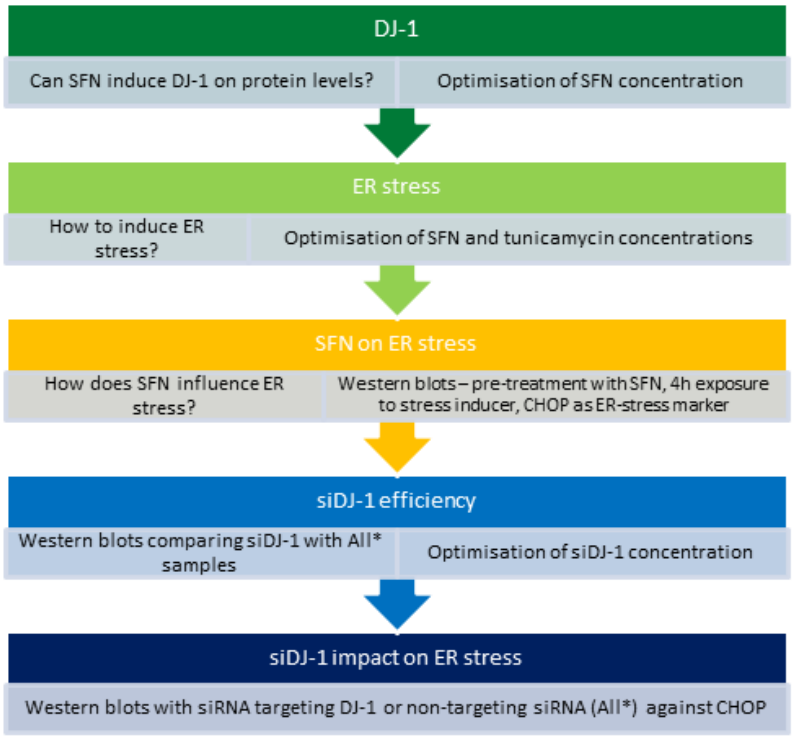

Figure 8.6 Flow diagram of DJ-1 related experiments This lists the experiments planned to determine whether DJ-1 can influence the ability of SFN to protect PC-12 cells from tunicamycin-induced ER-stress.

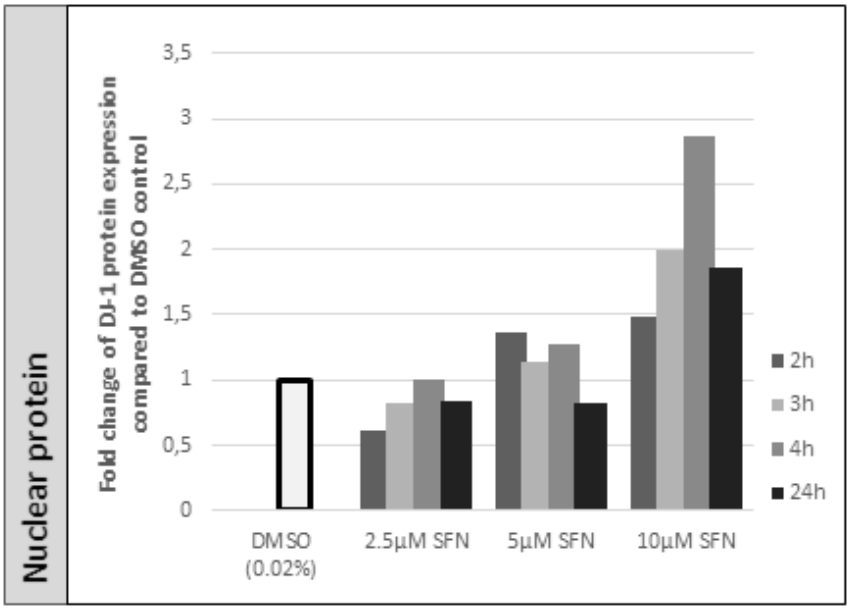

Figure 62: DJ-1 expression in PC-12 cells after SFN treatment as determined by western blot.
Cells were treated with 0.02% DMSO (vehicle control) or different SFN concentrations and incubated for 2, 3, 4 or 24h. Nuclear protein was collected. Blots were imaged with Odyssey and data calculated from DJ-1 bands (23kDa) against SAM68 (68kDa). The bars represent one biological replicate.

8.4.1 ANALYSIS OF DJ-1 EXPRESSION AFTER TREATMENT WITH EMETINE, ANISOMYCIN AND CYCLOHEXIMIDE

To investigate the increased DJ-1 levels, protein inhibitors like emetine, anisomycin and cycloheximide (CHX) were added to SFN treatment. All three compounds are commonly used to block protein synthesis through various pathways. This experiment has also been carried out at various time points. **Figure 63** shows an example of the resulting western blot experiments. Interestingly, protein levels are increasing over time, especially in combined SFN + CHX, which suggests that either the amount of CHX used was not enough to inhibit protein translation, that the production of DJ-1 is in fact not due to an increase in translation, or that SFN itself is regulating the production of DJ-1 by inhibiting another protein responsible for degrading DJ-1. This was not investigated further.

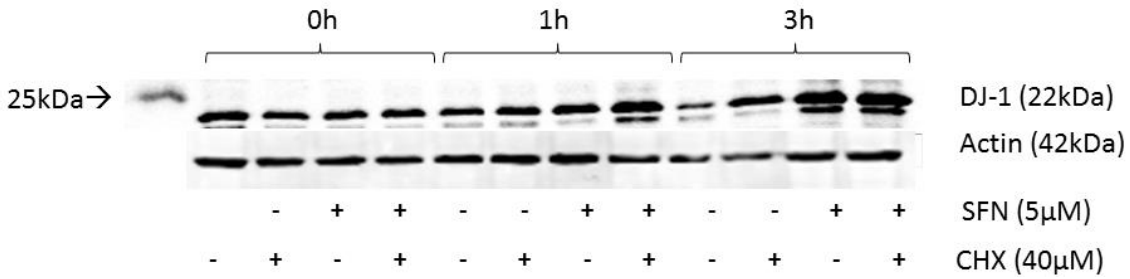

Figure 63: DJ-1 expression in PC-12 cells after SFN and CHX treatment as determined by western blot.
Cells were treated with 5µM SFN and/or 40µM CHX for 0, 1 or 3h. The blots were imaged by Odyssey and show DJ-1 bands at 22kDa and actin at 42kDa.

8.4.2 CHOP EXPRESSION WITH SIDJ-1

CHOP levels were observed under ER-stress conditions induced by tunicamycin and compared to basal levels when cells were transfected either with All* or DJ-1 siRNA. No difference could be observed between SFN pre-treated cells exposed to All* or siDJ-1. Since the knock-down of siDJ-1 was not successful, these results do not reflect any influence of DJ-1 in the ER-stress capabilities of SFN **(Figure 64)**. Although these results were not relevant regarding siDJ-1, the findings once again demonstrate the capability of SFN to reduce tunicamycin-induced ER-stress in PC-12 cells **(which can be seen in Figure 35)**. One biological replicate represented in the DJ-1 **Figure 37** had to be omitted due to outliers.

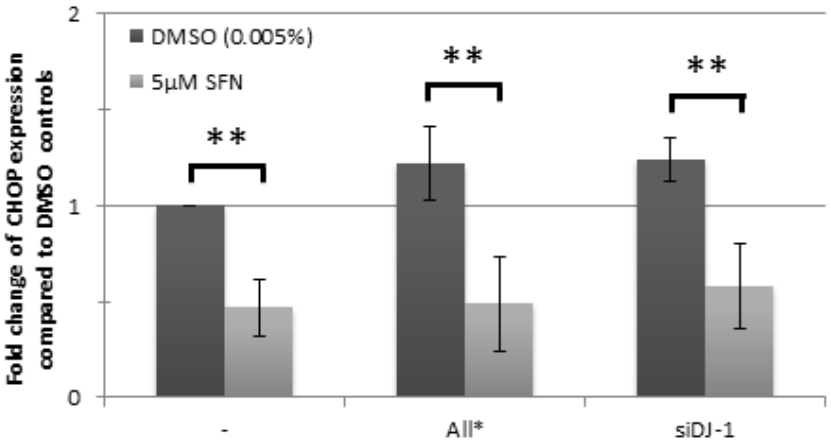

Figure 64: CHOP protein expression and recovery from tunicamycin-induced ER-stress by SFN in presence of siDJ-1.
PC-12 cells were treated with siDJ-1 before a 24h incubation with 5µM SFN. This was replaced by 1µg/ml tunicamycin for another 4h. Blots were imaged using Odyssey looking at CHOP (27kDa) and β-actin (42kDa) levels. The graph shows the quantification of CHOP after normalisation with β-actin expressed as fold change compared to the DMSO control. Each bar represents the average of 3 biological replicate. **P<0.02

8.5 ADDITIONS TO CHAPTER 5

8.5.1 ACTION OF SFN AND 3-MA AGAINST H_2O_2 INDUCED CELL DEATH

Cell protective effects of SFN against H_2O_2 induced apoptosis in presence of 3-MA. The autophagy inhibitor 3-MA leads to more death in combination with H_2O_2 than H_2O_2 on its own. SFN cannot rescue as many cells from H_2O_2 induced apoptosis in the presence of 3-MA **(Figure 65)**. However, due to the fact that the autophagic pathway could not be fully suppressed with 3-MA **(see Figure 39, p.103)**, these results may not reflect an absence of autophagy at all. This however led to a different approach, using Atg16L1-KO PNCs instead.

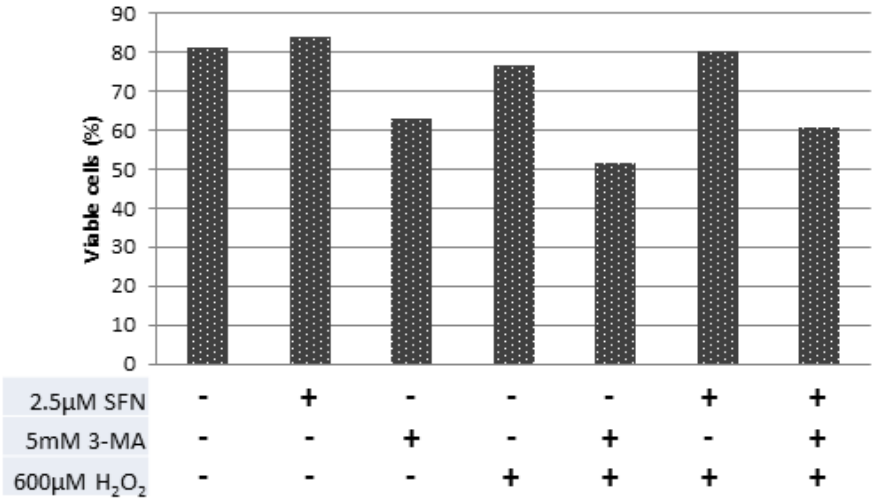

Figure 65: Effect of SFN on H_2O_2-induced apoptosis in PC-12 cells in the presence or absence of 3-MA, measured by flow cytometry.
Cells were pre-treated with either DMSO (0.025%) or 2.5µM SFN and/or 5mM 3-MA for 24h. Then, the treatment solution was replaced with either serum-free media alone or 600µM H_2O_2 for another 24h. The collected samples were analysed using the AnnexinV/PI kit and run on a flow cytometer. Results show the percentage of viable cells. Each bar represents a single biological replicate with about 10.000 events each (n=1).

8.5.2 GATING OF AV/PI EXPERIMENTS OF PNCS

Flow cytometry gate settings. As usual, events were gated to remove any debris from further calculation. Next, a graph plotting height and area of the forward scatter was used to gate only single cells. A forward and side scanner would usually be used as it is to set the gating for apoptosis. However, there was a clear differentiation in two cell groups visible, which were therefore gated separately as well as together **(Figure 66Figure 67Figure 68)**.

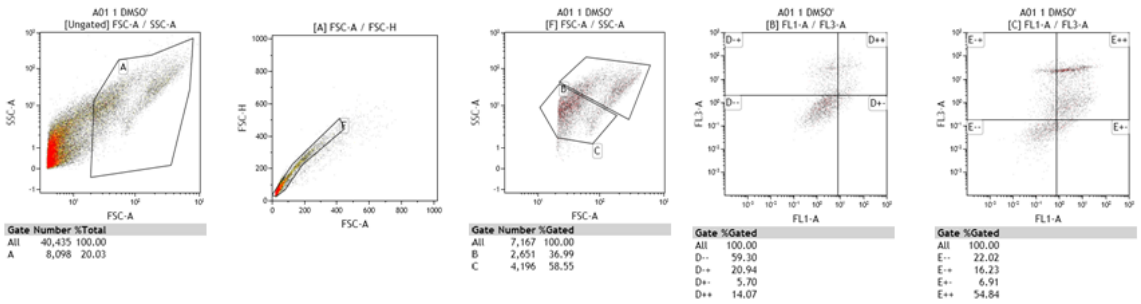

Figure 66: General Gating – splitting into top and bottom cells

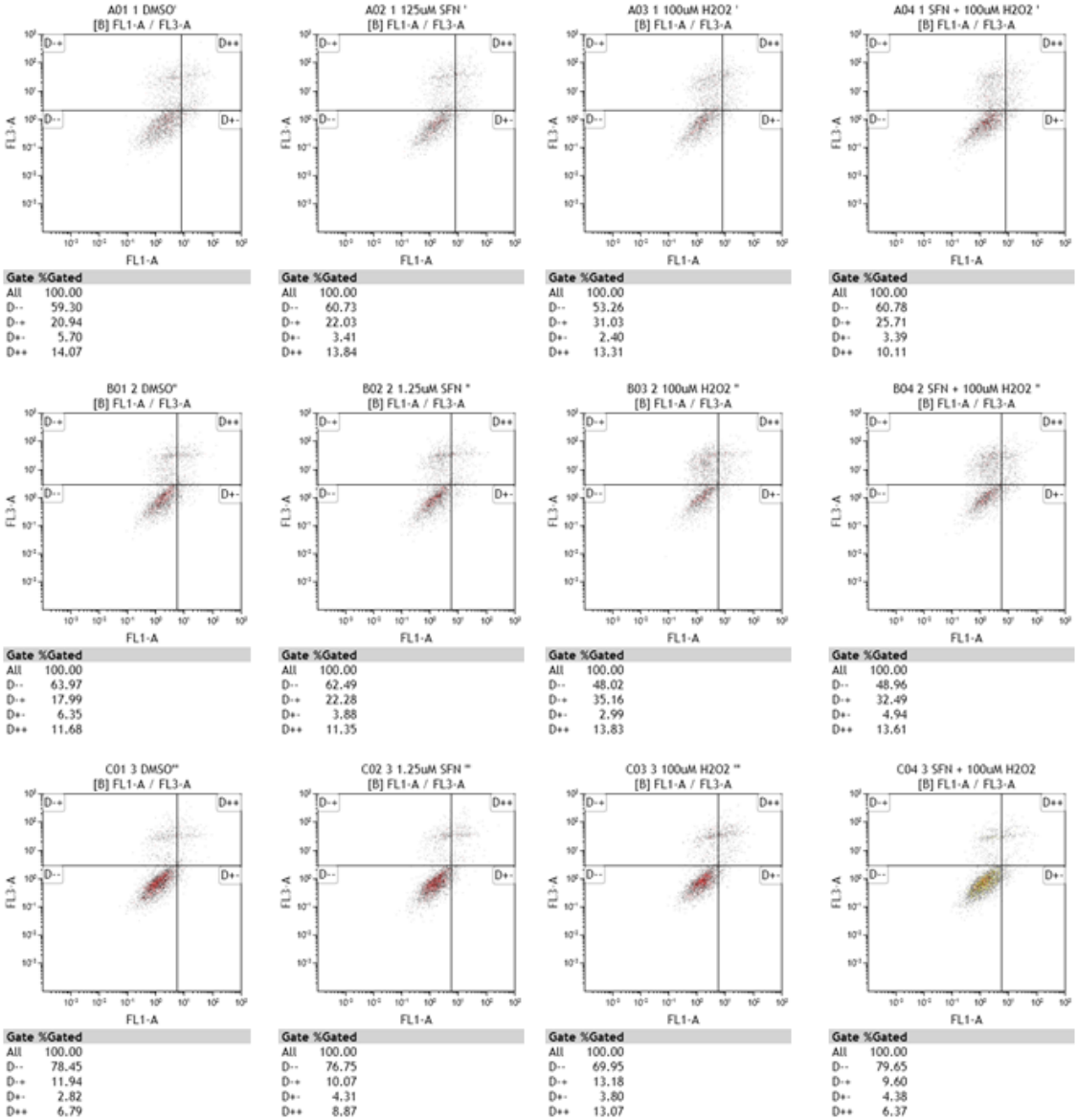

Figure 67: AV/PI graphs of top gated cells.

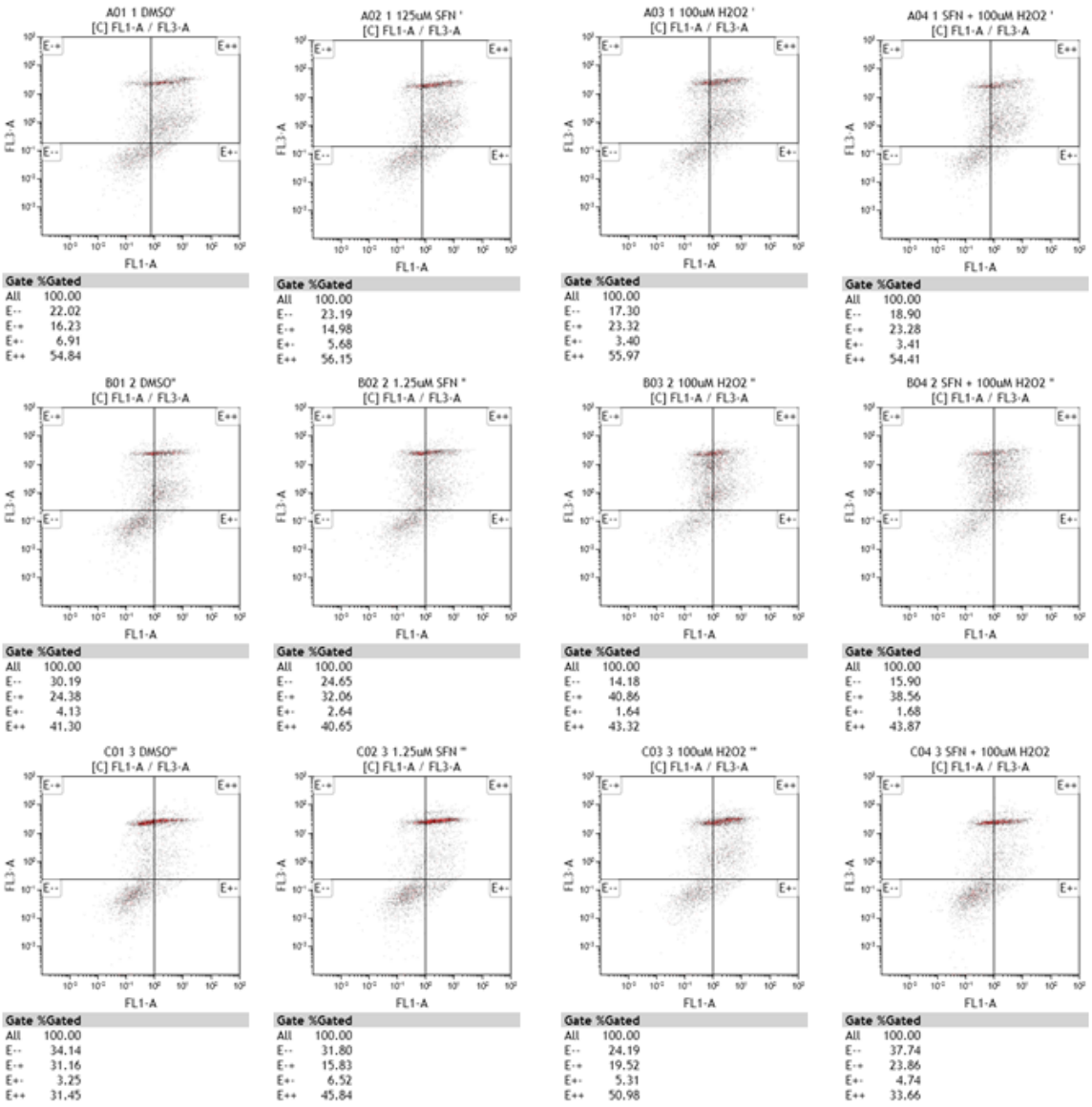

Figure 68: AV/PI graphs of top gated cells

8.5.3 GENOTYPING

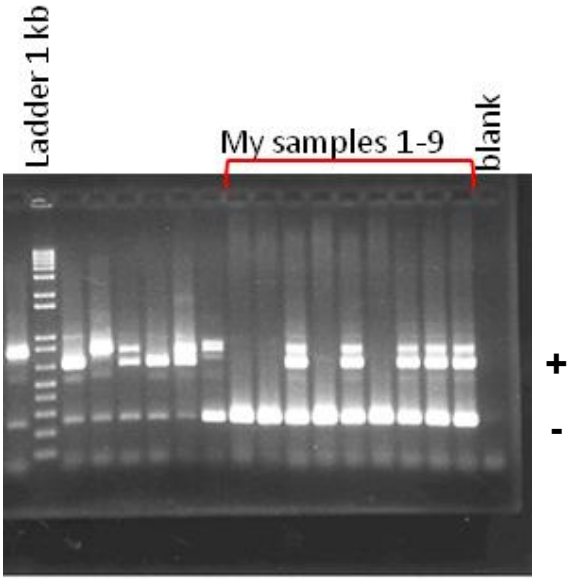

Figure 69: Atg16L1 genotyping of mice by PCR. Using end-point PCR and gel electrophoresis, Atg16L1 alleles were genotyped as wild-type (+/+ or +/-) and knock-out (-/-).

8.5.4 COATING PROTOCOL OF PLATES FOR PNCS

Poly ornithine Coating. A solution of 15µg/ml poly-ornithine solution was prepared. The wells were covered with it (1ml for 12well plate) and left in the incubator at 37°C over night.

Poly-D-lysine. A working solution of 50µg/ml was prepared. The surface of the culture vessel was covered (400µl for 12well plate) and then incubated at room temperature for 1h. The plates were thoroughly rinsed 3x with distilled water, as excess poly-D-lysine can be toxic to the cells. The coated plates are left uncovered under the hood until the wells have dried. Plates were used the next day, but can be stored at 4°C for one week when wrapped tightly in parafilm.

Before the cells are seeded, the plates are washed twice with sterile water and once with sterile filtered PBS. Then the PBS is replaced by DMEM/F12 +10% FBS (v/v) and left in the incubator at 37°C for 2h before cells are plated.